UNDERSTANDING CYTOTOXIC T LYMPHOCYTE FUNCTION USING MODELS OF PRIMARY IMMUNODEFICIENCIES

by
Senta Kapnick

A dissertation submitted to Johns Hopkins University in conformity with the requirements for the degree of Doctor of Philosophy

Baltimore, Maryland
July 2016

Abstract

CD8+ cytotoxic T lymphocytes (CTLs) are critical for the elimination of virally-infected cells, and defects in CTL responses can lead to primary immunodeficiencies and secondary lymphoproliferative syndromes. One such defect is caused by mutations in the gene encoding Inducible T cell Kinase (ITK), a kinase that serves as an amplifier of T cell receptor (TCR) signaling. Patients with mutations in ITK develop lymphoproliferative disease associated with susceptibility to viral infections. We found CTLs from ITK-deficient mice exhibit impaired killing of multiple different targets, indicating that ITK-deficiency leads to global defects in cytolysis. Treating WT CTLs with an ITK-specific inhibitor during cytolysis assays could reproduce impaired killing, suggesting that these defects were not necessarily due to altered T cell development or CTL differentiation. To further evaluate this killing defect, we examined the discrete steps involved in CTL activity, including TCR-triggered adherence to cells, immunological synapse formation, centrosome polarization, and degranulation inducing cytolysis in targets. Although early events following TCR-mediated target cell engagement, such as actin ring formation and polarization, were intact in ITK-deficient CTLs, we found defects in degranulation, suggesting ITK may play an unappreciated role in the final stages of killing. Nonetheless, prolonged culture of ITK-deficient CTLs in IL-2 could rescue defects in degranulation, similar to observations in NK cells from certain primary immunodeficiencies in which cytotoxicity is enhanced in culture after IL-2 stimulation. Together these experiments provide clues to novel roles for ITK and TCR signaling in regulating late stages of cytolysis, and further insight into the defects that may account for the susceptibility to

viral infections observed in patients with mutations in ITK and TCR signaling components.

In parallel work, we also examined the role of actin in regulating degranulation in normal CTLs. While previous work showed a reduction in actin density at the synapse prior to secretion of lytic granules, we found that cortical actin recovers concomitant with the termination of secretion. Disruption of this actin network via treatment with an actin depolymerization agent resulted in a resumed degranulation, suggesting that actin acts as a reversible barrier to prevent lytic granule exocytosis. Furthermore, we provide evidence that degranulation is required to reestablish the actin barrier. Our results suggest that actin is both regulated by, and regulates, degranulation in CTLs. Experiments further revealed a correlation between the recovery of actin and phosphatidylinositol 4,5-biphosphate (PIP_2) at the synapse, suggesting that the distribution of phosphatidylinositols in the membrane represent a potential mechanism through which CTLs regulate the density of cortical actin during cytolysis. Our work provides insight into actin-related mechanisms regulating secretion in CTLs, which may preserve serial killing capacity during immune responses.

Thesis advisor/reader: Pamela Schwartzberg, MD, PhD

Reader: Michael Edidin, PhD

Acknowledgments

First and foremost, I would like to thank my mentor, Dr. Pam Schwartzberg, for both her scientific and personal mentorship over the years. I feel incredibly privileged to have had the guidance of someone so brilliant and engaging throughout my PhD research, and have benefitted immensely from her experience and generosity. I sincerely thank you for your patience and support, Pam, and hope I can continue my scientific endeavors with your same dedication and fervor.

I would also like to thank the past and present members of the Schwartzberg lab, with whom it is has been an absolute pleasure to learn from, and exchange ideas with, every day. In particular, Dr. Jennifer Cannons and Dr. Julio Gomez-Rodriguez for sharing their extensive expertise with me, teaching me virtually everything I know about immunology and molecular biology. A special thanks as well to my dear friend and mentor, Dr. Zach Kraus, who always encourages me to imagine big – both in science and otherwise.

Much gratitude to all of our collaborators who have generously shared reagents, equipment, and their expertise. To Dr. Jane Stinchcombe and Dr. Gillian Griffiths for their helpful comments and scientific contributions to the ITK story. Thank you to my late-night imaging partner, co-author on the actin story, and friend, Alex Ritter; I look forward to many more years of productive collaboration. I'd like to also thank our mutual mentor, Dr. Jennifer Lippincott-Schwartz, for her direction in pulling the actin story together.

Thanks to my thesis committee members for their guidance over the years. Especially Dr. Michael Edidin, for his healthy dose of enthusiasm and willingness to

share his vast knowledge of all things. I'd also like to thank the support staff that enable us to do our science: in the lab, Julie Reilley and Robin Handon, Stacie Anderson and Martha Kirby in the Flow Cytometry Core, Stephen Wincovitch in the Microscopy Core, and the staff in the Mouse House.

Camaraderie is especially important during any adventure, and I feel fortunate to have shared this one with Mary Weston, Kristie Wrasman, Casey Hemmis, Pavol Genzor, and Christoph Lepper. The memories are precious, and I can't wait for those still to come.

I feel especially privileged to have had the love and unwavering support of a partner as incredible as Charlie Moore. Thank you for helping me finally find that elusive "work/life balance."

My humble gratitude and love goes to all of my family, who are still the most interesting people I know. Especially to two of the greatest gifts my parents ever gave me, my brothers: Markus and Izzy. Thanks for always reminding what "PhD" actually stands for.

To my strong, beautiful, and selfless mom – the truest friend I have. All that I am, or hope to be, I owe to you.

And to my dad, who gave me my first bottle and countless necessities since: you always say you're my #1 fan, but I hope you know that the truth is, I am yours.

“Be patient toward all that is unsolved in your heart and try to love the questions themselves, like locked rooms or like books that are written in a very foreign tongue. Do not seek the answers, which cannot be given to you now. Live the questions and perhaps you will then one day, without noticing it, live along some distant day into the answer.”

-- Rainer Maria Rilke

Table of Contents

List of Tables

List of Figures

Chapter 1: Introduction

1.1 Historical perspective

The concept of immunity, or the resistance to a particular condition due to a special status, dates back to 5th century BCE when the Greek historian, Thucydides, described a plague that killed one third of the Athenian population in a single summer. Although he attributed the cause of the disease, now known to be typhoid fever, to the “will of the Gods,” remarkably, he noted that individuals who had contracted the disease and survived became exempt from recurrence of plague. Although attempts to intentionally induce immunity were reported for centuries, even before Edward Jenner used variolation to protect individuals from smallpox, it was not until the 1860’s that Louis Pasteur serendipitously discovered that immunity could be acquired after exposure to attenuated bacterial cultures. This discovery was followed by the development of a vaccine against cholera in chickens, and the rationale that made immunology a science was born.

By the turn of the 19th century, a number of paradigms that laid the groundwork for the field of immunology were established. These included Emil von Behring and Shibasaburo Kitasato’s discovery that transferring serum with “anti-toxic activity” from animals immune to tetanus provided protection to recipients of that serum, and Ilya Metchnikoff’s description of phagocytosis, the pioneering study of cellular immunology.

1.2 The specificity of immune responses and their effectors

Host responses against invading pathogens are basic physiological reactions of most living organisms. Even prokaryotes protect themselves by use of restriction enzymes and clustered regularly interspaced palindromic repeats (CRISPRs) to degrade unfamiliar viruses [1]. Not surprisingly, the immune systems of humans and other mammals are significantly more complex, comprised of a network of organs, tissue, cells, and their associated molecules that have evolved in close contact with both benign and pathogenic organisms and environmental factors. This co-evolution has produced a system composed of two primary branches – the innate and adaptive arms, each with their own humoral and cellular components. Through extensive communication with one another, the innate and adaptive arms mount appropriate and effective immune responses to combat pathogen invasion and tumor growth and development.

Innate immune mechanisms rely primarily on the recognition of certain pathogen or danger-associated molecular patterns, and include physical barriers such as the skin and mucosa. Innate immunity comprises a wide range of humoral and cell-mediated defenses including phagocytes and natural killer (NK) cells, other hematopoietic cells from the myeloid lineage, and humoral components such as interferons, antimicrobial peptides, lysozymes, and complement. Together, components of the innate arm provide a rapid, general immune response that represents the first line of defense against invading pathogens.

Unlike the innate arm that controls pathogens through pattern recognition, the adaptive immune response has evolved to recognize a variety of individual antigens,

providing specificity and importantly, long-term memory in response to pathogen invasion. Key players during an adaptive immune response include B lymphocytes, which make up the humoral component of the adaptive arm via the production of immunoglobulins, and T lymphocytes, which provide cell-mediated immunity. T lymphocytes can be further divided into cells that express either the CD4 or the CD8 receptor on their surface. CD4+ T lymphocytes function mostly as T helper (T_H) cells, while CD8+ T cells function primarily as cytotoxic T lymphocytes (CTLs). CD4+ cells have an important role in orchestrating the adaptive immune response through cross talk with B lymphocytes and the production of cytokines that influence a wide variety of immune and non-immune cells both locally and systemically. In contrast, CD8+ T lymphocytes acquire cytolytic function and are primarily responsible for the elimination of cells infected with intracellular pathogens and tumorigenic cells through direct cell:cell interactions, in addition to cytokine production. Although a successful outcome to pathogen invasion usually requires a fully integrated response that includes optimal responses from B cells, T_H cells, and CTLs, this thesis will primarily focus on the mechanisms important for proper CTL effector function and the defects that are associated with genetic disorders that affect the functionality of this lymphocyte subset.

1.3 T lymphocytes

The T cell receptor complex

Antigen receptors are the means through which T lymphocytes recognize antigen on the surface of neighboring cells. Surface antigens generally take the form of short peptides derived from proteins being degraded through normal processes in a cell, intracellular pathogens replicating within the cell, or pathogens that have been internalized from extracellular space. However, no matter where a peptide is derived from, a T cell primarily recognizes antigen through the interaction of its T cell receptor (TCR) and that peptide in the context of specialized glycoproteins called Major Histocompatibility Complex (MHC) molecules. There are two classes of MHC molecules: class I (MHCI) and class II (MHCII), which differ in their structure as well as their expression pattern in tissues. The TCR of CD8+ cells sees antigen in the context of MHCI, which is expressed on virtually all nucleated cells in the body. This TCR:MHCI interaction allows CD8+ T lymphocytes that have acquired cytolytic activity to probe the surface of any MHCI-expressing cell, allowing cytolysis of virally infected or tumorigenic targets.

The polypeptide chains of αβ TCRs each consist of an extracellular amino-terminal variable region that together make up the single antigen-binding site, a constant region, and stalk segments that contain a cysteine residue through which a disulfide bond forms to link the two chains together. Unlike its extracellular domain, the cytoplasmic tails of the TCR are quite short, each chain consisting of only five amino acids. Even early on, this suggested to researchers that the α and β chains were not sufficient to mediate signaling in T cells on their own and that additional components were required. Additional evidence for this came when cells transfected with cDNA encoding the α and β chains did not display heterodimers at the surface

[2], implying that additional molecules were needed for trafficking as well. It wasn't until the 1990s that these components began to be better characterized; the transmembrane molecules we now know as the CD3 complex and the ζ chain. The CD3 complex consists the CD3γ, CD3δ, and two CD3ε chains (reviewed in [3, 4]). All three of the CD3 proteins have an extracellular immunoglobulin-like domain, and an intracellular domain with a single immunoreceptor tyrosine-based activation motif (ITAM) consisting two tyrosines with conserved spacing and charges. The δ chain on the other hand, has a short extracellular region and three ITAMs on its intracellular domain; all are critical for TCR signal propagation. In its mature form, the TCR complex consists of the antigen-binding αβ TCR heterodimer associated with four signaling chains; the α chain with a CD3ε:CD3δ heterodimer and the β chain with a CD3ε:CD3γ heterodimer. Assembly of the TCR complex occurs in the endoplasmic reticulum, thus ensuring that receptors that are expressed on the surface of cells are fully functional signaling complexes (reviewed in [5]).

T cell receptor signal transduction

When a TCR is engaged by peptide-MHC (pMHC), a signaling cascade begins with the phosphorylation of ITAMs in the cytoplasmic tail of the CD3:ζ complex. Phosphorylation of these tyrosine motifs is primarily mediated by the Src family kinase LCK that is constitutively associated with the CD4 and CD8 co-receptors, and is activated in response to TCR engagement. Phosphorylation of the multiple ITAMs in the CD3:ζ complex by LCK generates a binding site for ζ chain-

associated protein (ZAP-70) through its two Src homology-2 (SH2) phosphotyrosine-binding domains. Once recruited to the CD3:ζ complex, ZAP-70 is phosphorylated and activated, allowing it in turn to phosphorylate conserved tyrosines on two important scaffold proteins: linker of activated T cells (LAT), and SH2 domain-containing leukocyte phosphoprotein of 76kDa (SLP-76). Formation of the LAT:SLP-76 complex following TCR engagement is the critical first step during T cell activation. These two proteins form a complex with a number of additional SH2 domain-containing proteins that propagate downstream signaling. LAT binds phospholipase Cγ1 (PLCγ1), GRB2, and the GRB2-related adaptor (GADS) which links it to SLP-76. SLP-76 also contains tyrosine residues that promote recruitment and activation of the guanine nucleotide exchange factor (GEF) VAV1, the adaptor protein NCK, and the Tec family tyrosine kinase, Inducible T cell kinase (ITK).

One of the most important proximal steps in TCR signaling is the recruitment and full activation of PLCγ1 to the TCR complex at the plasma membrane. Recruitment of PLCγ1 is facilitated by both protein:protein interactions with the LAT:SLP-76 complex, and the binding of its Pleckstrin homology (PH) domain to phosphatidylinositol 3,4,5-triphosphate (PIP_3), a product of the phosphorylation of phosphatidylinositol 4,5-biphosphate (PIP_2) by phosphoinositide 3-kinase (PI3K). PLCγ1 activity is critical for T cell function because it cleaves PIP_2 to generate two major second messengers during TCR signaling: inositol triphosphate (IP_3) and diacylglycerol (DAG). Both products of PLCγ1 activity influence short-term cytoskeletal and long-term transcriptional changes in the cell through the initiation of calcium flux and the nucleation of downstream signaling.

Full activation of PLCγ1 requires phosphorylation by ITK, whose role in CD8+ T cell function will be the focus of chapter 2 in this thesis. ITK is recruited to the plasma membrane both via interactions of its PH domain with phospholipids, including PIP_3 [6], and interactions with the LAT:SLP-76 complex via its SH2 and SH3 domains (reviewed in [7, 8]). ITK is activated by protein interactions with SLP-76 and phosphorylation on its activation loop by LCK. Once activated, ITK phosphorylates Y783 on PLCγ1 to fully activate its primary substrate [9, 10]. However, it is essential to note that despite the importance of PLCγ1 activation by ITK during TCR triggering, the absence of ITK does not completely abrogate TCR signaling or Ca^{2+} flux. Instead, ITK-deficiency leads to impaired downstream signaling resulting in altered development and differentiation of the T cell lineages [11-13]. For that reason, ITK is thought of as an amplifier, or modulator, of TCR signaling (reviewed in [14]). The redundant mechanisms in place for PLCγ1 activation are not fully understood, but may involve other kinases such as LCK, ZAP-70, or the Tec family member Resting Lymphocyte Kinase (RLK), as evidenced by more significant defects in T cell activation in *Itk*$^{-/-}$*Rlk*$^{-/-}$ mice when compared with ITK single knockouts (reviewed in [7]). Because of the graded nature of these signaling defects, mice deficient in Tec family kinases have been used as a model for understanding suboptimal signaling through the TCR.

The activation of PLCγ1 by ITK leads to PIP_2 hydrolysis, which generates DAG and IP_3, two of the major secondary messengers in TCR signaling. IP_3 binds IP_3 receptors (IP_3R) on the plasma membrane of the endoplasmic reticulum (ER) and perhaps other intracellular organelles, which induces Ca^{2+} release from ER

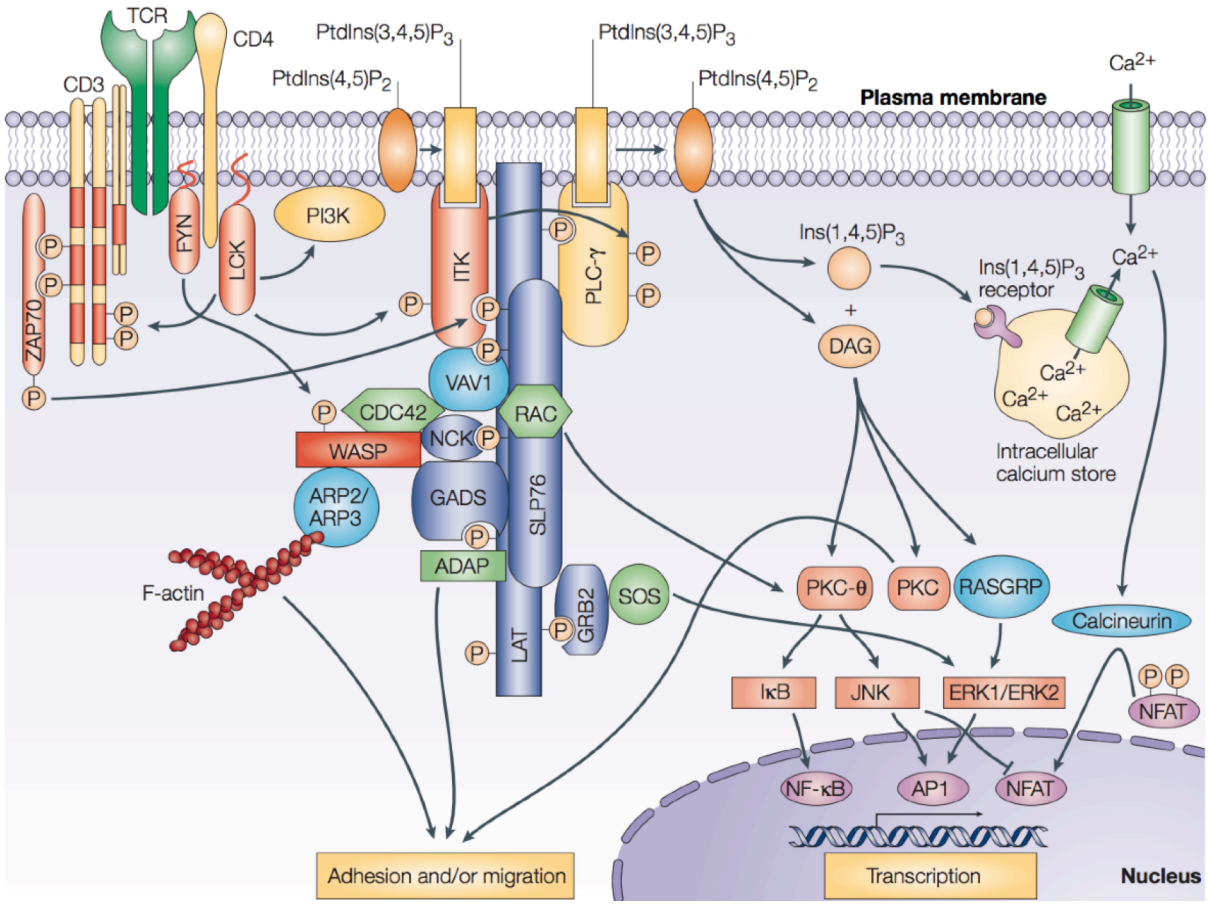

Figure 1.3.1: T cell receptor signal transduction. T cell receptor (TCR) engagement by peptide:MHC leads to the phosphorylation of ITAMs in the cytoplasmic tails of CD3 and ζ chains by LCK. ZAP-70-mediated phosphorylation of LAT leads to the assembly of a signaling complex that includes proteins such as SLP-76, PI3K, and PLCγ1, among others. PI3K phosphorylates PIP_2 to generate PIP_3, which acts as a docking site for PH-domain containing proteins. PLCγ1 is fully activated following phosphorylation by ITK, and cleaves PIP_2 to generate DAG and IP_3. DAG activates RASGRP and members of the PKC family, which go on to activate MAPKs that directly affect transcription. IP_3 triggers Ca^{2+} release from ER stores, increasing cytosolic calcium concentration. VAV1 recruitment to the LAT:SLP-76 complex activates CDC42, which enhances WASP activity through its interaction with NCK. Activation of WASP results to recruitment of ARP2/3, leading to actin polymerization controlling adhesion, polarization, and cell motility. Reproduced from [7].

stores into the cytoplasm. Stromal interaction molecules 1 and 2 (STIM1 and STIM2) act as Ca^{2+} sensors in the ER via their N-terminal EF hand motifs located in the ER lumen. Ca^{2+} efflux from the ER causes STIM proteins to aggregate in the membrane; this oligomerization in turn triggers sustained store-operated Ca^{2+} entry (SOCE) at the plasma membrane through the calcium release activated channel (CRAC), ORAI1. As a result, the tightly regulated nanomolar-range Ca^{2+} concentration in resting T cells can reach micromolar levels following TCR triggering. This elevated intracellular Ca^{2+} activates several Ca^{2+}-dependent signaling proteins and their target transcription factors. These include calmodulin and the phosphatase calcineurin, and its major target transcription factor, nuclear factor of activated T cells (NFAT), as well as calmodulin-dependent kinase (CaMK) and its target, cyclic-AMP-responsive element binding protein (CREB) (reviewed in [15]).

Production of DAG at the membrane recruits members of the protein kinase C (PKC) family, such as PKCθ, and Ras guanyl-releasing protein 1 (RASGRP1) via a DAG-binding domain. PKCθ goes on to induce a signaling cascade leading to nuclear translocation of the transcription factor, nuclear factor κB (NF-κB). RASGRP1 recruitment by DAG also in turn activates the small GTPase, RAS. Activation of RAS triggers the mitogen activated kinase (MAPK) cascade, a series of serine/threonine kinases that act directly on a number of transcription factors.

Together, TCR-triggered DAG production and Ca^{2+} flux play pivotal roles in T cell proliferation, differentiation, and effector function. Evidence for this comes from the ability of the pharmacological agents phorbol 12-myristate 13-acetate (PMA), a DAG mimic, and the calcium ionophore, ionomycin, to rescue downstream defects

resulting from suboptimal PLCγ1 signaling [16, 17]. As described, these integrated pathways (among others) can work at the transcriptional level to affect the long-term behavior or even overall identity of a T lymphocyte, but Ca^{2+} flux and DAG production can also have short-term consequences. These include the regulation of lymphocyte polarization, cytoskeletal reorganization, and degranulation, the specific role in CTLs of which will both be discussed in the following chapters.

IL-2 signaling

Although signaling in the context of antigenic responsiveness through the TCR has been extensively studied in T lymphocytes, work in the last decade has greatly expanded our understanding of how T cell activation can be modulated by environmental cues as well. One such example of this is through cytokine receptor signaling. Cytokines are proteins secreted in response to extracellular stimuli. They can act on the cell that produces them, neighboring cells, or even mediate distance effects through transport in blood or lymph, and can have profound effects on gene expression for both development and activation. Although the many different details of cytokine signaling are beyond the scope of this thesis, signaling downstream of the cytokine interleukin-2 (IL-2) in particular is worth briefly mentioning because of its influence on the differentiation, overall function, and homeostasis in virtually all T cell subsets.

IL-2 is produced and secreted by T cells, activated dendritic cells, and B cells. The cytokine signals through a trimeric receptor composed of the common cytokine

γ_c chain, the IL-2Rβ (CD122), and the IL2Rα (CD25) subunit. IL-2 signaling induces transcription of a variety of target genes, including its own high-affinity receptor subunit, CD25, through the Janus kinase (JAK) and signal transducer and activator of transcription (STAT) (specifically JAK3 and STAT5), PI3K/AKT, and the MAPK pathways (reviewed in [18] and [18]). Many studies have shown the particular importance of IL-2 for the generation of effective CD8+ T cell responses. For example, the expansion of CD8+ T cells in *Il2*$^{-/-}$ mice in response to acute viral infection is approximately three-fold lower than in WT controls, leading to impaired viral clearance by CTLs [19]. Additionally, persistent PI3K and STAT5 signaling through the IL-2R are required for the expression of perforin, granzyme B, and interferon γ (IFNγ) during the generation of CTLs [20]. Collectively, these data indicate that in addition to the TCR, the strength and duration of IL-2 signaling can modulate primary expansion in response to antigen stimulation and the generation of CTL effectors. While exactly how and where IL-2 signaling pathways converge with the TCR downstream of engagement is still under intense investigation, a recent elegant study demonstrated that the PI3K and AKT have an important role in integrating antigen and cytokine responses in CD8+ T lymphocytes [21]. Further work on how IL-2 can modulate TCR signaling and T lymphocyte function will not only help us better understand the mechanisms required for an effective immune response, but may also have clinical implications.

1.4 CD8+ T lymphocyte differentiation into CTLs

In order to become effector CTLs with the capacity to kill targets in a granule-mediated fashion, naïve CD8+ T cells must be activated through their TCR in conjunction with co-stimulatory signals and IL-2, a process that can take up to six days in culture, although it occurs more rapidly *in vivo*. The combination of receptor-specific stimulation and co-stimulation induces rapid clonal cell division and protein synthesis to generate a population of activated antigen-specific CD8+ T cells, CTLs, which express cytotoxic proteins such as perforin and the serine-proteases known as granzymes that upon secretion are capable of inducing death in target cells.

The energy demands of activation of naïve CD8+ T cells require the upregulation of nutrient and amino acid transporters and the transcription of genes important for protein and lipid synthesis. One key regulator of genes important for metabolic programming is mammalian target of Rapamycin (mTOR), a serine/threonine kinase located on lysosomal membranes. MTOR is activated by the PI3K/AKT axis and nutrient cues, and integrates signals from the environment to promote survival and differentiation in T cells. Phosphorylation of S6 kinase (S6K) by mTOR leads to increased protein synthesis and activates both MYC and hypoxia inducible factor 1α (HIF1α), which in turn promote expression of genes involved in glucose uptake and glycolysis (reviewed in [22]). In CD8+ T cells, activated mTOR and HIF1α are required for the expression of perforin and granzymes during differentiation, while not affecting the expression of FasL and IFNγ [23]. Thus in addition to activation downstream of the TCR and IL-2, co-stimulatory molecule–mediated activation of mTOR also controls a diverse transcriptional program that

regulates both the metabolic reprogramming required for clonal expansion, and the expression of specific effectors during CD8+ T cell differentiation.

In addition to TCR-induced NFκB and NFAT activation that help promote survival and differentiation of CD8+ T cells, TCR:MHC interactions in conjunction with cytokine signaling also affect the induction of the transcription factors T-BET and Eomesodermin (EOMES) [24, 25]. These factors modulate genes important for IFNγ production [26] and the expression of perforin and granzymes in CTLs [27-29]. Thus, TCR and cytokine signaling work in concert to activate transcription factors during the generation of CTLs that express the cytolytic proteins critical for their effector function.

1.5 Granule-dependent cytolysis by CTLs

Although CTLs can produce cytokines with cytotoxic capacities and utilize death receptor-mediated pathways to trigger apoptosis in targets, the granule exocytosis model first proposed by Berke in 1975 has now been established as the major pathway of rapid cytolysis by CTLs. Many of the stages of target cytolysis by CTLs have been characterized through the study of rare mutations that cause inherited diseases by affecting cytotoxic function of lymphocytes (Table 1.5.1). Although a number of different phenotypic consequences of defective cytolysis are observed, common themes include an inability to clear viral infections, and fulminant infectious mononucleosis often driven by infection with Epstein-Barr virus (EBV) and other herpes virus family members. In addition, many of these mutations manifest in

Table 1.5.1: Primary immunodeficiencies affecting CTL function

Genetic disorder	Inheritance	Gene	Protein	Function	Stage of cytolysis affected
FHL type 2	AR	*Prf*	Perforin	pore-forming	cytolysis of targets
FHL type 3	AR	*Unc13d*	MUNC13-4	granule priming	secretion
FHL type 4	AR	*Stx11*	Syntaxin 11	granule fusion	secretion
FHL type 5	AR	*STXBP2*	MUNC18-2	granule fusion	secretion
GS2	AR	*Rab27a*	RAB27A	granule fusion	secretion
CHS	AR	*Lyst*	LYST	lysosomal trafficking	granule biogenesis
HPS2	AR	*Ap3b1*	AP3B1	protein sorting	polarization of granules
ITK-deficiency	AR	*Itk*	ITK	TCR signaling	activation, secretion (granule fusion?)
XLP	X-linked	*SH2D1A*	SAP	co-receptor signaling	adhesion and immunological synapse formation
CD27-deficiency	AR	*CD27*	CD27	TNFR signaling	T:B interactions
XMEN	X-linked	*MAGT1*	Mg^{2+} transporter	Mg^{2+} flux	activation of T cells
DOCK8-deficiency	AR	*Dock8*	DOCK8	GEF, actin cytoskeletal rearrangements	normal cytolytic activity, defective trafficking in tissue , immunological synapse formation
Coronin1A-deficiency	AR	*Coro1A*	Coronin1A	actin cytoskeletal rearrangement	T cell trafficking, immunological synapse formation (NK cells)
MST1-deficiency	AR	*Stk4*	serine-threonine kinase 4	activation and survival	activation
PI3K hyper-activation	AR	*p110δ*	PI3K	co-receptor signaling	elevated mTOR signaling, impaired centrosome polarization, survival
LCK-deficiency	AR	*Lck*	LCK	TCR signaling	T cell development and activation, lytic granule convergence in CTLs (LCK OFF)
ORAI1-deficiency	AR	*Orai1*	ORAI1	Ca^{2+} flux	normal thymic development, impaired cytokine/lytic granule
STIM1/2-deficiency	AR	*Stim1, Stim2*	STIM1, STIM2	Ca^{2+} flux	

Table 1.5.1: Primary immunodeficiencies affecting CTL function, continued

Genetic disorder	EBV	Other recurrent infections	Other clinical features	Mouse model
FHL type 2	+	common viral infections, TB	cytopenia, hepatosplenomegaly, lymphoma agammaglobulinemia, fever, HLH	*Prf1-/-*
FHL type 3	+	Herpes, common viral infections		jinx
FHL type 4	+	common viral infections		*Stx11-/-*
FHL type 5	+	Herpes, calcivirus, adenovirus, rotavirus		*Stxbp1-/-*
GS2	+	CMV, adenovirus	hypopigmentation, hepatosplenomegaly, neuro impairment, HLH	ashen
CHS	+	recurrent sinopulmonary infections, skin infections	hepatosplenomegaly, albinism, pancytopenia, leukemia, HLH	beige
HPS2	-	respiratory tract infections, otitis media	hearing loss, albinism	pearl
ITK-deficiency	+	CMV, BK polyoma, CMV, respiratory viral infections	agammaglobulinemia, lymphomas	*Itk-/-*
XLP	+		agammaglobulinemia, lymphomas, HLH	*SH2D1A-/-*
CD27-deficiency	+	None	varied; memory B cell deficiency, malignant lymphoma, HLH	*CD27-/-*
XMEN	+	viral infections	lymphomas	none
DOCK8-deficiency	-	HSV, HPV, MCV, VZ, salmonella enteritis, giardiasis	hyper IgE, carcinoma, cardiac anomalies	*Dock8-/-*
Coronin1A-deficiency	+	VZV, rotavirus	lymphopenia, delayed language and motor development	*Coro1a-/-*
MST1-deficiency	+	HSV, VSV, MCV, HPV, bacterial, Candidal	defective humoral responses, lymphomas, lymphopenia, autoimmune cytopenia, cardiac anomalies	*Stk4-/-*
PI3K hyper-activation	+	CMV	sinopulmonary infections, lymphadenopathy, nodular lymphoid hyperplasia	E1024K (un-published)
LCK-deficiency	-		Lymphopenia	*Lck-/-*, inducible LCK OFF
ORAI1-deficiency	-	bacterial, viral (HSV), fungal	defective calcification, ectodermal dysplasia	*Orai-/-*
STIM1/2-deficiency	-	bacterial, viral (HSV, HHV8), fungal infections	autoimmune cytopenia, Kaposi sarcoma	*Stim1-/-* *Stim2-/-*

patients as lymphoproliferative disorders with Hemophagocytic Lymphohistiocytosis (HLH) or HLH-like syndromes. HLH is a severe disorder characterized by the unchecked expansion of CTLs in which excessive IFNγ production by CTLs leads to the secondary activation of macrophages, their organ infiltration, and secretion of damaging pro-inflammatory cytokines (reviewed in [30]). Thus, HLH symptoms are directly related to the inability of CTLs to control viral infection.

Granule-dependent contact-mediated killing of virally infected cells by CTLs is initiated when the TCR is engaged by antigen in the context of MHCI. Once the TCR is engaged, a signaling cascade is initiated that leads to the cytolysis of target cells through a number of distinct stages. Killing begins with the TCR-triggered adhesion of CTLs to target cells and the rapid accumulation of an actin meshwork at the CTL:target cell interface [31]. Actin then clears to form a ring that marks the periphery of the immunological synapse, the special organization of membrane and signaling proteins that forms in a T cell at the interface between it and its target. Actin clearance is followed by reorientation of the centrosome toward the target cell [32], where it then docks at the plasma membrane [33]. This centrosome polarization is accompanied by the movement of lytic granules toward the docked centrosome along a reorganized microtubule network [33, 34]. Polarized granules then fuse in the secretory domain of the synapse, releasing their lytic contents. The pore-forming activity of perforin allows granzymes to enter the cytoplasm of target cells and initiate cell death [35-38]. Thus, CTLs are able to rapidly and effectively eliminate virally infected targets during the adaptive immune response (Figure 1.5.1). In the following sections, the distinct stages of cytolysis by CTLs will be reviewed.

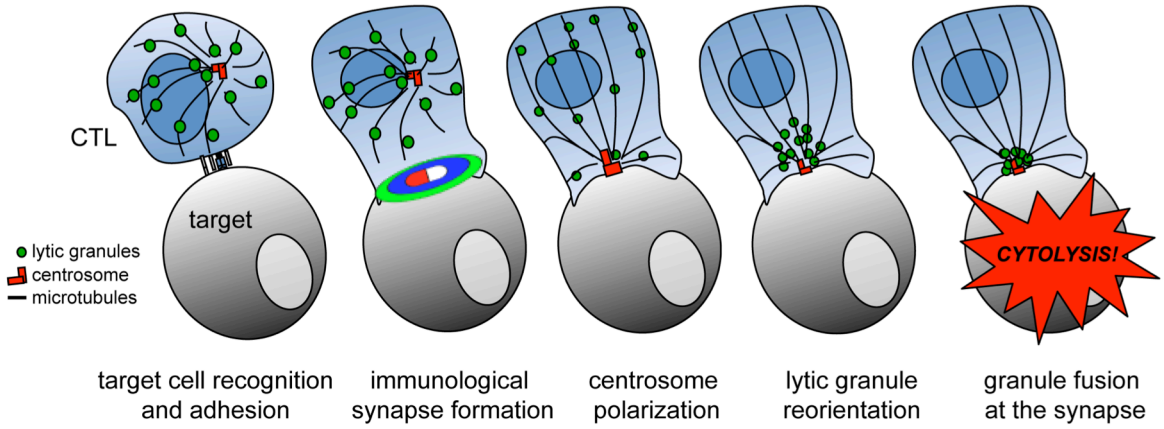

Figure 1.5.1: Stages of cytolysis. Killing by CTLs is initiated when the TCR triggers activation and adherence of CTLs to targets, followed by accumulation of actin at the interface between the T and target cell. Actin clears to form a ring that marks the periphery of the immunological synapse. Immunological synapse formation is followed by polarization of centrosome and lytic granule toward the target cells and finally, fusion of lytic granules at the plasma membrane to induce death in target cells. Figure created by Senta Kapnick.

The immunological synapse

First described as a “small space for the directed secretion of cytokines” [39], the TCR-triggered immunological synapse is a highly organized structure composed of signaling and adhesion molecules, and cytoskeletal components that forms in the T cell at the interface between T and target cells. Early seminal reports using confocal microscopy to examine single cell:cell contacts described a classic bulls-eye patterned contact between CD4+ T cells and antigen-presenting cells (APCs) during antigen-specific interactions. The researchers speculated (correctly) that the spatially segregated components at the synapse, which they called supramolecular activation clusters (SMACs), could determine the effector function and fate of T cells

[40]. In 2001, the Griffiths lab first described the immunological synapse in CTLs. While the overall structure of the synapse was determined to be similar between CD4+ and CD8+ T cells, an additional “secretory domain,” or region near the center of the synapse at which lytic granules fuse with the plasma membrane, was noted [41]. Additionally, compared with the longer-lived, more stable synapses formed between CD4+ T cells and APCs, CTLs have been observed to form shorter-lived, patterned synapses. In support of this, one study showed that formation of a classic bulls-eye synapse is not necessarily required for cytolytic effector function [42]. This suggests that CTL:target interactions may only need to be long enough for the rapid fusion of a few lytic granules, allowing CTLs to move on the next target during an immune response. Thus while immunological synapses form and are grossly similar in both CD4+ and CD8+ T cells, structural and temporal differences may reflect the diverse functions of T cells subsets during an immune response.

The finding that the immunological synapse structure could be recapitulated by stimulation with ligands on lipid bilayers has greatly advanced its molecular dissection [43]. At the center of the synapse is the central (c)SMAC where the TCR, CD28, and other signaling components such as LCK and PKCθ are found. Given the concentration of these molecules in the cSMAC, this area was originally presumed to be a region of TCR signaling initiation and propagation [40, 44]. Work in the early 2000’s in Jurkat cells and an additional CD4+ T cell line showed that TCR signaling initiates the formation of microclusters: micron-sized assemblies of TCR, pMHC, co-receptors, and their associated signal transduction molecules which are sites of tyrosine phosphorylation [44, 45]. Not long after they were identified, signaling

microclusters were observed to form at the periphery of the synapse and precede immunological synapse formation in CD4+ T cells from transgenic mice [46]. Finally, images revealed decreased pY at the synapse [47], supporting the idea that the cSMAC instead represents a site of TCR signaling termination where TCR microclusters are internalized and degraded [46]. Although most of the work examining signaling at the cSMAC has been performed in CD4+ T cells, studies have reported microcluster formation in CD8+ T cells as well [48-50]. However, whether the details of microcluster formation and signaling at the cSMAC differ between CD4+ and CD8+ T cells remains to be seen.

The cSMAC is surrounded by the peripheral (p)SMAC, a ring composed of adhesion molecules and cytoskeletal linkers such as talin. While these molecules facilitate CTL adhesion to their targets, the tight junctions formed in the pSMAC between lymphocyte function associated antigen 1 (LFA-1) molecules and its ligand on target cells, intracellular adhesion marker 1 (ICAM-1), have been proposed to prevent the diffusion of secreted proteins beyond the junction between a T and target cell [39, 51]. In support of this idea, electron microscopy (EM) of CTLs in conjugates with their targets revealed a cleft in the membrane at the synapse [41]. The position of the secretory domain and this synaptic cleft in the center of the pSMAC is believed to concentrate and sequester secreted components of the lytic granules, including perforin and granzymes, in the space between CTLs and their targets, increasing the efficiency of killing and protecting surrounding cells from cytotoxic effectors.

The periphery of the immunological synapse, called the distal (d)SMAC, is marked by a ring of dense, polymerized actin enriched in actin nucleating proteins that maintain the symmetry of the synapse itself. During TCR-triggered actin remodeling, monomeric g actin polymerizes to form filamentous f actin. The instability of small actin oligomers makes spontaneous nucleation of filaments by g actin an unfavorable event [52]. Therefore cells use nucleation-promoting factors (NPFs) at the synapse, such as Wiskott Aldrich syndrome protein (WASp) in T cells, to initiate the formation of new actin filaments. Patients with mutations in WASp develop a primary immunodeficiency associated with defects in T cell differentiation linked to the impaired formation of stable synapses [53]. Once activated by GTPases in a TCR-dependent manner, NPFs induce actin polymerization through the actin

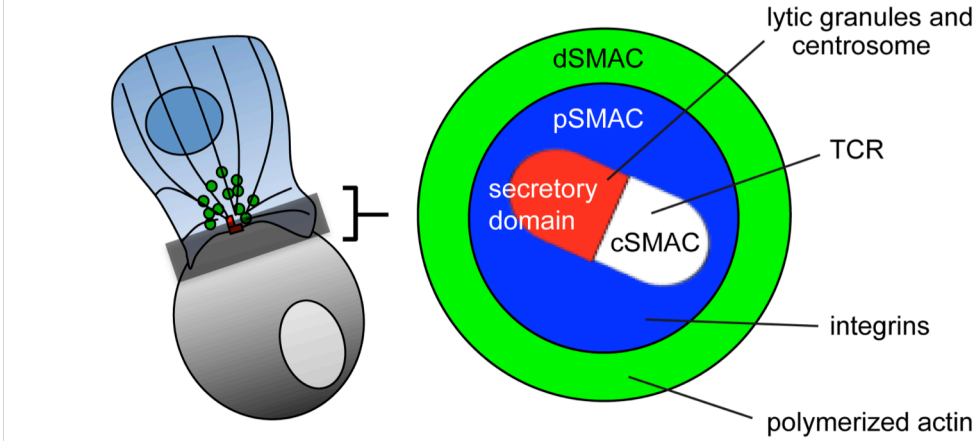

Figure 1.5.2: Schematic of the immunological synapse. The cytolytic immunological synapse is a highly organized, TCR-triggered structure composed of signaling and adhesion molecules, and cytoskeletal components that forms in the T cell at the interface between the CTL and target cell. The dSMAC is a densely polymerized ring of actin that marks the periphery of the synapse. Inside the actin ring is the pSMAC, where integrins such as LFA-1 are found. In the center of the synapse lies the cSMAC, characterized by accumulated TCR bound to MHCI. Adjacent to the cSMAC, and unique to the CTL synapse, is the secretory domain, where the centrosome docks to facilitate the directed secretion of lytic granules. Figure created by Senta Kapnick.

related protein 2/3 (ARP2/3) complex and formins (reviewed in [54], and [55]). ARP2/3 drives polymerization of branched f actin found in the cortex and leading edge of migrating cells. Formins, on the other hand, mediate the formation of unbranched actin filaments. Where knockdown of ARP2/3 in T cells impairs spreading over the surface of APCs, formin-deficiency leads to defective centrosome polarization and cytolytic activity [56].

While TCR-mediated regulation of NPFs at the synapse has received considerable attention, actin-severing factors are also important contributors to synaptic architecture. Patients with mutations in the actin-binding protein, Coronin1a, develop immunodeficiencies with broad susceptibility to viral infections, reminiscent of syndromes associated with defects in CTL and NK function. Indeed, Coronin1A is required for NK cell cytotoxicity, where loss of the protein results in increased f actin density at the synapse associated with decreased secretion [57]. However, the mechanistic understanding of how these proteins contribute to synaptic actin depolymerization is complicated by local conditions in the cell. For example, severing of actin filaments by the actin severing protein, cofilin, could actually increase the availability of g actin monomers. Thus if NPFs are active at the site of depolymerization, actin-severing protein activity could provide the monomeric actin needed for new filament growth.

While questions remain regarding the regulation of synaptic actin architecture, the formation of the dSMAC and subsequent reduction of actin density at the center of the synapse permits the polarization of lytic granules and their secretion toward the target cell [58-60]. For example, actin-binding proteins such as RAS GTPase-

activating-like protein 1 with IQ motifs (IQGAP-1) localize to the dSMAC in CTLs during immunological synapse formation [33]. These proteins tether plus-end microtubules to the actin cytoskeleton, either in conjunction with adaptors [61] or through the recruitment of the cytoskeletal motor dynein [62], suggesting that formation of the dSMAC may also play a role in generating forces that propel the centrosome forward during cytolysis. Thus together, the immunological synapse establishes the zones within which T cell activation and effector function occur.

Polarization of cytolytic machinery

Following formation of the immunological synapse, the centrosome, which is normally located in the uropod of a migrating CTL, reorients toward the target cell and docks at the plasma membrane where cortical actin is reduced. This docking is believed to bring lytic granules close enough to the plasma membrane for degranulation to occur [33]. In T cells, the centrosome is also the microtubule-organizing center (MTOC) and is associated with the Golgi apparatus and other vesicular compartments. Therefore as the centrosome moves toward the synapse, its movement is accompanied by a restructuring of the microtubule cytoskeleton. This establishes polarity in CTLs, and aligns the cellular machinery involved in protein trafficking with the synapse to presumably facilitate the directional secretion during target killing [33]. Centrosome polarization in the context of CTL:target conjugates was first reported over 30 years ago [31, 63-65] but only recently have we begun to understand the molecular mechanisms driving this stage of CTL killing.

Studies using a doxycycline-inducible system to turn off the expression of LCK in mature CTLs [66], and analog-sensitive ZAP-70 mutants allowing for reversible inhibition of ZAP-70 activity [67, 68], established that like CD4+ T cells, centrosome polarization in CTLs is driven by TCR signaling. In the mid-2000s, a new technique was employed that used a photo-activatable pMHC reagent that was turned on when irradiated with ultraviolet (UV) light to control the spatiotemporal activation of T cells, further facilitating the study of pathways linking TCR-triggered responses to cytoskeletal components using microscopy [69]. Although CD4+ T cells were used, Huse and colleagues utilized this technique to show that that PLCγ1 activity was required for MTOC polarization. They went on to demonstrate that local activation of caged DAG using UV irradiation was sufficient to induce transient centrosome polarization in the absence of TCR-triggering. Interestingly, this DAG-driven centrosome polarization occurred in a Ca^{2+}-independent manner, where blocking $Ca2^{+}$ flux using ethylene glycol-bis β-aminoethyl ether-N,N,N',N' tetra acetic acid (EGTA) or 1,2-bis o-aminophenoxy ethane-N,N,N’,N’ tetra acetic acid (BAPTA-AM) had no effect on centrosome reorientation induced in their photo-activatable system [70]. Later work demonstrated that this DAG-dependent polarization led to PKCθ activation and the subsequent recruitment of cytoskeletal motors [62, 71, 72], although only partial defects in centrosome polarization in PKCθ-deficient mice suggest redundant activity in the PKC subfamily [73]. Thus, the full contributions of DAG to centrosome polarization in CTLs are still not fully understood.

Like the centrosome, lytic granules must reorient toward the target cell for directional secretion during killing to occur. This process of lytic granule polarization

is intimately linked to centrosome polarization. A recently published comprehensive study described the convergence of granules at the centrosome prior to its arrival at the synapse during cytolysis of target cells. Thus the centrosome and granules were simultaneously delivered to the synapse in areas of reduced cortical actin [34]. Additional work has showed that unlike centrosome polarization, granule convergence in CTLs is responsive to the strength of TCR signaling [67], although it is not well understood how signal strength controls this stage. In addition, studies of Hermansky-Pudlak syndrome type 2 (HPS2) patients with mutations in the gene encoding the β-3A subunit of the adaptor protein 3 (AP3) complex, important for shuttling cargo from the Golgi to the endosome-lysosomal pathway [74], have revealed a role for AP3 in granule reorientation. AP3-deficient CTLs from HPS2 patients have enlarged granules, and while TCR-triggered centrosome polarization is intact, lytic granules showed an abnormal distribution throughout the cell [75]. CTLs from HPS2 patients have a decreased ability to kill targets [75], emphasizing the importance of granule convergence and polarization for proper CTL function.

Finally, although controversial, there is evidence that the plus-end directed motor protein, kinesin-1, mediates the final delivery of granules to the synapse. In one study, expression of a dominant-negative form of kinesin, or silencing of the motor protein, did not effect centrosome polarization, but transport of lytic granules to the synaptic membrane was inhibited [76].

Lytic granule secretion

Following centrosome and lytic granule reorientation, several steps are still required for the killing of target cells. These include granule docking, priming, and finally, fusion. While there remain a number of questions surrounding the precise mechanisms that regulate lytic granule secretion in CTLs, much of the machinery required for granule fusion has been fairly well characterized through the study of human mutations that affect cytotoxic function of lymphocytes and so cause disease (Table 1.5.1).

Efficient docking of mature lytic granules at the plasma membrane is dependent on RAB27a, a small GTPase critical for vesicle trafficking. RAB27a-deficiency is responsible for Griscelli syndrome in humans [77] and the ashen phenotype in mice [78]. The loss of RAB27a in CTLs results in impaired granule fusion while leaving TCR-mediated centrosome and granule polarization intact [77]. Electron microscopy of both mice and human cells showed that lytic granules from RAB27a-deficient CTLs fail to dock at the plasma membrane [79, 80], offering mechanistic insight into the critical role of this GTPase in granule fusion. RAB27a interacts with effectors such as synaptotagmin-like proteins (SLP)-1 and SLP-2 [81, 82]. SLP1 and SLP2 contain two C2 domains that can interact with vesicle and plasma membrane phospholipids in a Ca^{2+}-dependent manner. While individual knockouts of *Slp1* or *Slp2* do not affect CTL killing, expression of a dominant negative form of SLP2 results in reduced cytolysis of targets associated with impaired degranulation [81, 82]. This suggests that SLP proteins could be involved in tethering to stabilize interactions between lytic granules and the membrane with which they fuse.

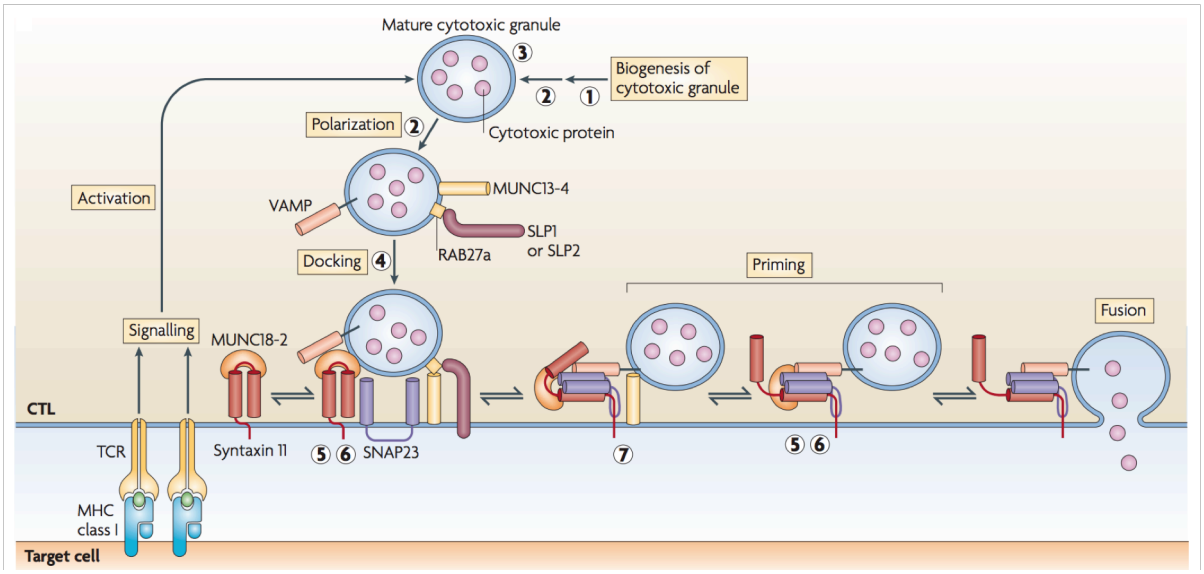

Figure 1.5.3: Lytic granule biogenesis and secretion. Following TCR stimulation and immunological synapse formation, mature granules polarize toward the plasma membrane. Docking occurs via the interaction of vesicle-associated RAB27A with SLP1 or SLP2, and the membrane-associated MUNC18-2 with Syntaxin 11. MUNC13-4 binding to Syntaxin 11 changes it from a closed to open conformation. Priming occurs during formation of SNARE complexes between VAMPs and Syntaxin 11/SNAP23, followed by MUNC18-2-mediated fusion through zippering of SNAREs. Numbers indicate different stages that are impaired in various primary immunodeficiencies: (1) LYST, (2) AP3, (3) perforin, (4) RAB27A, (5) Syntaxin 11, (6) MUNC18-2, and (7) MUNC14-4. Reproduced from [83].

Once lytic granules are tethered to the plasma membrane, vesicle-associated MUNC13-4 proteins prime docking complexes in a Ca^{2+}-dependent manner. Like RAB27a-deficiency, loss of MUNC13-4 leads to defects in lytic granule secretion while other pathways such as IFNγ secretion are unaffected [84, 85]. Lytic granules in CTLs from patients with mutations in MUNC13-4, the cause of the primary immunodeficiency Familial Hemophagocytic Lymphohistiocytosis (FHL) type 3 that has a phenotype indistinguishable from that of perforin deficiency, are able to dock at the plasma membrane although degranulation was significantly impaired [84, 86].

MUNC13-4 mediates lytic granule fusion at the plasma membrane by regulating interactions between vesicle and target-associated soluble N-ethylmaleimide sensitive factor attachment protein receptor (SNARE) proteins. Since only specific combinations of SNARE proteins result in successful membrane fusion, it is thought that SNAREs also confer targeting specificity in cells. Although many related SNARE proteins are expressed in CTLs, it is thought that the MUNC13-4-mediated change in the SNARE protein syntaxin-11 (STX11) from its closed conformation to its open form initiates fusion in CTLs. In its open conformation, STX11 is able to form a SNARE complex with the vesicle-associated membrane proteins (VAMPs) 7 and 8, and synaptosomal-associated protein of 23kDa (SNAP23). The importance of STX11 for CTL killing was demonstrated when CTLs from FHL type 4 patients with mutations in STX11 were shown to exhibit partially impaired lytic granule secretion despite normal centrosome and granule polarization [87, 88]. Interestingly, defects in granule secretion in STX11-deficient NK cells can be partially rescued by IL-2 treatment [88]. This suggests that cytokine signaling can either increase expression of proteins with redundant function, or possibly induce alternative secretory mechanisms in cells.

Finally, SNARE interactions are regulated by the SEC1/MUNC18 family of accessory proteins [89]. Mutations in MUNC18-2 cause FHL type 5, yet another immunodeficiency associated with defective cytotoxic lymphocyte function [90, 91]. MUNC18-2 interacts with STX11 to promote trans-SNARE complex formation, thus facilitating lytic granule fusion at the membrane.

As described, many parts of the machinery required for lytic granule fusion have been characterized. What is not well understood is what exactly triggers vesicle fusion in CTLs, and whether additional proteins provide a layer of regulation beyond those described, as is the case in the neurological synapse. Granzyme release in CTLs has long been considered Ca^{2+}-dependent [92]; chelation of extracellular Ca^{2+} using EGTA or intracellular Ca^{2+} with BAPTA-AM completely abolishes secretion in CTLs. NK cells from ORAI1-deficient patients exhibit defects in granule secretion leading to impaired target lysis [93], emphasizing the importance of Ca^{2+} flux in lymphocyte cytotoxicity. However, while some components of the granule fusion machinery mentioned above contain Ca^{2+}-binding domains, precisely which molecule(s) determine the dependence of granule secretion on Ca^{2+} is still unclear.

One additional series of candidates for Ca^{2+} sensors in CTLs are the synaptotagmins, a family of proteins that bind SNAREs in a calcium-dependent manner [94]. CTLs from OT-I transgenic synaptotagmin VII (SYTVII)-deficient mice exhibit reduced killing of peptide-pulsed targets, although lytic granule secretion was unaffected by the cross-linking of soluble anti-CD3 antibodies [95]. However, unlike the brain-specific synaptotagmin I that functions as a Ca^{2+} sensor for neurotransmitter release [96], SYTVII has a low affinity for Ca^{2+} [97], making the argument for its involvement in Ca^{2+}-mediated granule secretion unclear.

Lastly, early studies using cyclosporine A, an inhibitor of the Ca^{2+}/calmodulin-dependent phosphatase calcineurin, reported reduced granzyme release in murine CTLs [98, 99]. These data provided an additional hypothesis for another molecular

basis of the Ca^{2+} dependence on granule secretion. More extensive work in TALL-104 CTLs, a human leukemic cell line, showed that overexpression of either full-length calcineurin or a mutant Ca^{2+}-independent truncated version augmented granule secretion [100]. Again, they saw no granule secretion in the absence of extracellular calcium, highlighting the importance of Ca^{2+} in the granule fusion process. Although the contribution of calcineurin to granule secretion is established, once again the substrate mediating the effect of calcineurin on granule secretion remains elusive.

1.6 Aims of this thesis

Work in this thesis is aimed towards increasing our understanding of the requirements for proper CTL function through the study of mutants affecting TCR signaling pathways. This work has uncovered a previously unappreciated role for the TCR signaling factor, ITK, in regulating the late stages of CTL killing. A second series of work focused on understanding how the actin cytoskeleton regulates the cessation of secretion in CTLs. It is hoped that these studies provide additional insight into the requirements for cytolysis, and an improved understanding of primary immunodeficiencies associated with impaired CTL function.

In chapter 2, I present work examining the contribution of ITK to CTL effector function using *Itk*$^{-/-}$ mice. I show that the absence of ITK results in a global defect in the killing of target cells by CTLs. Although I found that ITK-deficiency affects differentiation of CD8+ T cells, using pharmacological inhibitors of ITK in WT CTLs, I also present evidence that this defect is associated with impaired lytic granule

secretion, independent of the effects of ITK on CTL differentiation. Lastly, I report that IL-2 can rescue functionality of ITK-deficient CD8+ T cells.

In chapter 3, I characterize the role of the cortical actin cytoskeleton in secretion of lytic granules during target cytolysis. Although previous work has examined the contribution of actin in the initiation of secretion by CTLs, I present data that directly evaluates the role of cortical actin throughout the entire course of CTL:target interactions. Combining specialized microscopy techniques with mouse models of primary immunodeficiencies and pharmacological manipulation, I show a novel role for actin in the termination of cytolysis by CTLs. Additional work presented here implicates PIP_2 as a potential regulator of cortical actin during CTL effector function.

Chapter 2: Inducible T cell kinase regulates expression of cytolytic effectors and degranulation in CD8+ cytotoxic T lymphocytes

2.1 Introduction

Inducible T cell kinase (ITK) is one of five members of the Tec family of non-receptor tyrosine kinases, which are predominantly expressed in hematopoietic cells and are important for lymphocyte signaling [101, 102]. Although three of the five Tec kinase family members are expressed in T cells (ITK, resting lymphocyte kinase (RLK), and Tec), ITK is most highly expressed and has the most clearly defined function. For this reason, ITK is considered to be the predominant family member contributing to T cell development and differentiation.

ITK activity is regulated by localization, phosphorylation, and interaction with adaptor proteins (reviewed in [8]). It is recruited to the plasma membrane by the interaction of its PH domain with IP_4 and PI3K-generated PIP_3 [6, 103]. At the plasma membrane, ITK interacts with the TCR-triggered LAT:SLP-76 complex via its SH2 and SH3 domains [104, 105]. The kinase activity of ITK is activated following phosphorylation of its activation loop by LCK [105-107], leading to the phosphorylation of its major target, PLCγ1. Accordingly, the loss of ITK results in profound impairment of Ca^{2+} flux, leading to significant defects in NFAT activation and other Ca^{2+}-dependent functions in T cells [12, 108]. ITK has also been shown to have a kinase-independent role in TCR signaling, probably due to its function as an adaptor molecule, helping recruit or stabilize interactions of proteins within the LAT:SLP-76 complex, such as the GEF, VAV1. Kinase-deficient mutants rescue the

ability of actin to accumulate at the immunological synapse [109], and activate Serum Response Factor, a transcription factor dependent on cytoskeletal changes for its activation [110] in ITK-deficient cells. Studies on CD4+ T cells from *Itk*$^{-/-}$ mice have shown that suboptimal TCR signaling in the absence of ITK can lead to dramatic effects on T_H cell differentiation, and alter functional T cell outcomes including impaired Type II responses. Some of these defects are secondary to either decreased IL-2 production or altered responses to IL-2 [12, 13, 111-114]. Notably however, these studies have primarily focused on either total T cell or CD4+ T cell populations, leaving the role of ITK in CD8+ T cells less well explored.

As a modulator of TCR signaling and cell differentiation, ITK has been shown to have a role in the control of infection in several disease models. Relevant to CTLs, *Itk*$^{-/-}$ mice can mount protective immune responses against vaccinia virus, vesicular stomatitis virus, and lymphocytic choriomeningitis virus (LCMV) [115, 116]; however, viral clearance is delayed in these studies. While delayed viral clearance may reflect poor activation of CD8+ T cells under conditions of suboptimal TCR signaling, whether or not there were specific defects in granule-mediated cytolysis on a per cell basis has not been examined.

In 2009, the first patients with loss of function mutations in ITK were reported. They exhibited severe fulminant infectious mononucleosis triggered by Epstein Barr virus (EBV) infection [117-119]. EBV is a common Herpes virus family member transmitted through mucosal secretions, notably saliva. Primary infection generally occurs in the pulmonary epithelium, but chronic infection persists in B cells where the virus can enter a latent phase. EBV is best known to cause infectious

mononucleosis, characterized by fatigue, fever, and lymphadenopathy associated with lymphoproliferation in healthy individuals. However, in patients with primary immunodeficiencies, such as ITK-deficient patients, EBV infection can lead to the severe immune dysregulation that manifests as a fatal mononucleosis, Hemophagocytic Lymphohistiocytosis (HLH) or HLH-like syndromes (as previously described), the development of lymphomas, and defective antibody responses. Nine ITK-deficient patients have now been described, some of whom, in addition to high EBV viral loads, present with viral infections including cytomegalovirus (CMV), severe varicella, and respiratory complications due to progressive pulmonary infections (reviewed in [120], see Table 2.1.1).

Together, this clinical phenotype resembles a number of other primary immunodeficiencies (Table 1.5.1 in chapter 1), most notably X-linked lymphoproliferative syndrome (XLP-1), a disease caused by mutations affecting the small adaptor molecule, signaling lymphocyte activation molecule (SLAM)-associated protein (SAP). Our lab has previously shown that CTLs from SAP-deficient mice exhibit specific defects in killing B cells, despite normal cytolysis of other targets [50]. Analogous observations have been made in cells from patients with XLP-1 [121], providing mechanistic insight into the particular inability of SAP-deficient CTLs to kill EBV-infected B cells. The similar clinical phenotypes in ITK-deficiency, and XLP-1, raise the question of whether ITK-deficiency may also specifically affect cytolysis of EBV-infected B cells. Thus, a more complete characterization of the role of ITK in CTL effector function is critical for our understanding of the pathogenesis of ITK-deficiency.

Table 2.1.1: ITK patient information

	patient 1, Turkey	patient 2, Turkey	patient 3, Palestine	patient 4, Palestine	patient 5, Palestine
mutation	R335W (SH2 domain)	R335W (SH2 domain)	Y588X (kinase domain)	Y588X (kinase domain)	Y588X (kinase domain)
gender	female	female	female	male	male
age at diagnosis	5	6	4	5	3
current status	died at age 10	died at age 7	died at age 6	remission after chemotherapy	healthy after HSCT
lymphadenopathy	+	+	+	+	+
hepatosplenomegaly	+	+	+	+	+
defective antibody responses	+	+	+	+	+
pulmonary infections	+	none	none	+	+
histology	B cell LPD, Hodgkin's	B cell LPD, Hodgkin's	Hodgkin's	Hodgkin's	Hodgkin's
autoimmunity	none	none	none	nephritis, thyroiditis	thyroiditis
HLH	none	+	+	none	none
CD8+ T cell numbers	normal	decreased	increased	decreased	normal
EBV status	acute	acute	past infection	acute	n.d.
other infections	BK polyomavirus, *Pneumocystis jirovecii*	n.d.	n.d.	common respiratory viral infections	common respiratory infections
references	Huck, Feyen 2009	Huck, Feyen 2009	Stepensky, Weintraub 2011	Stepensky, Weintraub 2011	Stepensky, Weintraub 2011

ITK patient information, continued

	patient 6, Morocco	patient 7, India	patient 8, Iran	patient 9, Turkey
mutation	R29H (PH domain)	D500T, F501L, M503X (kinase domain)	P157P, R265X (SH3/2 domain)	Q17X (PH domain)
gender	male	female	female	male
age at diagnosis	11	6	14	18
current status	died at age 26	died after HSCT, age 8	died at age 15	unknown
lymphadenopathy	+	+	+	+
hepatosplenomegaly	+	+	+	none
defective antibody responses	+	+		
pulmonary infections	+	+	+	+
histology	B cell LPD	B cell LPD, Hodgkin's, LBL, lymphomatoid granulomatosis	B cell LPD	none
autoimmunity	autoimmune hemolytic anemia	none	none	none
HLH	none	+	none	none
CD8+ T cell numbers	normal	normal	normal	normal
EBV status	past infection	n.d.	n.d.	negative
other infections	CMV in serum and BAF	common respiratory viral infections	n.d.	n.d.
references	Linka, Risse 2012	Linka, Risse 2012	Mansouri, Mahdaviani, 2012	Serwas, Cagdas 2014

Abbreviations**:** BAF, bronchial aspiration fluid; CMV, cytomegalovirus; EBV, Epstein Barr virus; HLH, Hemophagocytic Lymphohistiocytosis; HSCT, hematopoietic stem cell transplantation; LBL, large B cell lymphoma; LPD, lymphoproliferative disorder; n.d., not determined.

Here, we used the OT-I TCR transgenic system to examine the role of ITK specifically in CD8+ T cell cytolytic effector function. We found that ITK was required for efficient killing of multiple different target cells. Surprisingly, examination of discrete stages of CTL function revealed that ITK-deficiency did not affect the early stages of killing, including adhesion to targets and polarization of the centrosome and granules, which were intact in ITK-deficient CTLs. Instead, ITK-deficiency in CTLs was associated with decreased expression of the effector molecules, granzyme B and perforin, combined with defects in degranulation, a late stage of target killing. Impairment of both killing and degranulation could be reproduced by treating WT murine CTLs or activated human CD8+ T cells from healthy donors with an ITK-specific inhibitor during cytolysis assays, suggesting that these defects were not due to altered T cell development or differentiation, and highlighting the effects of ITK on degranulation. Nonetheless, we also found that prolonged incubation with IL-2 rescued these defects, similar to a number of other immunodeficiencies with defective function of cytotoxic lymphocytes. These results suggest that ITK plays a previously unappreciated role in lytic granule secretion during CTL killing, and provide evidence for novel roles for ITK and TCR signaling in regulating late stages of cytolytic activity that may contribute to reduced viral clearance in patients with mutations in ITK.

2.2 Results

ITK-deficient CTLs have impaired cytolytic effector function against targets

Previous studies on the effects of ITK-deficiency on murine CD8+ T cell function revealed both decreased and delayed viral clearance, accompanied by decreased CTL expansion *in vivo* and *in vitro* [115, 116]. However, whether there may be specific defects in cytotoxicity on a per cell basis, and whether there are defects against distinct targets, have not been examined. To evaluate the effects of ITK on CD8+ T cell cytotoxicity, we used the OT-I TCR transgenic mouse model. T cells from OT-I mice express a clonal TCR that recognizes a peptide, $OVA_{257-264}$, derived from the ovalbumin protein in the context of $H2K^b$ [122]. This system allowed us to evaluate killing of different targets presenting the same antigen in a controlled environment, using defined numbers of effectors and targets. Furthermore, although ITK-deficient mice show altered thymic development of CD8+ T cells, expression of the OT-I transgene largely rescues these phenotypes [123].

To generate effector CTLs, splenocytes from WT and ITK-deficient OT-I mice were stimulated *in vitro* with the $OVA_{257-264}$ peptide for three days. Cells were washed and cultured in fresh medium with IL-2, which was changed every 48 hours throughout the duration of the culture. After six days, this culture program generated activated CTLs from naïve CD8+ T cells. To evaluate activation, we examined cell proliferation and surface expression of the TCR and additional surface markers. Consistent with their TCR signaling defects, $Itk^{-/-}$ OT-I CD8+ T cells exhibited delayed proliferation (Figure 2.2.1A) measured by the dilution of the amine reactive dye, Cell Trace Violet (CTV), as well as differences in the initial induction and down-regulation of surface activation markers (Figure 2.2.1B). However, by day six when CTLs were used in functional assays, the mean fluorescence intensity (MFI) of

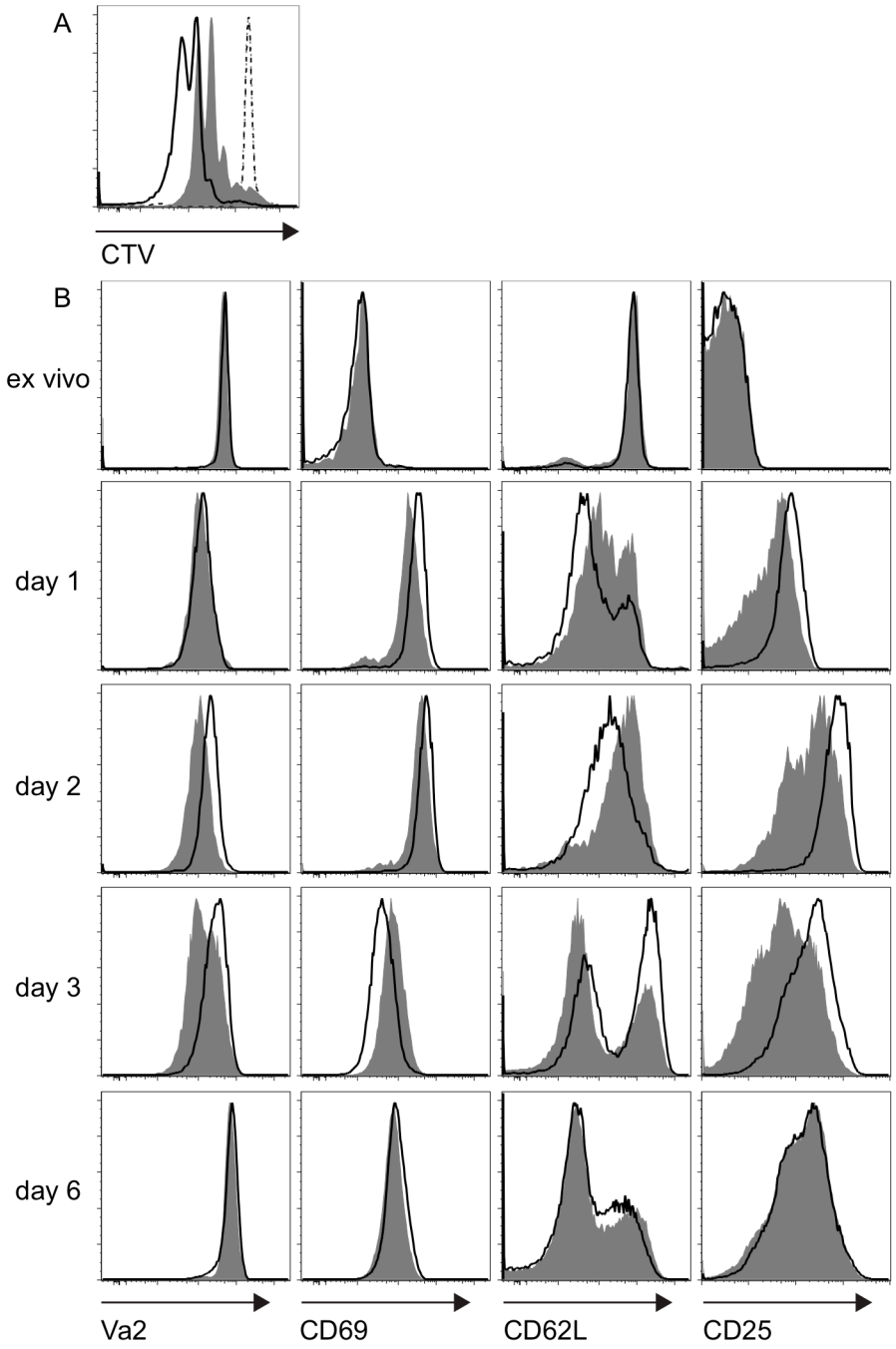

Figure 2.2.1: *in vitro* activation of WT and *Itk*$^{-/-}$ OT-I CD8+ T lymphocytes. (A) Representative histogram of CellTrace Violet (CTV) dilution in WT (black lines) or *Itk*$^{-/-}$ (gray solid) OT-I CD8+ T cells either directly *ex vivo* (dotted lines) or following 48-hour stimulation of whole splenocytes with 10nM $OVA_{257-264}$ (solid lines). (B) Representative histograms of Vα2, CD69, CD62L, and CD25 surface marker staining on WT (black lines) or *Itk*$^{-/-}$ (gray solid) OT-I CD8+ T cells at indicated time points during *in vitro* activation.

markers including Vα2, CD69, and CD25, as well as the percentage of CD62L+ cells, were similar between WT and *Itk*$^{-/-}$ OT-I CD8+ T cells. (Figure 2.2.1B). Therefore, we used day 6-7 stimulated CTLs to compare cytolysis between WT and *Itk*$^{-/-}$ cells.

CTLs from SAP-deficient patients who have phenotypes similar to ITK-deficient patients are unable to kill B cells, despite normal killing of other cellular targets. To evaluate whether *Itk*$^{-/-}$ OT-I CTLs also showed differential killing of targets, we used three target cell types that were pulsed with 1μM of $OVA_{257-264}$ peptide: LPS-activated B cells from WT C57Bl/6 mice, the EL4 thymoma cell line, and the MC57 fibrosarcoma cell line. While *in vitro* activated WT OT-I CTLs could kill WT B cells effectively, CTLs from *Itk*$^{-/-}$ OT-I mice had impaired cytotoxicity against B cell targets (Figure 2.2.2A). However, unlike SAP-deficient CTLs that show defective killing primarily of B cell targets and low-avidity T cell targets [50], ITK-deficient CTLs also failed to efficiently kill both the peptide-pulsed EL4 lymphocyte and MC57 non-

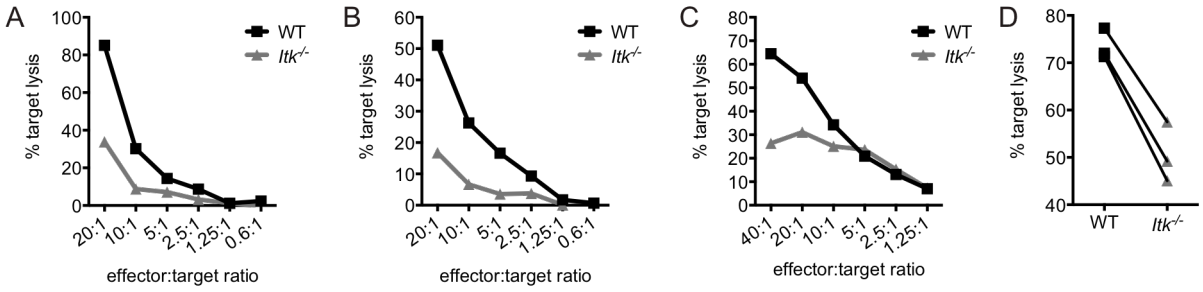

Figure 2.2.2: ITK-deficient CTLs have impaired cytolytic function against targets. *In vitro* cytolysis of (A) LPS-activated WT B cells, (B) EL4, or (C) MC57 targets pulsed with 1μM $OVA_{257-264}$ peptide by WT OT-I (black) or *Itk*$^{-/-}$ OT-I (gray) CTLs at decreasing CTL:target ratios. Graphs show percent target lysis. (D) *In vivo* cytolysis of 1 μM $OVA_{257-264}$ peptide-pulsed LPS activated B cell targets. Each connecting line represents paired mice from an individual experiment.

lymphocyte cell lines (Figure 2.2.2B and C). Defects were also seen in an *in vivo* transfer model; activated CTLs from *Itk*$^{-/-}$ OT-I mice had impaired cytotoxicity against WT C57Bl/6 B cell targets pulsed with $OVA_{257-264}$ peptide when co-transferred into WT C57Bl/6 recipients (Figure 2.2.2D). Together these data suggest that unlike SAP-deficiency, ITK–deficiency leads to a global defect in CTL killing.

ITK-deficient cells show decreased expression of effector molecules

During activation, CD8+ T cells differentiate into CTLs, which express cytolytic effector molecules critical for the cytolysis of target cells. The expression of several of these effector molecules is dependent on IL-2, mTOR, and PI3K-mediated pathways [20, 23]. Our lab recently found that ITK-deficient CD4+ T cells show impaired activation of mTOR, as evidenced by decreased phosphorylation of ribosomal protein S6, which is phosphorylated by S6 Kinase, a direct target of the mTORC1 complex [114]. Similarly, we observed decreased phosphorylation of S6 on the S6K phosphorylation site during early activation of ITK-deficient CD8+ T cells (Figure 2.2.3A). Consistent with reports that mTOR controls a diverse transcriptional program that includes the expression of lytic effector molecules [23], both granzyme B and perforin levels were reduced in *Itk*$^{-/-}$ OT-I CTLs when compared with WT cells (Figure 2.2.3B and C).

To determine whether decreased expression of these effector molecules was the sole cause of reduced cytotoxicity in the absence of ITK, we treated previously

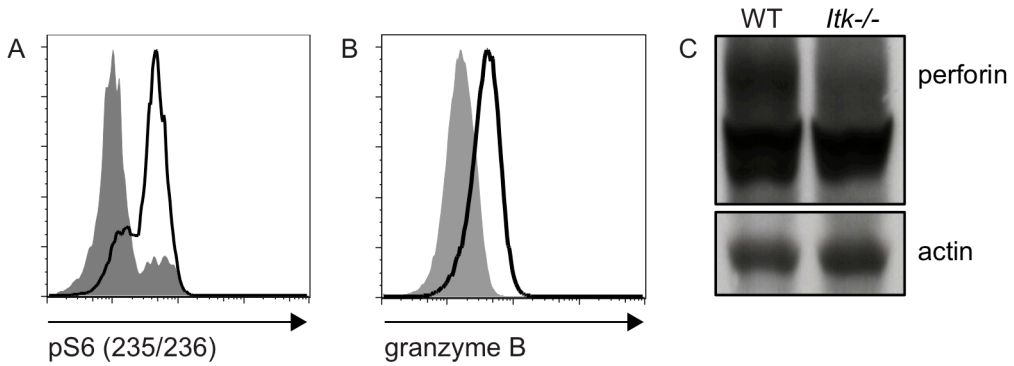

Figure 2.2.3: ITK-deficient CTLs show decreased expression of lytic effector molecules. (A) Whole splenocytes from WT (black) or *Itk*$^{-/-}$ (gray) OT-I CD8+ T cells were activated in the presence of 10nM $OVA_{257-264}$ peptide and stained for pS6 (S235/236) using flow cytometry. Histograms are representative of two independent experiments. (B) Representative histogram of granzyme B expression levels in day 6 *in vitro* activated WT (black, solid line) or *Itk*$^{-/-}$ (gray, solid line) OT-I CTLs. (C) Perforin expression in total lysates from day 7 activated WT and ITK-deficient CD8+ T lymphocytes, probed for perforin and for actin as a loading control. Representative of three independent experiments.

activated WT OT-I CTLs with 10n, an inhibitor of ITK, immediately prior to their use. This treatment allowed for short-term inhibition of ITK during cytolysis, while minimizing non-specific effects that could alter differentiation. Treatment of activated WT CTLs with 10n led to impairments in Ca^{2+} flux comparable to that seen in *Itk*$^{-/-}$ CTLs (Figure 2.2.4A), confirming its ability to reproduce phenotypes associated with loss of ITK activity. Incubation of WT CTLs with 10n during the cytolysis assay reproduced the defects in killing seen in activated ITK-deficient OT-I CTLs (Figure 2.2.4B). Similarly, treatment with 10n of allo-activated human CD8+ T cell blasts generated from healthy peripheral blood mononuclear cell (PBMC) donors also led to impaired killing of P815 targets, a mouse mastocytoma cell line expressing high levels of Fc receptors that can present anti-CD3, making it a target for human CD8+ T cells (Figure 2.2.4C). Thus treatment with the 10n inhibitor leads to similar defects in TCR-triggered responses as in ITK-deficient CD8+ T cells. These data suggest

that while suboptimal TCR signaling in the absence of ITK affects the kinetics of activation and the expression of cytolytic effectors, impaired killing is not fully attributable to altered activation and differentiation of CD8+ T cells.

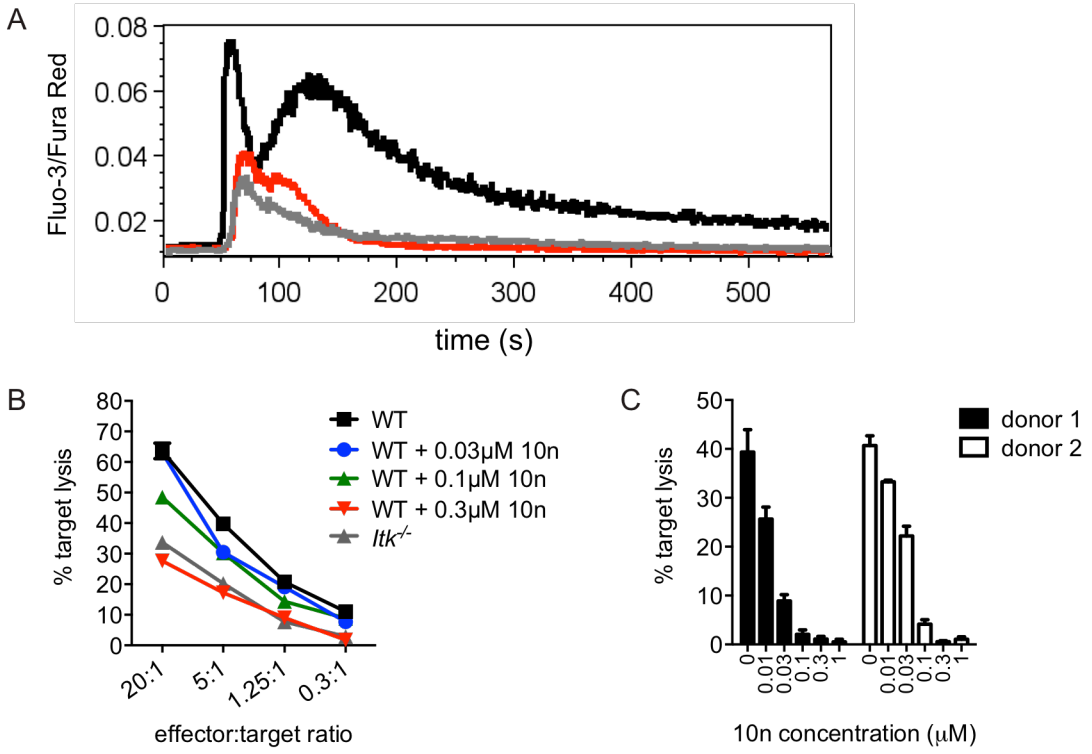

Figure 2.2.4: Pharmacological inhibition of ITK results in impaired killing of target cells. (A) Intracellular Ca^{2+} flux in WT (black), *Itk*$^{-/-}$ (gray), or WT OT-I CTLs treated with 300nM 10n (red) following 5μg/mL anti-CD3 and 10μg/mL anti-CD8 crosslinking, plotted as the ratio of Fluo-3 (FL-1)/FuraRed (FL-3) over time. Histograms are representative of two independent experiments. (B) *In vitro* cytolysis of EL4 targets by previously activated ITK-deficient (gray) or WT OTI CTLs treated with indicated concentrations of the ITK inhibitor, 10n (blue, green, and red) or left untreated as a control (black) at decreasing CTL:target ratios. (C) *In vitro* cytolysis of P815 target cells pulsed with 2μg/mL OKT3 by allo-reactive human CD8+ T cells generated from healthy donors and treated with 10n at indicated concentrations. Graphs show percent target lysis ± SD for each healthy donor at 4-hour time points using 20:1 T:target cell ratio.

Itk$^{-/-}$ CTLs show normal adhesion and actin ring formation

To better understand the roles of ITK and TCR signaling in regulating cytolytic activity, we examined the discrete stages of CTL function in *Itk*$^{-/-}$ cells. Killing by CTLs is initiated when TCR engagement triggers adherence of CTLs to targets. Previous data from our laboratory have shown that ITK-deficient CD4+ T cells have decreased adhesion to B cell targets [124]. Freshly isolated *Itk*$^{-/-}$ OT-I CD8+ T cells also showed decreased adhesion to B cell targets in a flow-based adhesion assay (Figure 2.2.5A). However, once activated, *Itk*$^{-/-}$ OT-I CTLs formed conjugates with peptide-pulsed LPS-activated WT B cell targets (Figure 2.2.5B) or EL4 targets (Figure 2.2.5C) as well as WT CTLs. These results suggest that once CTLs are generated, an impairment in adhesion does not likely contribute to defects in killing by *Itk*$^{-/-}$ CTLs.

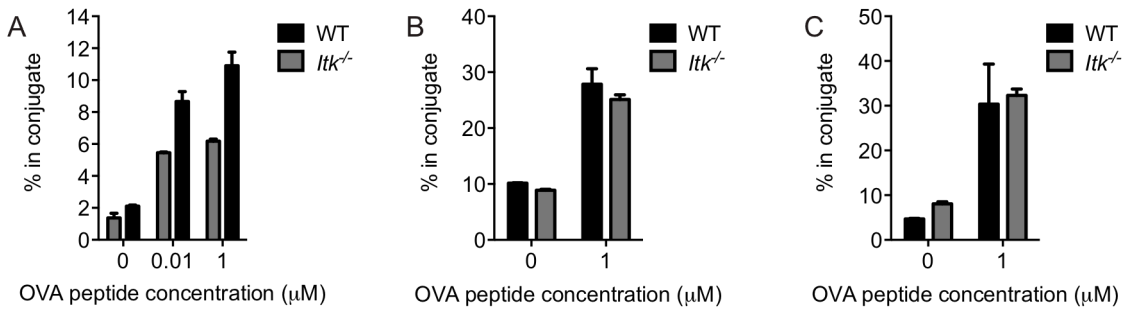

Figure 2.2.5: Activated ITK-deficient CTLs adhere normally to target cells. (A) Adhesion of *ex vivo* WT (black) or *Itk*$^{-/-}$ (gray) OT-I CD8+ T cells to LPS-activated WT B cells not pulsed or pulsed with $OVA_{257-264}$ peptide at indicated concentrations. Adhesion of previously activated WT (black) or *Itk*$^{-/-}$ (gray) CTLs to (B) LPS-activated WT B cells or (C) EL4 cells pulsed with 1μM $OVA_{257-264}$, or not pulsed as a control. Conjugation was performed at 1:2 T:target cell ratios for 20 minutes. Bars represent mean ± SD of the percent of CD8+ target+ cells in the CD8+ gate.

Following adhesion, an actin-rich meshwork accumulates at the interface between T and target cells. Actin then rapidly clears from the center of the synapse to form an enriched actin ring that marks the periphery of the immunological synapse [40, 41]. This central clearing is thought to be important for centrosome polarization and lytic granule reorientation toward the target cell [33, 34, 41]. Previous work has shown that ITK-deficient CD4+ T cells or Jurkat cells treated with siRNA to ITK have defects in actin polarization [109], likely due to a kinase-independent requirement for ITK in stabilizing SLP76:VAV1 interactions during signaling [109]. To examine actin organization in *Itk*$^{-/-}$ OT-I CTLs, we evaluated actin localization in CTLs by immunofluorescence confocal microscopy. Actin accumulation at the CTL:target interface appeared normal in *Itk*$^{-/-}$ OT-I CTLs (data not shown). The ring-like organization of the actin cytoskeleton as evaluated in 3-dimensional reconstructions, z-stacks turned *en face* (Figure 2.2.6A), also did not differ between WT and *Itk*$^{-/-}$ cells (Figure 2.2.6B and C). This, in combination with their normal adhesion, suggested that once activated, CTLs do not require ITK for the early stages of their interactions with target cells.

Itk$^{-/-}$ CTLs show normal centrosome and lytic granule reorientation during cytolysis of targets

Following immunological synapse formation, the centrosome reorients toward the interface between T and target cells, thus directing lytic granules toward their target for effective killing [33, 34]. Studies suggest that centrosome polarization in T

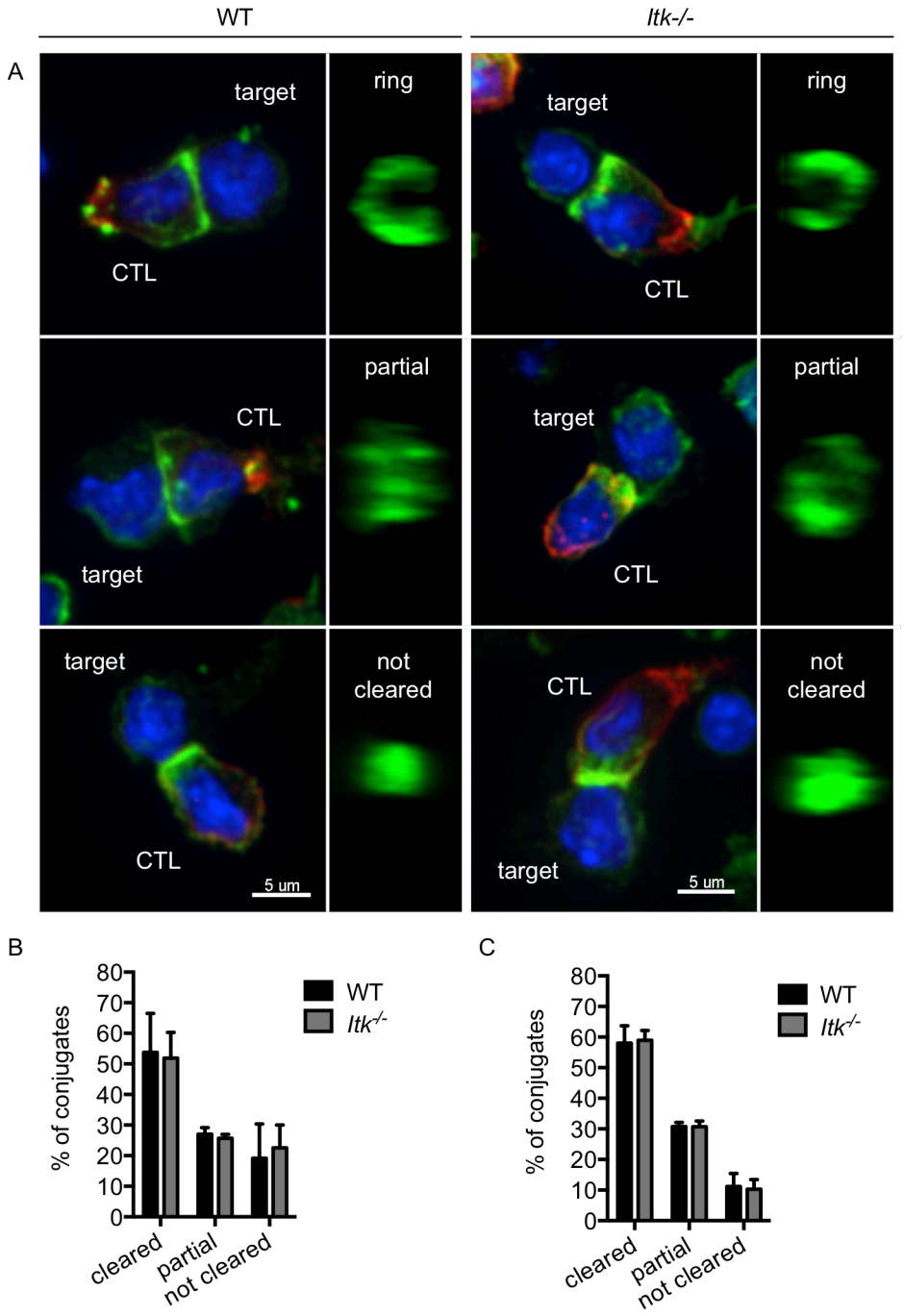

Figure 2.2.6: *Itk*$^{-/-}$ CTLs exhibit normal actin ring formation during immunological synapse formation. (A) Representative images of maximum projections of WT or *Itk*$^{-/-}$ CTLs in conjugate pairs with LPS activated WT B cell targets pulsed with 1μM $OVA_{257-264}$ (first and third columns, respectively). 1μm slice of reconstructed z stacks rotated in the yz plane are included (second and fourth columns). Nuclei (blue), CD8 (red), actin (green). Scale bars = 5μm. Quantification of actin ring localization at the immunological synapse between WT (black) and *Itk*$^{-/-}$ (gray) CTLs and (B) LPS activated WT B cell targets (WT n=105, *Itk*$^{-/-}$ n=82 from 3 independent experiments) or (C) EL4 targets (WT n=185, *Itk*$^{-/-}$ n=194 from 4 independent experiments) pulsed with 1μM $OVA_{257-264}$ peptide.

cells requires PLCγ1 activation, but is a DAG signaling-dependent, calcium-independent process [70]. Because ITK directly phosphorylates PLCγ1, which is responsible for DAG production during TCR signaling, we wanted to evaluate centrosome reorientation and lytic granule polarization in CTL:target conjugates. To examine centrosome polarization, we co-stained for actin and γ-tubulin as a marker for the centrosome (Figure 2.2.7A and B) and examined localization using confocal immunofluorescence microscopy. We found that ITK-deficient CTLs polarized their centrosomes normally in response to peptide-pulsed EL4 targets (Figure 2.2.7C). Nonetheless, consistent with previous reports [13, 71, 108], we found that Ca^{2+} mobilization in response to anti-CD3 stimulation was markedly abnormal in activated CTLs in the absence of ITK (Figure 2.2.4A), suggesting that PLCγ1 activation was still impaired in ITK-deficient CTLs.

The polarization of lytic granules has also been linked to the strength of TCR signaling in the OT-I system, where weak signals generated by low avidity ligands induced centrosome polarization without triggering concomitant lytic granule polarization [67, 125]. These data suggest that the reorientation of the centrosome and polarization of lytic granules can be decoupled under suboptimal TCR-triggering conditions. Although the absence of ITK during TCR engagement also results in suboptimal TCR signaling, we found normal polarization of lytic granules toward the immunological synapse, as evaluated by granzyme B staining of ITK-deficient CTLs in response to peptide-pulsed EL4 targets (Figure 2.2.8A, B, and C). Gross examination of granule convergence also did not reveal obvious defects in the absence of ITK. These results suggest that the impaired killing of targets by OT-I

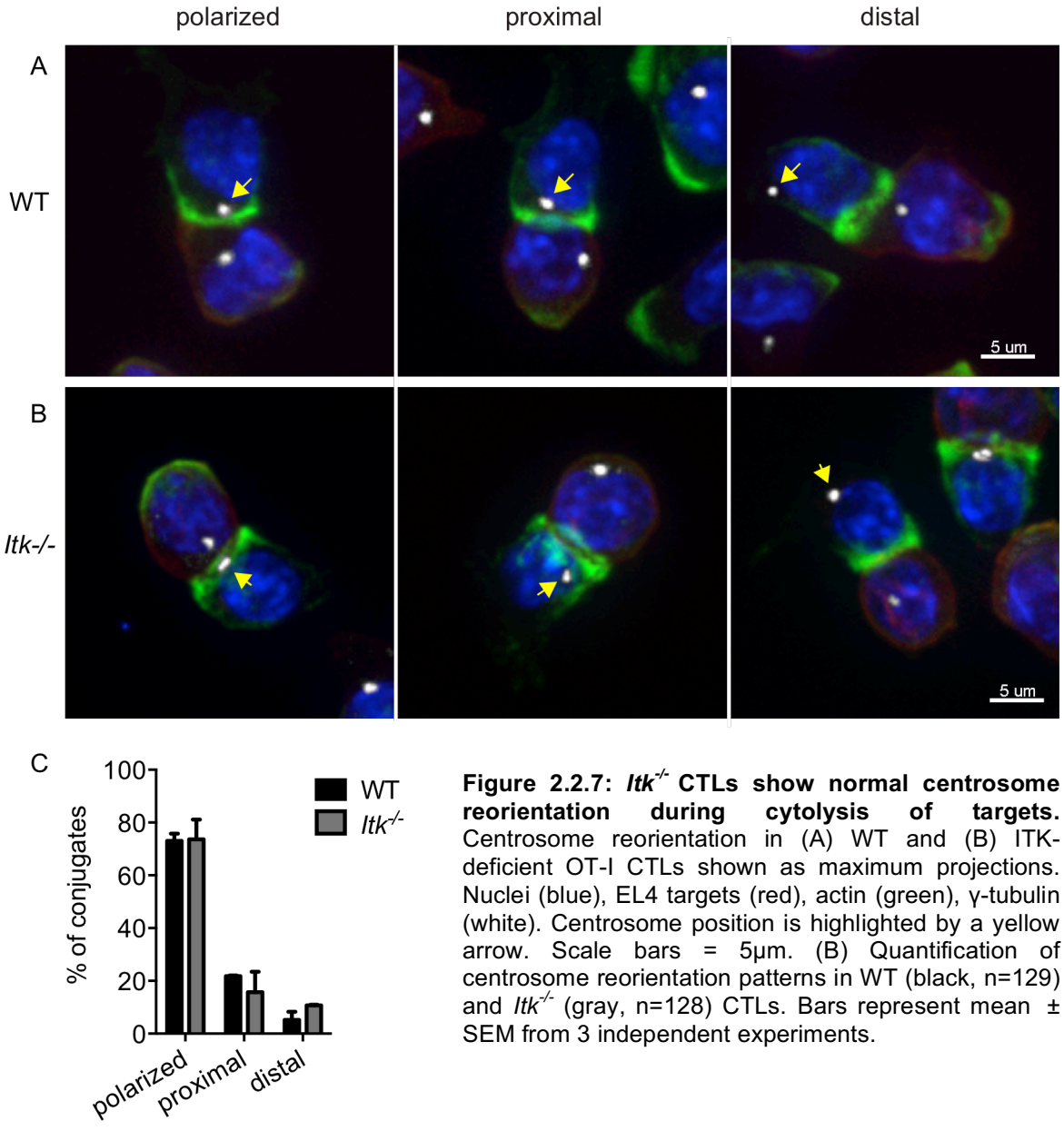

Figure 2.2.7: *Itk*$^{-/-}$ CTLs show normal centrosome reorientation during cytolysis of targets. Centrosome reorientation in (A) WT and (B) ITK-deficient OT-I CTLs shown as maximum projections. Nuclei (blue), EL4 targets (red), actin (green), γ-tubulin (white). Centrosome position is highlighted by a yellow arrow. Scale bars = 5μm. (B) Quantification of centrosome reorientation patterns in WT (black, n=129) and *Itk*$^{-/-}$ (gray, n=128) CTLs. Bars represent mean ± SEM from 3 independent experiments.

CTLs in the absence of ITK does not result from defects in lytic granule reorientation, and that once activated CTLs are generated, ITK is not required for centrosome or lytic granule polarization toward targets, despite defective activation of PLCγ1.

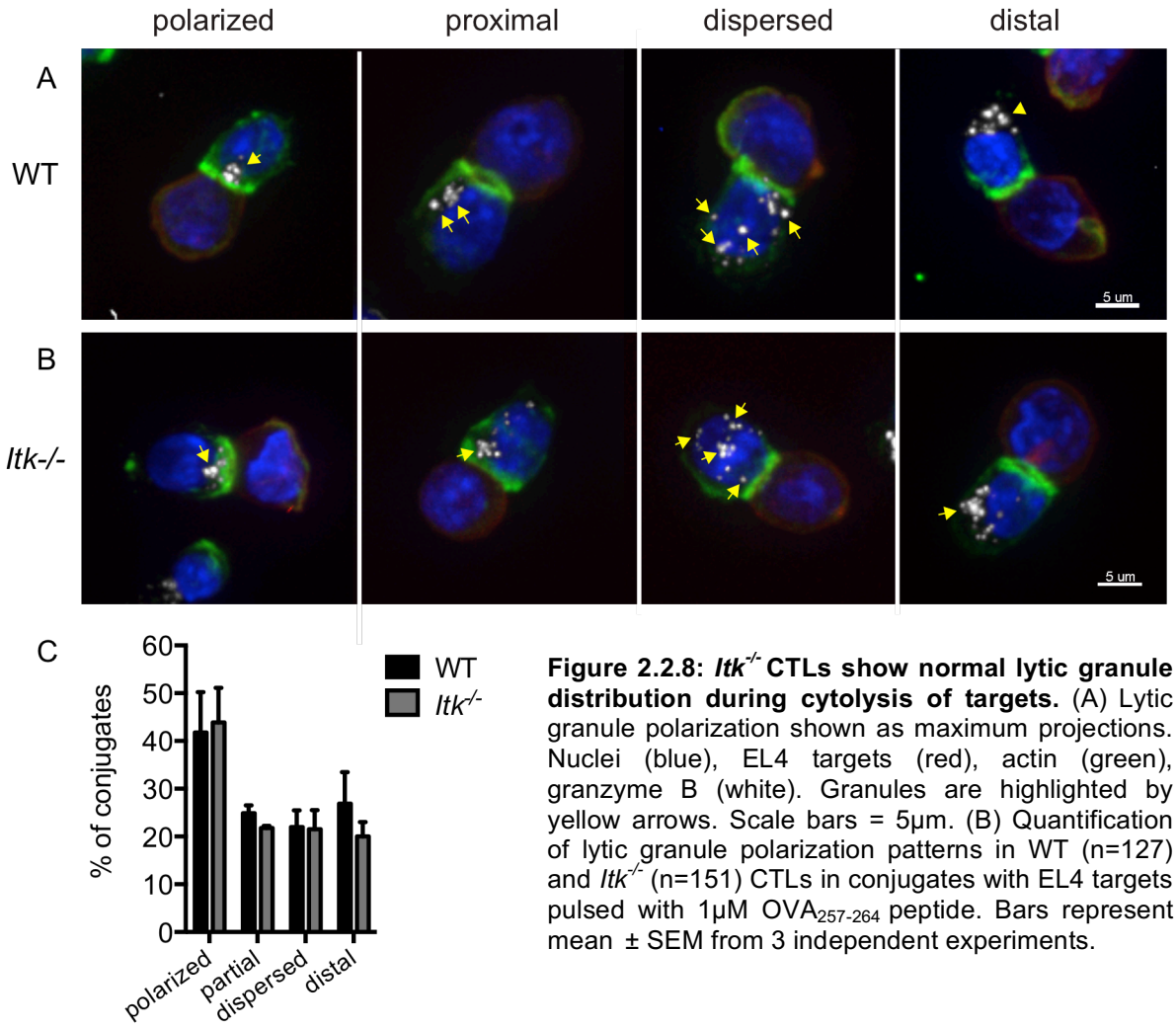

Figure 2.2.8: *Itk*$^{-/-}$ CTLs show normal lytic granule distribution during cytolysis of targets. (A) Lytic granule polarization shown as maximum projections. Nuclei (blue), EL4 targets (red), actin (green), granzyme B (white). Granules are highlighted by yellow arrows. Scale bars = 5μm. (B) Quantification of lytic granule polarization patterns in WT (n=127) and *Itk*$^{-/-}$ (n=151) CTLs in conjugates with EL4 targets pulsed with 1μM $OVA_{257-264}$ peptide. Bars represent mean ± SEM from 3 independent experiments.

TCR-triggered degranulation is reduced in ITK-deficient CTLs

The final stage of granule-dependent killing of target cells by CTLs is the fusion of the lytic granules to release their cytotoxic contents, leading to target cell killing. To evaluate this step, we used a flow-based degranulation assay that measures cycling of lysosomal associated membrane protein 1 (LAMP1) in response to TCR stimulation [126]. LAMP1 is a prominent component of lytic granule

membranes but is found at very low levels on the surface of resting cells. When TCR-engagement triggers fusion of lytic granules at the plasma membrane, LAMP1 is exposed to the surrounding environment where it can be bound by fluorophore-conjugated anti- LAMP1 antibodies in the medium, before being rapidly taken up and recycled. Thus, the accumulation of a fluorescent signal serves as readout for degranulation in CTLs. Using this assay, we found that *Itk*$^{-/-}$ OT-I CTLs exhibited reduced degranulation. Although the extent of this defect was more variable, and less severe, than the defect in cytotoxicity, we observed defective degranulation in response to plate-bound anti-CD3 (Figure 2.2.9A), as well activated targets, including both peptide-pulsed LPS-activated WT B cells (Figure 2.2.9B) and EL4

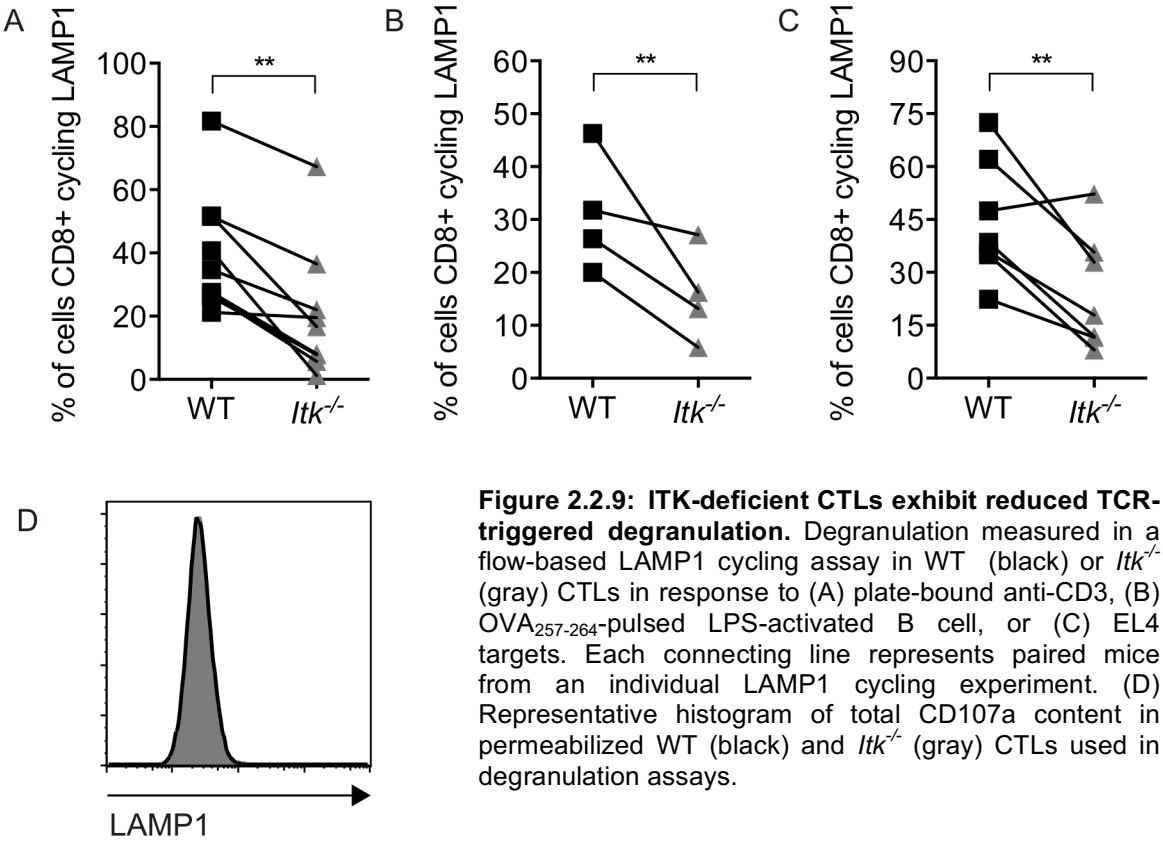

Figure 2.2.9: ITK-deficient CTLs exhibit reduced TCR-triggered degranulation. Degranulation measured in a flow-based LAMP1 cycling assay in WT (black) or *Itk*$^{-/-}$ (gray) CTLs in response to (A) plate-bound anti-CD3, (B) $OVA_{257-264}$-pulsed LPS-activated B cell, or (C) EL4 targets. Each connecting line represents paired mice from an individual LAMP1 cycling experiment. (D) Representative histogram of total CD107a content in permeabilized WT (black) and *Itk*$^{-/-}$ (gray) CTLs used in degranulation assays.

cells (Figure 2.2.9C). Importantly, intracellular staining confirmed that total LAMP1 content was equivalent between WT and ITK-deficient CTLs (Figure 2.2.9D), suggesting that reduced degranulation in the absence of ITK was not due to differences in total LAMP1 levels between WT and ITK-deficient CTLs. To confirm that impaired degranulation by *Itk*$^{-/-}$ CTLs was due to the loss of ITK activity, we again treated previously activated WT OT-I CTLs with increasing concentrations of the ITK-inhibitor, 10n, during LAMP1 cycling assays. Inhibitor treatment of WT CTLs led to reductions in degranulation similar to those seen in *Itk*$^{-/-}$ OT-I CTLs (Figure 2.2.10A). As was the case for *Itk*$^{-/-}$ cells, upstream processes such as adhesion were not affected by the ITK inhibitor (Figure 2.2.10B). Similarly, treatment of allo-activated human CD8+ T cells with 10n also led to impaired degranulation (Figure

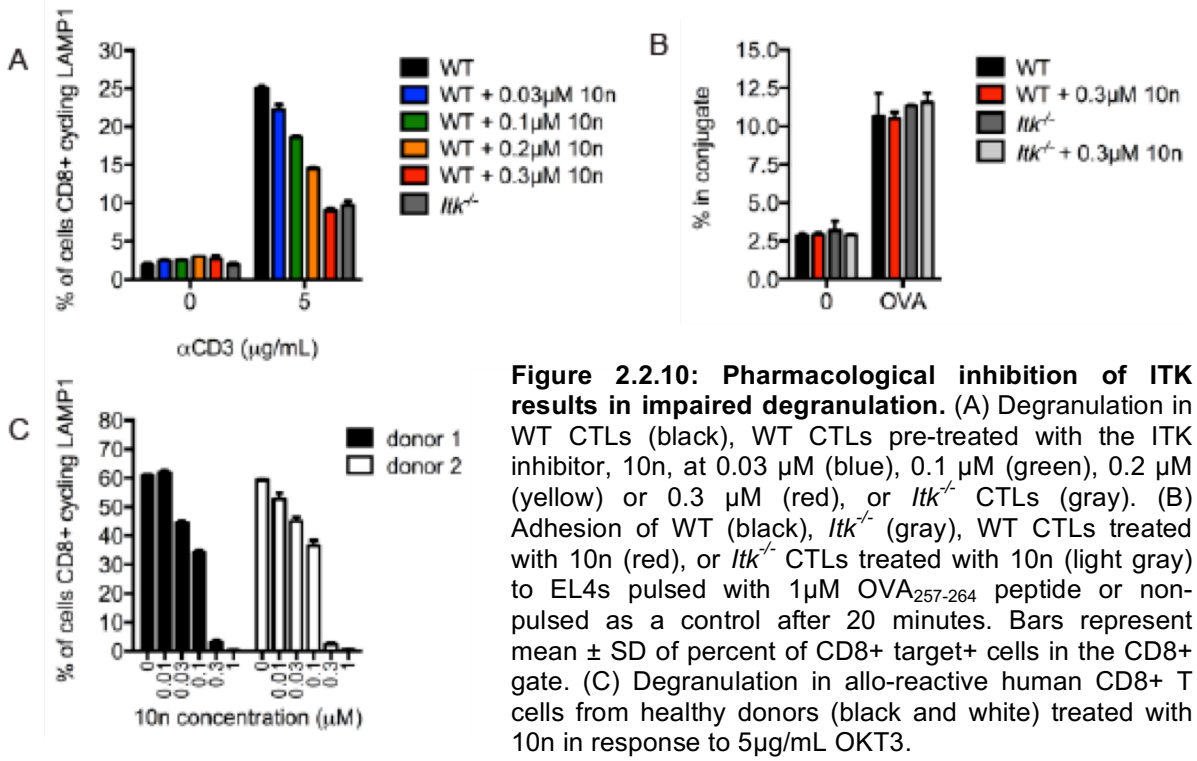

Figure 2.2.10: Pharmacological inhibition of ITK results in impaired degranulation. (A) Degranulation in WT CTLs (black), WT CTLs pre-treated with the ITK inhibitor, 10n, at 0.03 μM (blue), 0.1 μM (green), 0.2 μM (yellow) or 0.3 μM (red), or *Itk*$^{-/-}$ CTLs (gray). (B) Adhesion of WT (black), *Itk*$^{-/-}$ (gray), WT CTLs treated with 10n (red), or *Itk*$^{-/-}$ CTLs treated with 10n (light gray) to EL4s pulsed with 1μM $OVA_{257-264}$ peptide or non-pulsed as a control after 20 minutes. Bars represent mean ± SD of percent of CD8+ target+ cells in the CD8+ gate. (C) Degranulation in allo-reactive human CD8+ T cells from healthy donors (black and white) treated with 10n in response to 5μg/mL OKT3.

2.2.10C). These results suggest that ITK activity plays a previously unappreciated role in lytic granule fusion, the final stage of CTL killing, without affecting upstream events.

Evaluation by electron microscopy reveals subtle differences between the immunological synapses formed by WT and *Itk*$^{-/-}$ cells

In an effort to understand the cellular basis for the reduction in LAMP1 cycling observed in FACS-based secretion assays, we collaborated with Jane Stinchcombe in the Griffiths lab at the Cambridge Institute for Medical Research to closely examine the immunological synapse in WT or ITK-deficient CTL:target conjugates using transmission electron microscopy (TEM). This method provided us with structural information at a resolution that we could not obtain using immunofluorescence techniques.

TEM images revealed that ITK-deficient CTLs formed conjugates and made normal contact sites with targets; secretory clefts indicative of mature immunological synapses were observed in both WT and *Itk*$^{-/-}$ CTL:target conjugates. Polarized centrosomes, organized microtubule networks, and accumulated granules were evident in ITK-deficient CTLs (Figure 2.2.11A), to the same extent as in the WT cells. These EM data are consistent with our observations made using immunofluorescence that centrosome and lytic granule polarization are unaffected by the absence of ITK (Figure 2.2.7C and 2.2.8C).

However, when comparing populations of WT and *Itk*$^{-/-}$ CTLs, our

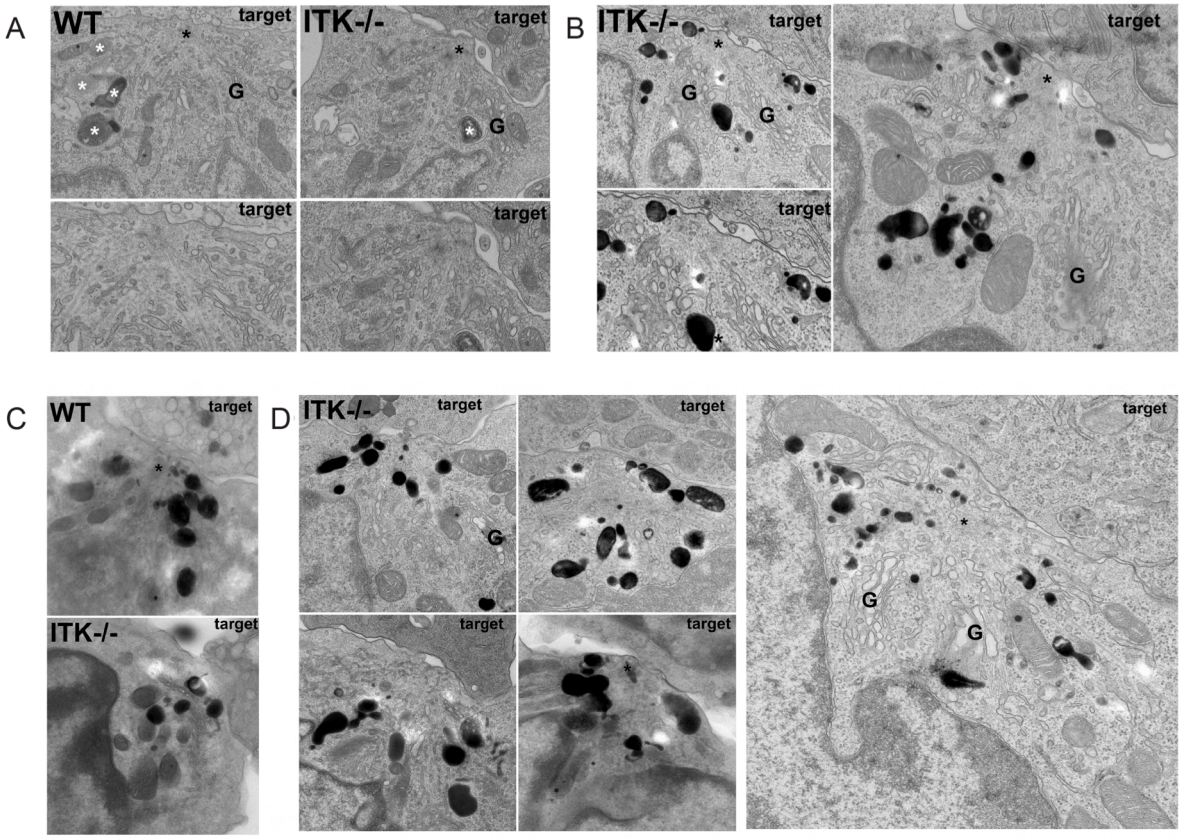

Figure 2.2.11: TEM images of WT or *Itk*$^{-/-}$ CTLs in conjugate with OVA$_{257-264}$ peptide-pulsed EL4 target cells. (A) WT and ITK-deficient CTLs prepared in the absence of HRP. The equivalent organization of the microtubule network from the membrane at the synapse can be seen. Looser contact site and debris in WT CTL:target conjugates can be seen, compared with *Itk*$^{-/-}$ CTL:target pairs. Bottom panels are the same images at higher magnification. (B) *Itk*$^{-/-}$ CTLs only, where the granules are labeled with HRP and microtubule reorganization from tightly polarized centrosome material at the contact site is observed. (C) Thick sections through CTL:target conjugates t provide an overview of organelle behavior in HRP-labeled cells. WT cell (top) shows classic phenotype with polarized centriole, granules, and Golgi. The image of the ITK-deficient CTL (bottom) was taken in the plane to side of the centriole to show granule position. Target in both cases are dying, indicated by vacuolation of the ER. (D) *Itk*$^{-/-}$ CTLs only, representing different profiles of granule polarization to the contact site in ITK-deficient cells. No target cell death noted. Black asterisk, site of centriole baral; white asterisks, lytic granules; G, Golgi apparatus. Images provided by Dr. Jane Stinchcombe.

collaborators also reported some interesting subtle differences that were consistent among three independent experiments. First, a looser contact site between WT CTLs and conjugates was noted, with evidence of released material visible in between the cells membranes. The contact site between ITK-deficient CTLs and targets appeared more flat, or tight, with less material visible between CTLs and targets (Figure 2.2.11A). WT CTLs also showed an organelle polarization that was more focused toward the synapse with fewer granules evident at the contact site (Figure 2.211A, B, C, and D). In WT cells, more of the tightly polarized conjugates were associated with dying targets, as indicated by the presence of apoptotic structures in some targets in TEM images (Figure 2.2.11C). Although dying targets were also observed in some conjugates formed with ITK-deficient CTLs, fewer *Itk*$^{-/-}$ CTLs were associated with apoptotic targets. This observation is consistent with the poorer killing in our *in vitro* cytolysis assays.

Although the differences cited between populations of WT and ITK-deficient CTLs were very subtle and therefore we must take precautions in their interpretation, a noted increase in the accumulation of lytic granules around the centrosome and at the contact site instead of along the membrane suggests that there may be a block in the dissociation of granules from the microtubule network before fusion, or in granule docking.

Total internal reflection fluorescence microscopy visualization of degranulation in WT and ITK-deficient CTLs

To further visualize the degranulation, we used total internal reflection fluorescence (TIRF) microscopy. This imaging technique uses an evanescent wave to only excite fluorescent proteins that are 200 nm from the cell:glass interface, making it particularly suited for examining events that occur at the plasma membrane in cells, such as secretion.

For TIRF imaging, we first crossed the ITK-deficient mice to mice expressing LifeAct-mRuby, a sensor for polymerized actin. However, we found that CTLs from these mice did not express high enough levels of LifeAct to reproducibly image using TIRF. We then proceeded by optimizing double transfections of activated WT and ITK-deficient CTLs with LifeAct-mApple and LAMP1-eGFP constructs. While transfection with LifeAct constructs alone did not dramatically reduce viability in cells when compared with cells that were electroporated in the absence of plasmid, transfection with the LAMP1-eGFP construct significantly affected cell survival (Figure 2.2.12). Since low viability greatly complicates imaging, as dead cells cannot be excluded via gating or other methods, we next moved to a hybrid system that combined transfection with retroviral transduction in order to reduce the cell death

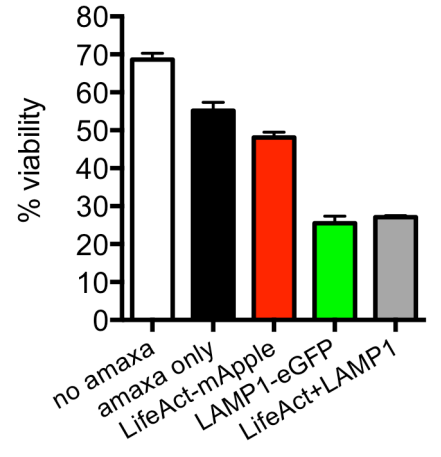

Figure 2.2.12: Viability following transfection with fluorescent constructs. WT CTLs cultured under previously described standard conditions, untransfected, transfected with empty vector, LifeAct-mApple alone, LAMP1-eGFP alone, or co-transfected with LifeAct-mApple and LAMP1-eGFP constructs. Graph shows percent viability ± SD in each group, as determined by the percent of cells in the live gate.

associated with transfection of the LAMP1-eGFP construct. For this method, CTLs were activated for 36 hours, transduced with a LAMP1-eGFP retrovirus, and then cultured in IL-2 for two days before sorting eGFP positive cells. The sorting step also eliminated a problem with interpretation of our TIRF data acquired using doubly-transfected cells; that is, the inability to distinguish between CTLs that did not appear to polarize and/or secrete because they were not expressing LAMP1-eGFP versus those where the absence of LAMP1 fusion in TIRF represented a real biological phenomenon. This was an important consideration, especially since FACS-based degranulation data indicated that the defect we were trying to visualize was partial. After sorting, cells were allowed to recover in culture before transfection with LifeAct-mApple to label actin in the cells, and then imaged the following day. This process required culturing cells for a total of eight days, i.e. six days after the initial addition of IL-2 to media, or three rounds of IL-2 stimulation in total.

Using cells prepared with this transfection/transduction hybrid system, we were able to confirm in TIRF that ITK-deficient cells could form actin rings as well as WT CTLs. Lytic granules were seen moving into the TIRF field, and degranulation was visualized by the diffusion of the eGFP signal into the plasma membrane upon granule fusion (Figure 2.2.13A). However, after six days in culture with IL-2, we found that the percent of cells that degranulated was equivalent between WT and ITK-deficient CTLs (Figure 2.2.13B). While lytic granules could polarize and fuse, there was a slight, albeit statistically insignificant, tendency toward decreased numbers of granules undergoing fusion in the absence of ITK when compared to WT CTLs (Figure 2.2.13C).

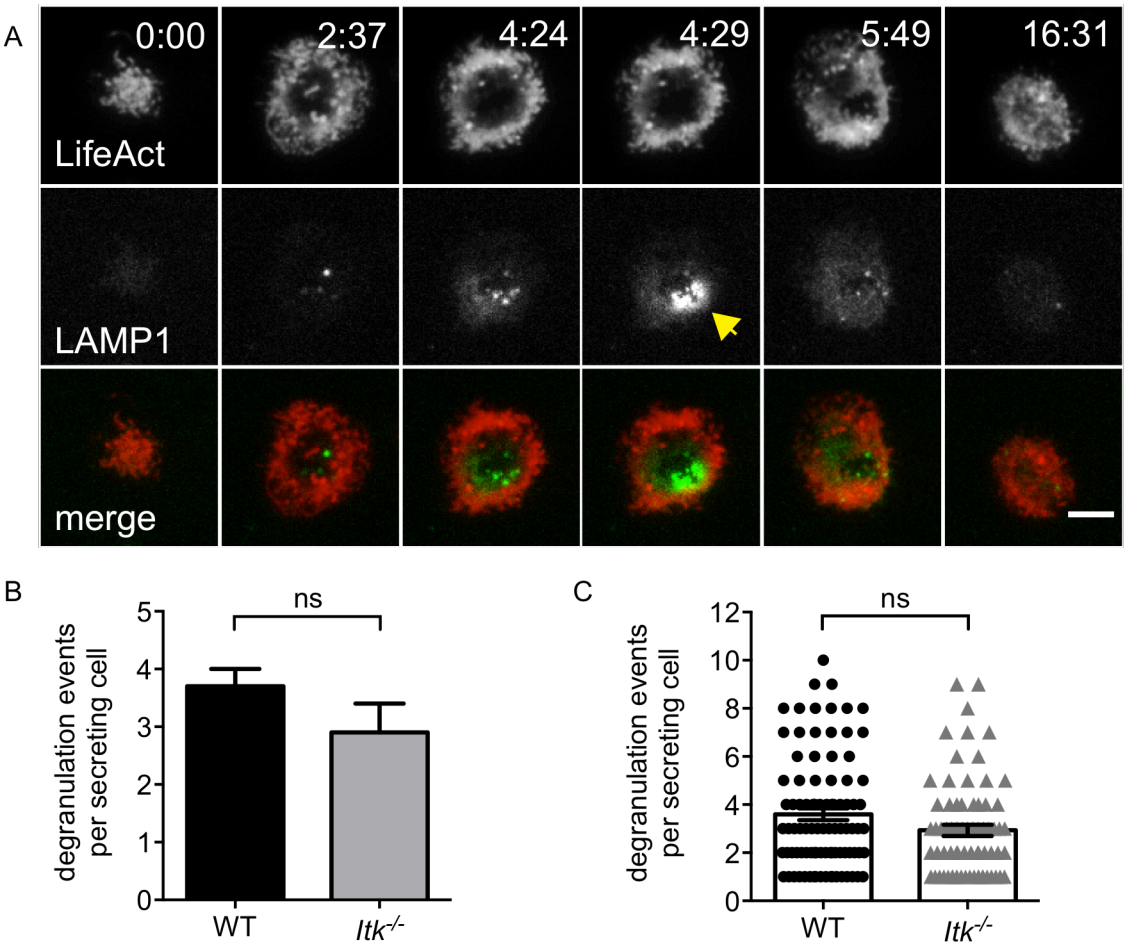

Figure 2.2.13: TIRF imaging of CTLs. (A) TIRF images of a WT CTL expressing LifeAct-mApple (red) and LAMP1-eGFP (green) degranulating on anti-CD3-coated glass surfaces. Top row displays signal from the LifeAct-mApple (561) channel and middle row from the LAMP1-eGFP (488) channel, shown in gray scale. Merged images are shown in bottom row. Degranulation in the middle row is highlighted by a yellow arrowhead. Time shown in minutes:seconds. Scale bar = 5μm. (B) Percent of LAMP1-eGFP-transduced, LifeAct-mApple-transfected WT (black) or *Itk*$^{-/-}$ (gray) OT-I CTLs that degranulated in response to anti-CD3-coated glass surfaces, imaged with TIRF microscopy. Mean ± SEM. WT n=109, *Itk*$^{-/-}$ = 59, from 5 independent experiments. (C) Number of granules that fused in each secreting WT (black) or *Itk*$^{-/-}$ (gray) OT-I CTL transduced with LAMP1-eGFP and transfected with LifeAct-mApple, then imaged via TIRF microscopy. Graphs represent mean ± SEM. WT n=103, *Itk*$^{-/-}$ = 75, from 5 independent experiments.

Degranulation and cytotoxicity are restored in ITK-deficient CTLs after prolonged culture in IL-2

Because we were unable to visualize the degranulation defect in ITK-deficient CTLs by microscopy, we decided to look more closely at differences between how the CTLs were prepared for the FACS-based assays versus TIRF imaging. A side-by-side comparison of cells under each activation condition using our FACS-based degranulation assay revealed that the preparation of cells for TIRF assays resulted in augmented granule fusion in the absence of ITK. After extensive studies to rule out the effects of retroviral transduction, cell sorting, or transfection itself (data not shown), we turned to the prolonged culture in IL-2 as a possible explanation for the augmented degranulation in ITK-deficient CTLs.

IL-2 has long been known to enhance lymphocyte cytotoxicity in culture, particularly for natural killer (NK) cells [127]. More recent data has shown that IL-2 stimulation of peripheral blood lymphocytes (PBLs) augments degranulation in healthy donor cells. In addition, IL-2 has been shown to partially restore degranulation in PBLs from Familial Hemophagocytic Lymphohistiocytosis type 4 (FHL4) patients that carry a mutation in STX11, a gene encoding a t-SNARE important for vesicle fusion in CTLs [88], and to a lesser extent in peripheral blood mononuclear cells (PBMCs) from FHL3 and FHL5 patients [74, 128] carrying mutations affecting UNC13D and STXBP2, all parts of lytic granule fusion machinery. Although different molecular requirements for NK cell and CTL cytotoxicity have not been described, very little is understood about the contribution

of IL-2 to CTL degranulation, in part due to the requirement for IL-2 for differentiation of CTLs. However, since IL-2 culture restored cytotoxic capability in NK cells from patients with primary immunodeficiencies with defects in lymphocyte degranulation, we hypothesized that prolonged exposure to IL-2 might also augment degranulation in ITK-deficient CTLs.

To test this, we continued culturing both WT and *Itk*$^{-/-}$ OT-I CTLs for six days after the initial addition of IL-2 to medium (nine days total), resuspending the cells in fresh medium plus IL-2 every 48 hours. Under these prolonged culture conditions, cells were exposed to an additional round of IL-2 stimulation. We noted that viability in WT OT-I CTLs cultures began to decrease after eight days from an average of 83.3% on day seven to 25.8% on day nine, while the viability of *Itk*$^{-/-}$ OT-I CTLs was much less affected over the same time in culture, changing only from 76% on day seven to 62.8% on day nine (Figure 2.2.14A). These observations are consistent with previous reports that ITK-deficient CD4+ T cells are resistant to cell death under a number of conditions [129].

To compare degranulation between cells activated for different periods of time, we put cells in culture each day for a series of five days. This provided us with cells from staggered cultures so that degranulation assays could be performed on the same day using cells at different time points following primary activation. Interestingly, prolonged exposure to IL-2 restored degranulation in *Itk*$^{-/-}$ OT-I CTLs, to levels equivalent to those seen in viable WT OT-I CTLs that were stimulated for the same period of time (Figure 2.2.14B). Notably, this was not secondary to reduced degranulation in the viable WT cells, but rather to an increase in ITK-deficient cells.

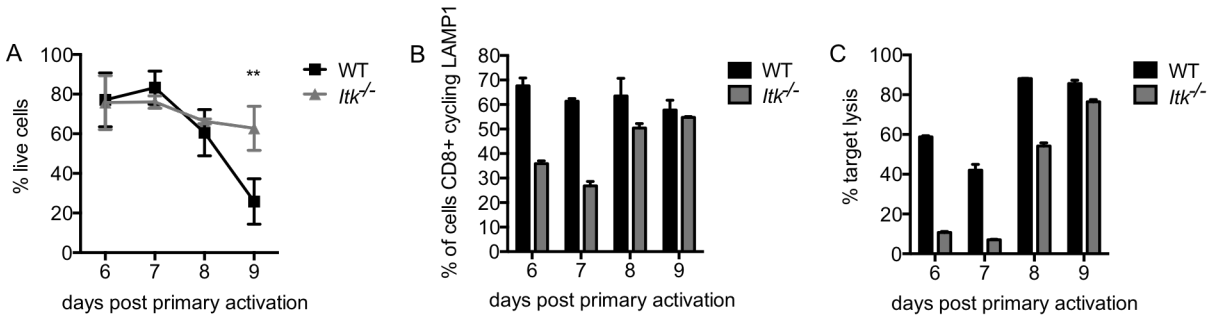

Figure 2.2.14: Degranulation and cytotoxicity are restored in ITK-deficient CTLs after prolonged culture in IL-2. (A) Degranulation in response to 5μg/mL of plate-bound anti-CD3 in WT (black) or ITK-deficient (gray) OT-I CTLs cultured under indicated culture conditions. Bars show ± SD. (B) WT (black) or *Itk*$^{-/-}$ (gray) OT-I CTLs were cultured and stained with Live/Dead dye to evaluate viability. Graph depicts percent of total CD8+ cells with dye excluded at indicated time points. Points represent mean ± SEM from two independent experiments. (C) Graph depicts percent of WT (black) or *Itk*$^{-/-}$ (gray) CTLs cycling LAMP1 in response to 5μg/mL of plate-bound anti-CD3 evaluated at indicated days after the start of primary activation. (D) *in vitro* cytolysis of EL4 targets pulsed with 1μM $OVA_{257-264}$ peptide by WT OT-I (black) or *Itk*$^{-/-}$ OT-I (gray) CTLs at a 20:1 effector:target ratio, evaluated at indicated days after primary activation. Graphs show percent cytotoxicity ± SD at 4-hour time points. Representative of 3 independent experiments.

To determine whether augmented degranulation in ITK-deficient CTLs during prolonged culture in IL-2 translated into increased cytolysis, we evaluated killing of peptide-pulsed EL4 target cells by CTLs. Similarly, prolonged incubation with IL-2 rescued the ability of ITK-deficient CTLs to kill targets (Figure 2.2.14C). Together these data suggest that, like NK cells from FHL3, 4, and 5 immunodeficient patients, prolonged IL-2 treatment can restore both degranulation and cytolysis in ITK-deficient OT-I CTLs.

2.3 Discussion

ITK is an important modulator of TCR signaling, required for maximum PLCγ1 activation and Ca^{2+} signaling in T cells. Previous work has suggested that viral

clearance was delayed in ITK-deficient animals, although ultimately *Itk*$^{-/-}$ mice mount a protective immune response against viral infection [115, 116]. This information, coupled with reports that patients with mutations in ITK are particularly susceptible to viral infections, led us to further probe how ITK-deficiency directly affects the process of killing in CTLs. Our results provide new insight into the effect of ITK and suboptimal TCR signaling on CD8+ T cell function, and how it may contribute to phenotypes associated with ITK-deficiency in humans.

Here, we show that ITK-deficient CTLs have an intrinsic defect in cytolysis. Despite delays in activation and expression of effector molecules, once CTLs were generated, early TCR-driven events of target cell recognition, adhesion, and cell polarization were normal in the absence of ITK. However, we found that degranulation in ITK-deficient CTLs was impaired. We further found that this defect could be overcome by prolonged exposure to IL-2 in culture. Similar observations have been made for other primary immunodeficiencies where IL-2 was reported to enhance cytotoxic lymphocyte function, notably in the FHL family of diseases [88, 128].

Given altered actin accumulation in ITK-deficient CD4+ T cells, we were surprised to find that the early stages of CTL killing were normal in the absence of ITK. Indeed, *ex vivo* CD8+ T cells from *Itk*$^{-/-}$ OTI mice exhibited reduced adhesion to target cells, similar to ITK-deficient CD4+ T cells. We do not think this is strictly due to developmental defects during thymocyte maturation, since the OT-I transgene improves many features of altered development seen in non-transgenic *Itk*$^{-/-}$ mice [123]. For example, we observed similar surface levels of TCR and other surface

markers in cells directly isolated *ex vivo* from WT and ITK-deficient OT-I mice. However, once CTLs were fully activated, ITK-deficiency did not alter adherence or actin recruitment to target cells. This suggests that the cells that expanded during *in vitro* activation were now more functional. We speculate that this rescue may be at least partially attributable to the presence of IL-2 in culture, as adhesion and other defects in NK cell populations from patients with primary immunodeficiencies have also reportedly been rescued by IL-2 (see below for further discussion) [74, 128, 130].

Downstream of TCR engagement, the activation of PLCγ1 leads to the hydrolysis of PIP_2 to generate two major second messengers in T cell signaling: DAG and IP_3. Localized DAG gradients generated by TCR activation serve as a polarizing signal, regulating centrosome reorientation toward target cells by recruiting PKC isozymes [71, 73]. We found that both centrosome and lytic granule polarization toward target cells were normal in *Itk*$^{-/-}$ CTLs. Thus, although ITK is important for the full activation of PLCγ1 in T cells, the DAG gradient generated in ITK-deficient CTLs is sufficient to drive cell polarization, despite evidence that PLCγ1 activation was defective, as indicated by the decreased Ca^{2+} mobilization. It is possible that ITK affects other downstream effectors that influence DAG concentrations, such as the diacylglycerol kinase (DGK) α and ζ, thereby diminishing the effects of decreased DAG generation by PLCγ1. Consistent with the idea that ITK-deficient cells have sufficient levels of DAG, we found that treatment of ITK-deficient cells with a DGK inhibitor, which would increase DAG concentrations by preventing conversion of DAG to phosphatidic acid, did not augment degranulation

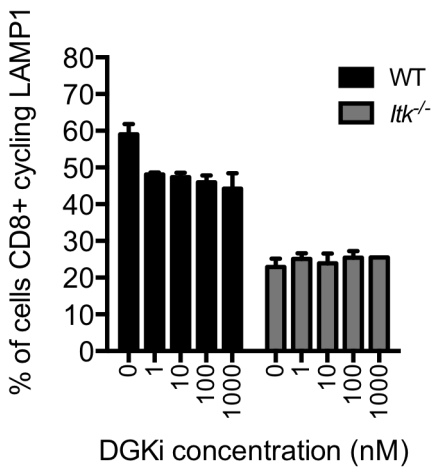

Figure 2.3.1: Inhibition of DGK in ITK-deficient does not rescue degranulation. Graph depicts percent of WT (black) or *Itk*$^{-/-}$ (gray) CTLs treated with indicated concentrations of a DGK inhibitor and cycling LAMP1 in response to 5μg/mL of plate-bound anti-CD3. Mean ± SD.

by ITK-deficient CTLs (Figure 2.3.1). This is in contrast with SAP-deficient CTLs, whose defect in cytolysis is partially rescued by treatment with the same inhibitor [131].

Once granules reach the plasma membrane, TIRF microscopy has revealed them to be highly dynamic structures that must dock before fusion can occur. Previous work has suggested that efficient granule docking, defined as the tethering of vesicles to the plasma membrane (reviewed in [132]), is dependent on the strength of TCR signaling [67, 125]. Since ITK-deficiency leads to impaired degranulation, and CTLs undergo suboptimal TCR signaling due to the loss of ITK, one possible explanation for the impaired degranulation is that docking is defective in *Itk*$^{-/-}$ CTLs. Although the precise upstream signals controlling docking are not known, the importance of this step in degranulation has been established through the study of patients with mutations in membrane- or vesicle-associated fusion machinery who have inherited forms of HLH syndromes. TEM data from our collaborators in the Griffiths lab indicates that while ITK-deficient CTLs are able to polarize their centrosome, granules, and microtubule network, there exists a subtle but reproducible difference in the pattern of lytic granules accumulating at the synapse. This observation suggests a problem in transfer of granules from the microtubule network to the membrane, or possibly in

granule docking. Although high-resolution images of the synapse provide clues to how the absence of ITK affects granule fusion specifically, it is difficult to quantify the subtle defects observed. The extensive EM studies required to do so are beyond the scope of this thesis.

Efficient granule docking and priming in CTLs is dependent on membrane- or vesicle-associated fusion machinery, including RAB27a, tethering proteins, and SNAREs, that lead to abnormal CTL responses. We found that protein expression of STX11 (33kDa), MUNC13-4 (120kDa), MUNC18-2 (66kDa), SNAP23 (23kDa), and SYT7 (60-90kDa) was equivalent in WT and ITK-deficient CTLs (Figure 2.3.2A-D).

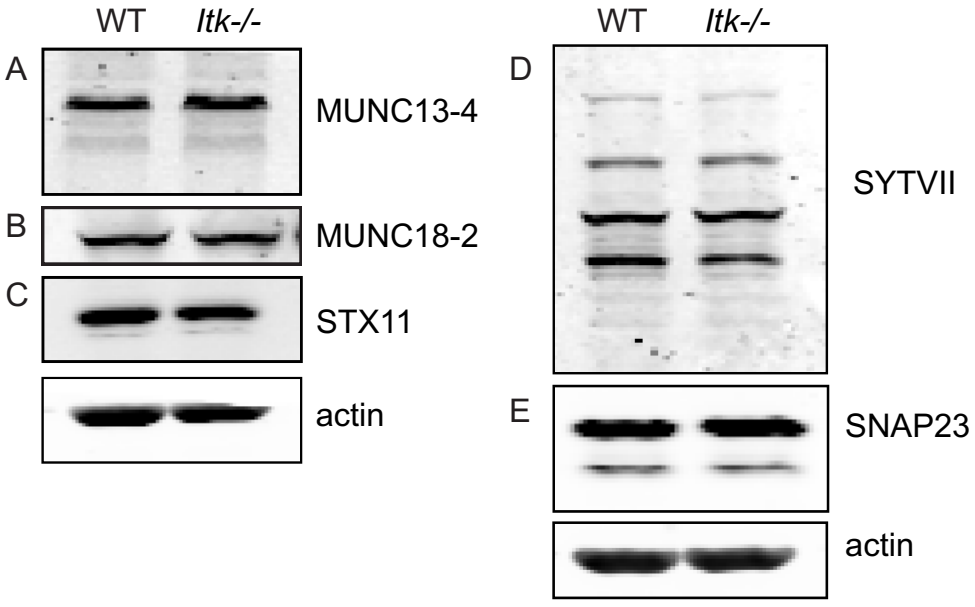

Figure 2.3.2: Lytic granule fusion machinery is expressed at equivalent levels in WT and ITK-deficient CTLs. Expression of (A) MUNC13-4 (120kDa), (B) MUNC18-2 (66kDa), (C) STX11 (33kDa), (D) SYTVII (60-90kDa), or (E) SNAP23 (23kDa) in total lysates obtained from day 7 WT or *Itk*$^{-/-}$ OT-I CTLs. Blotted for actin as a loading control.

However, interpretation of protein expression levels is complicated in some cases by data that mouse STX11 antibodies also recognize other syntaxins (possibly STX3, since reactivity is seen in STX11 gene-targeted mice) (Gillian Griffiths, unpublished observations). Likewise, most studies probing RAB27a function have relied on the overexpression of a tagged form of the protein. Examining endogenous RAB27a protein levels, as well as the localization of other components of the fusion machinery, has proven difficult due to the limited availability of good reagents for western blotting and microscopy. We therefore cannot rule out impaired localization of these molecules, nor lytic granule biogenesis or the generation of mature granules containing the necessary machinery for efficient TCR-triggered fusion at the plasma membrane, as a possible explanation for our phenotype in ITK-deficient CTLs. Alternatively, components of fusion machinery may be dependent on TCR-triggered post-translational modifications to regulate degranulation in CTLs. This is not unprecedented; Fc receptor-induced phosphorylation of SNAP23 in mast cells by IκB kinase, a kinase downstream of IgE receptor signaling, is essential for degranulation, as expression of a phospho-mimetic SNAP23 mutant partially rescues degranulation in IκB kinase-deficient mice [133].

The hydrolysis of PIP_2 by PLCγ1 to produce IP_3 triggers store-operated calcium entry (SOCE) into the cell through the action of ER calcium sensors, STIM1 and 2, and the subsequent activation of the calcium release-activated channel (CRAC), ORAI1, at the plasma membrane. Some components of fusion machinery, such as MUNC13-4 and SYT7, have both calcium and phospholipid-binding domains that are thought to mediate SNARE assembly and lytic granule fusion by

increasing affinity. Thus, the balance between calcium flux and phospholipid composition could fine-tune lytic granule fusion in CTLs. While the precise signals that couple surface receptor signaling to degranulation machinery in CTLs are still not fully understood, there is an absolute dependence on Ca^{2+} for lytic granule secretion. CTLs do not degranulate in the presence of EGTA, a potent chelator of calcium, and cytotoxic lymphocytes from patients with mutations in STIM1 or ORAI1 have defects in secretion [93, 134, 135] (and data not shown), while polarization in these cells remains intact. Similarly, we find Ca^{2+} flux defects in *Itk*$^{-/-}$ CD8+ T cells, and the defects we observe in degranulation in the absence of ITK are reminiscent of those seen in NK cells from patients harboring mutations in ORAI or STIM proteins. Nonetheless, treatment of WT CTLs with ionomycin, a calcium ionophore that bypasses TCR signaling for calcium flux minimally induced degranulation (from 2-3% in non-treated cells to 6-10% in cells treated with 1ug/mL of ionomycin (Figure 2.3.3). While degranulation in ITK-deficient CTLs treated with ionomycin in the

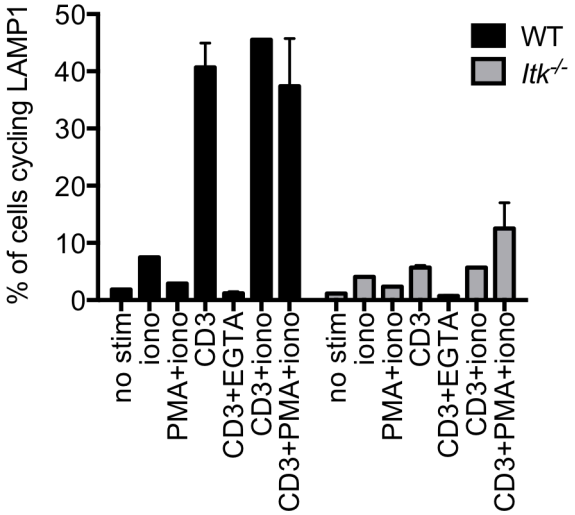

Figure 2.3.3: TCR-triggered degranulation in ITK-deficient is not rescued by PMA/ionomycin treatment. Degranulation measured in a flow-based LAMP1 cycling assay in WT (black) or *Itk*$^{-/-}$ (gray) CTLs in response to 0 (no stim) or 5µg/mL plate-bound anti-CD3 in the presence of ionomycin (1µg/mL), ionomycin + PMA (20ng/mL), or EGTA (0.5mM). Bars represent mean ± SD, representative of three or more experiments.

absence of TCR engagement could reach levels equivalent to WT CTLs, this result was not always consistent, and in any case was small. Furthermore, ionomycin (or PMA and ionomycin) treatment was unable to elicit levels of degranulation achieved in WT cells with TCR stimulation, or rescue degranulation in *Itk*$^{-/-}$ CTLs in the presence of TCR stimulation (i.e. in response to either anti-CD3 or peptide-pulsed targets) (Figure 2.3.3). Nonetheless, ionomycin treatment could rescue FACS-based calcium flux assays and cytokine production, where ionomycin treatment induced robust calcium flux and IFNγ and TNFα production in ITK-deficient CTLs in conjunction with PMA (data not shown). Although there are reports in the literature that NK cells, and both human CD8+ T cells and T cell clones degranulate in response to ionomycin alone [93, 136], there is virtually no evidence that Ca^{2+} flux can induce robust degranulation in primary murine CTLs (Ritter, unpublished observations). This suggests that Ca^{2+} flux is necessary, but not sufficient, for degranulation in primary murine CTLs, at least under the conditions we have examined.

Although our inhibitor data suggest that ITK plays an activation-independent role in TCR-triggered degranulation, the stages of docking or fusion are probably not the only problem in ITK-deficient CTLs. We find that expression of downstream effectors, such as granzyme B and perforin, is also reduced in the absence of ITK. Previous work has shown that through the HIF1α pathway, mTORC1 signaling controls a diverse transcriptional program including the expression of cytolytic effectors in T cells [23]. We have previously shown that CD4+ T cells from ITK-deficient mice have reduced mTORC1 signaling and HIF1α expression [114].

Similarly, we show here that ITK-deficient CD8+ T cells have altered mTORC1 signaling at early time points during activation, as well as decreased granzyme B and perforin expression. Together the results suggest that ITK-deficiency in CD8+ T cells has two consequences: when naïve CD8+ T cells in the periphery encounter antigen, a suboptimal TCR signal in the absence of ITK generates a population of CTLs with altered maturation kinetics, expressing less granzyme B, perforin and perhaps other effectors. Upon second antigen encounter, that population of sub-optimally activated CTLs is further unable to efficiently degranulate in the absence of ITK. In this scenario, the lytic granules that do undergo fusion may contain less granzyme B and perforin, thus together making ITK-deficient CTLs poor cytotoxic lymphocytes that are less effective at clearing virally infected targets at early time points during infection (Figure 2.3.4). Whether ITK affects other mediators of lytic granule secretion and cytolysis is an important question for the future.

However, we show here that prolonged culture of ITK-deficient CTLs in IL-2 rescues degranulation and cytolysis of target cells. To our knowledge, this is the first report that IL-2 can rescue cytolytic functionality of CTLs cells with TCR signaling defects. IL-2 treatment has long been known to increase cytolysis in NK cells and PBLs from patients with a variety of immunodeficiencies [130, 136-138]. Whether this is the result of increased expression of gene products important for cytolytic function, or whether there are direct effects on fusion is not clear. For example, Wiskott-Aldrich syndrome (WAS) is a primary immunodeficiency associated with an increased susceptibility to Herpes virus infections and decreased NK cell cytotoxicity. NK cytotoxicity in the absence of WASp improves with IL-2 in culture,

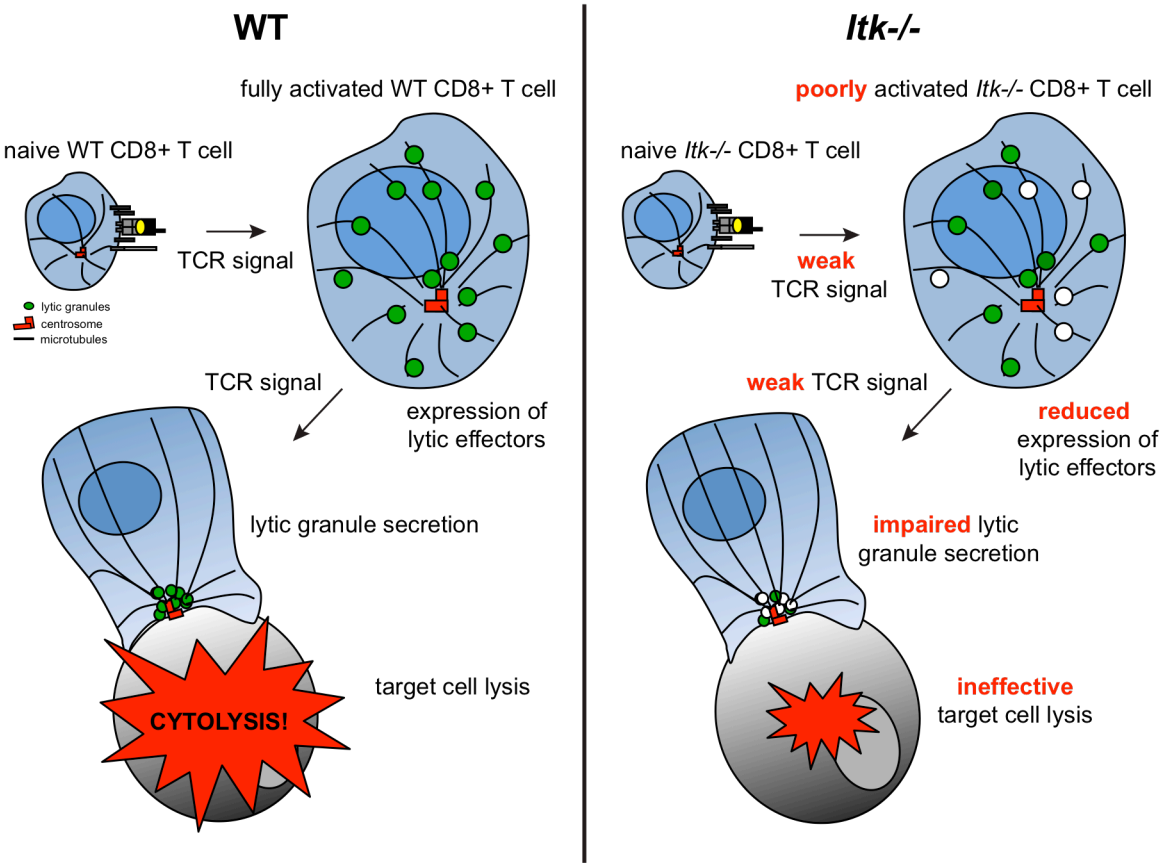

Figure 2.3.4: The dual consequences of ITK-deficiency.

and IL-2 treatment of a patient with WAS enhanced the cytotoxicity of their NK cells. Intriguingly, IL-2 stimulation of NK cells *in vitro* led to increased phosphorylation of the WASp homolog WAVE2, which was required for inducing WASp-independent NK cell function, but not for baseline activity [130]. These results suggest a potential signaling mechanism through which IL-2 can rescue defects in cytotoxic lymphocyte function. More recently, an elegant study investigating how T cells integrate intrinsic signaling with environmental cytokine cues showed that IL-2, in conjunction with strength of TCR signaling, regulates cell cycle entry through the activation of the

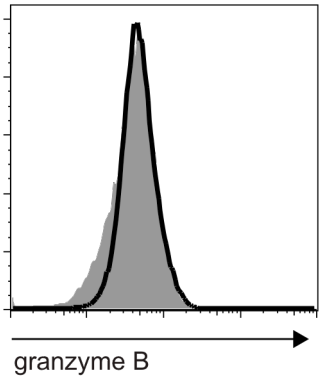

Figure 2.3.5: ITK-deficient CTLs show equivalent expression of granzyme B after prolonged culture in IL-2. WT (black) or *Itk*$^{-/-}$ (gray) OT-I CTLs activated in the presence of 10nM $OVA_{257-264}$ peptide and cultured for nine days in the presence of IL-2. Histogram is representative of two independent experiments.

PI3K signaling [21]. The loss of ITK in CTLs is reminiscent of many phenotypes associated with altered peptide or reduced TCR signaling: delayed proliferative responses, impaired mTORC signaling, reduced expression of effector molecules, and decreased Ca^{2+} flux. It is therefore possible that in our system and others, IL-2 provides a synergizing signal that enables complete activation of CTLs in the absence of optimal TCR signaling. Indeed, expression of surface markers in ITK-deficient CTLs improved after addition of IL-2 on day three of culture. Likewise, the expression of granzyme B also improves after prolonged culture (>8 days) of ITK-deficient CTLs with IL-2 (Figure 2.3.5). It is interesting to speculate that these effects may contribute to the eventual clearance of viral infections in ITK-deficient mice.

Overall, this work demonstrates two significant effects of ITK-deficiency on CTL function: first, a decrease expression of effectors and second, a potentially novel role for ITK in regulating degranulation without affecting upstream processes such as adhesion or cell polarization. Importantly, we also offer additional evidence for the role of IL-2 in integrating TCR and costimulatory signaling pathways for the generation of fully functional CTL responses. Together, this work provides insight into the defects that may account for the particular susceptibility to viral infections observed in patients with mutations in ITK and TCR signaling components.

Chapter 3: Cortical actin regulates secretion of lytic granules in CD8+ cytotoxic T lymphocytes

3.1 Introduction

CTLs carry out their cytolytic functions through the directed polarization and secretion of lytic granules, specialized structures that contain perforin and granzymes, molecules that induce death of target cells. Our studies of CTL function have led us to further investigate the mechanisms regulating this final stage in killing. A single CTL is capable of killing multiple target cells during an immune response [139, 140], hence they are thought to act as “serial killers”. As such, CTLs need to tightly regulate secretion, both in order to kill only appropriate target cells on contact, and to preserve the finite number of lytic granules for effective serial killing of targets. Data suggest that each CTL releases only a handful of granules per productive killing outcome. However, how CTLs regulate the number of granules secreted during an individual T:target interaction is still not yet understood.

One mechanism that has been proposed to play a role in regulating exocytosis in cells is through the control of the dense network of F actin known as the actin cortex. The contributions of the actin cytoskeleton at the plasma membrane to CTL activation and signaling have been explored (reviewed in [141] and [142]), but the dynamics of cortical actin at the synapse throughout the entire course of T:target interactions have not been well described. Upon interaction with target cells, T cells rapidly accumulate actin to the site of contact. However, within minutes of the T cell encountering the target, the cortical actin density at the center of the synapse undergoes a dramatic reduction compared with the rest of the cell [41]. This

reduction in cortical actin density has been spatially and temporally correlated with the secretion of lytic granules [34], yet how actin may contribute to the regulation of secretion during later stages of T:target interactions, and the maintenance of the serial killing capability of CTLs, is largely unknown.

To further explore the role of the cortical actin in regulating both the initiation and the termination of secretion of cytolytic granules in CTLs, we used live cell spinning disk confocal microscopy and total internal reflection fluorescence (TIRF) microscopy to directly examine the relationship of actin to secretion during T:target interactions. Our results suggest that the cortical actin meshwork contributes to regulation of both the initiation and the termination of secretion. Additional experiments further revealed a correlation between the recovery of actin and PIP_2 and the synapse, suggesting that the distribution of phosphatidylinositols in the membrane represent a potential mechanism through which CTLs regulate the density of actin during cytolysis. This work provides insight into actin-related mechanisms regulating through which CTLs can carefully control secretion and preserve serial killing capacity during immune responses.

3.2 Results

Cortical actin recovers at the synapse during CTL cytolytic activity

To examine actin dynamics during the termination of T:target cell interactions, we first used live cell spinning disk confocal microscopy to follow actin during the

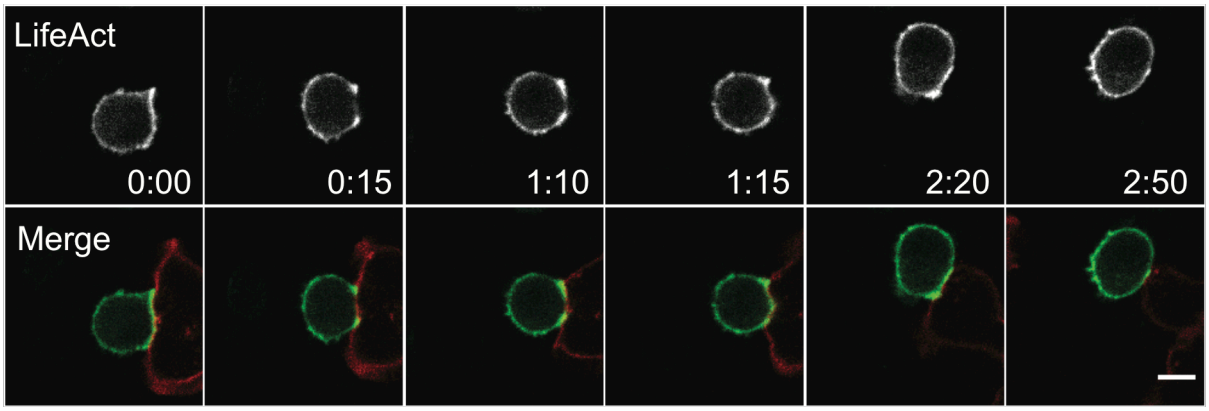

Figure 3.2.1: Actin recovers at the synapse during T:target interactions. Spinning disk confocal time lapse of a WT OT-I CTL expressing LifeAct-mEmerald (green) interacting with an EL4 target cell expressing tagRFP (red) pulsed with 1μM OVA_{257-26} (merge, bottom row). Images showing signal from the LifeAct (488) channel in a single slice correspond to the center of the synapse and are shown in gray scale (top row). n=11 cells from 3 independent experiments. Time shown as minute:second; scale bars = 5μm.

entire course of CTL interactions with their targets. To visualize actin dynamics in real time, we used CTLs expressing LifeAct-mEmerald, a fluorescently labeled actin-binding protein that allows visualization of polymerized actin in cells [143], in conjunction with fluorescently labeled targets. As previously shown [34], CTLs exhibit reduced actin at the site of contact with labeled targets. However, during the course of CTL:target interactions, the density of cortical actin at the synapse recovered across the synapse (Figure 3.2.1).

Because of the availability of fluorescence sensors, it was difficult to simultaneously image actin cortex dynamics and secretion of lytic granules in CTL:target conjugates. Therefore, to examine the relationship between actin dynamics and granule fusion with greater resolution and sensitivity in the context of secretion, we turned to total internal reflection fluorescence (TIRF) microscopy. CTLs were engineered to co-express both LifeAct-mApple to monitor actin dynamics

and LAMP1-eGFP to follow secretory granules. Cells were activated on anti-CD3-coated glass, allowing us to simultaneously visualize cortical actin density and lytic granule secretion over time. When cells engaged the stimulating coverslip, we observed a rapid reduction in central cortical actin density at the synapse that was followed by movement of lytic granules into the TIRF field. At various points after the appearance of these granules, we saw the disappearance of a concentrated vesicle fluorescence associated with the rapid diffusion of the green fluorescent signal through the membrane, indicative of degranulation. Similar to CTL:target interactions in our live confocal microscopy, TIRF images confirmed that cortical actin recovered at the immunological synapse following secretion (Figure 3.2.2A). Sixty-five cells in total were captured before actin had cleared or early enough after clearance that lytic granules had not yet appeared in the TIRF field. Cells included in our analysis were also large enough that granule secretion events were sufficiently spatially separated for accurate quantification. Over time, 78% (51/65) of these cells degranulated, indicated by the diffusion of LAMP1-eGFP in the plasma membrane, with an average of 3.8 ± 2.9 (mean ± SD) number granules fused per cell (Figure 3.2.2B). Of the 51 cells that degranulated, 94% (48/51) recovered cortical actin density within the 20 minute window in which they were imaged in TIRF. The mean time to actin recovery following fusion of the last granule in TIRF was observed at 1.59 ± 1.0 minutes (mean ± SD) (Figure 3.2.2C). We also noted that although granules could still be seen in the TIRF field behind the newly increased cortical actin density, fusion was no longer observed. Thus, secretion only occurred during

the period of actin clearance; actin recovery only occurred after secretion and once actin recovered, we no longer observed secretion. These data suggest that although granules remained polarized toward the contact site after secretion, recovery of the actin network may serve as barrier for secretion.

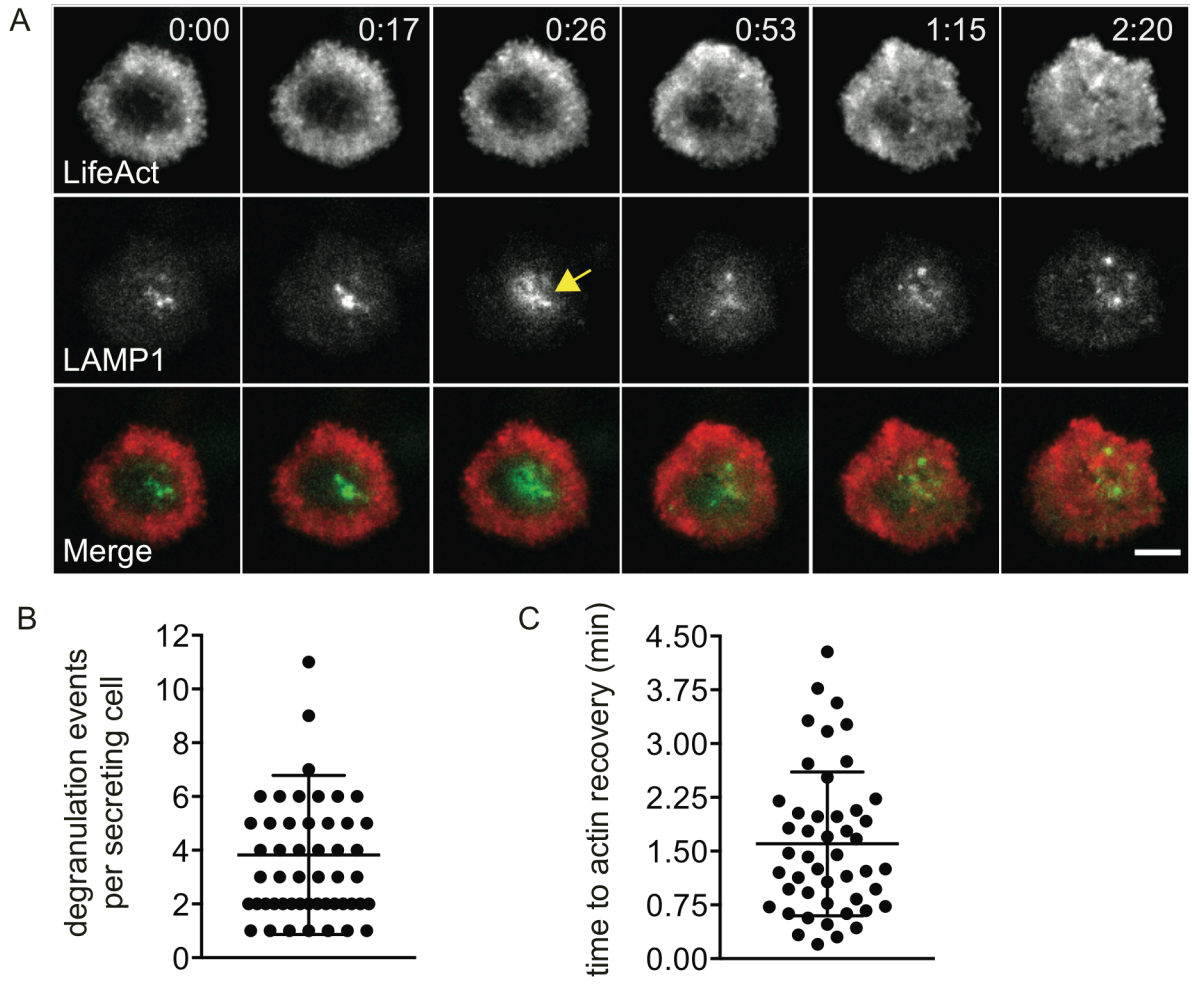

Figure 3.2.2: Actin recovers at the synapse following lytic granule secretion. (A) TIRF images of a CTL expressing LifeAct-mApple (red) and LAMP1-eGFP (green) degranulating on anti-CD3-coated glass surfaces (merge, bottom row). Top row displays signal from the LifeAct (561) channel and middle row from the LAMP1-eGFP (488) channel, shown in gray scale. Degranulation event in the middle row is highlighted by a yellow arrowhead. Time shown as minute:second; scale bars = 5μm. (B) Graph of time to actin recovery following secretion, where each circle represents an individual cell. n=48 cells from 9 independent experiments.

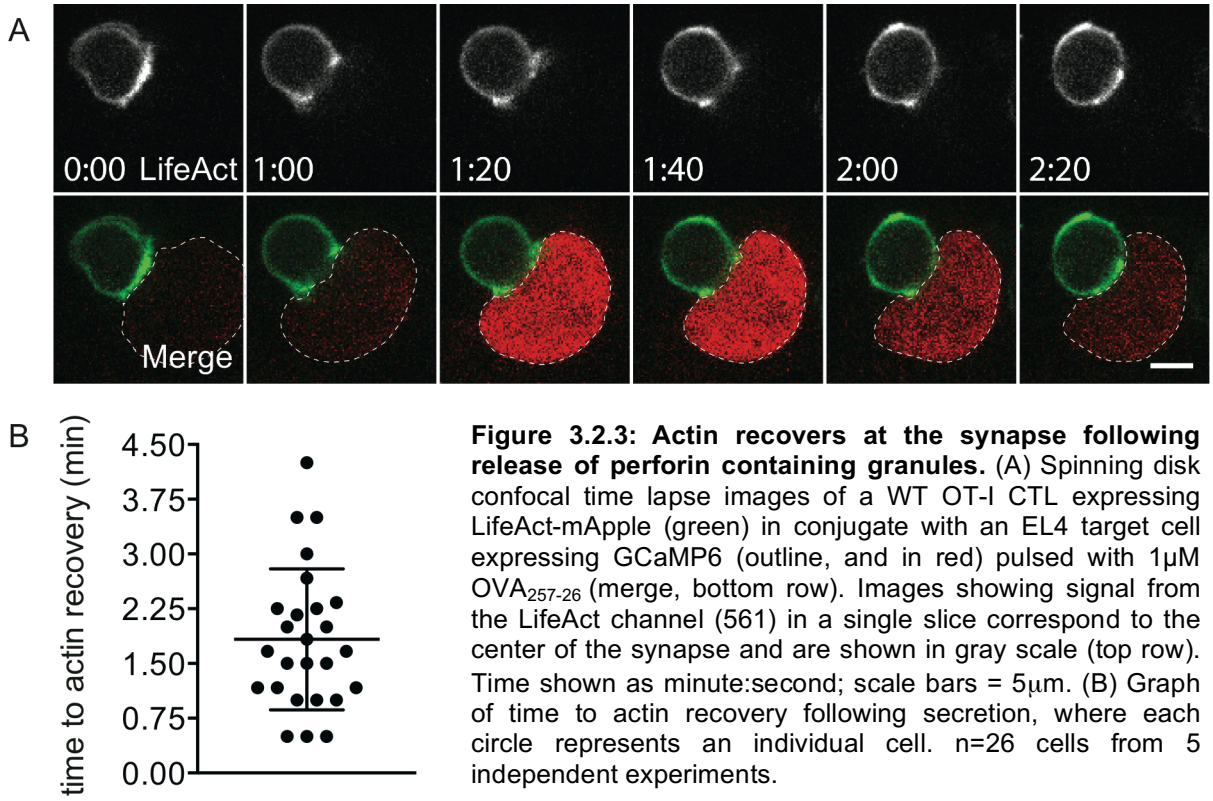

Figure 3.2.3: Actin recovers at the synapse following release of perforin containing granules. (A) Spinning disk confocal time lapse images of a WT OT-I CTL expressing LifeAct-mApple (green) in conjugate with an EL4 target cell expressing GCaMP6 (outline, and in red) pulsed with 1μM OVA_{257-26} (merge, bottom row). Images showing signal from the LifeAct channel (561) in a single slice correspond to the center of the synapse and are shown in gray scale (top row). Time shown as minute:second; scale bars = 5μm. (B) Graph of time to actin recovery following secretion, where each circle represents an individual cell. n=26 cells from 5 independent experiments.

To further correlate actin dynamics with CTL function, we used target cells expressing the Ca^{2+} indicator GCaMP6 that fluoresces upon increased intracellular Ca^{2+} concentration [139, 144, 145]. Previous work has shown that Ca^{2+} increases are associated with very early loss of membrane integrity [146], thus GCaMP6 fluorescence is a readout for loss of the target cell membrane integrity induced by CTL degranulation. As in our earlier results, we saw a reduction in cortical actin density at the synapse after contact with target cells using live cell spinning disc confocal microscopy (Figure 3.2.3A). The mean time to actin recovery after GCaMP fluorescence was 1.83 ± 0.96 minutes (mean ± SD) minutes (Figure 3.2.3B). However, once Ca^{2+} flux was seen in targets, we observed a recovery in the actin density at the synapse in greater than 90% of the CTL:target conjugates. Together

these experiments suggest that 1. cortical actin recovers at the synapse following cytolytic activity, and 2. the secretion of lytic granules only occurs during the period of actin clearance, i.e. once cortical actin recovers, secretion is no longer observed.

Removal of dense cortical actin permits granule secretion

The correlation between actin recovery and the cessation of secretion suggested to us that recovered cortical actin could act as a physical barrier, and thus serve as a mechanism for regulating secretion in CTLs. To test this hypothesis, CTLs expressing LifeAct-mApple and LAMP1-eGFP were allowed to interact with anti-CD3-coated glass, secrete lytic granules, and recover cortical actin. Following actin recovery, cells were treated with a carrier control (Figure 3.2.4A), or Latrunculin A (LatA) to depolymerize actin (Figure 3.2.4B), and monitored using TIRF microscopy to observe the effect of treatment on lytic granule secretion. Before treatment (-0:15, minutes:seconds), we often observed movement of lytic granules in the TIRF field behind the recovered cortical actin meshwork, but no fusion. After treatment with LatA (at 0:00), we saw a reduction in the intensity of cortical actin, indicating disassembly of the actin network (0:15-0:45) (Figure 3.2.4B). The reduction in cortical actin density was followed by lytic granule movement closer to the plasma membrane in the TIRF field, as indicated by an increase in LAMP1-eGFP fluorescence intensity (0:45). Furthermore, within one minute of this increase in lytic granule (eGFP) intensity, lytic granule secretion was again observed at the plasma membrane, as indicated by the diffusion of eGFP in the TIRF plane (1:30)

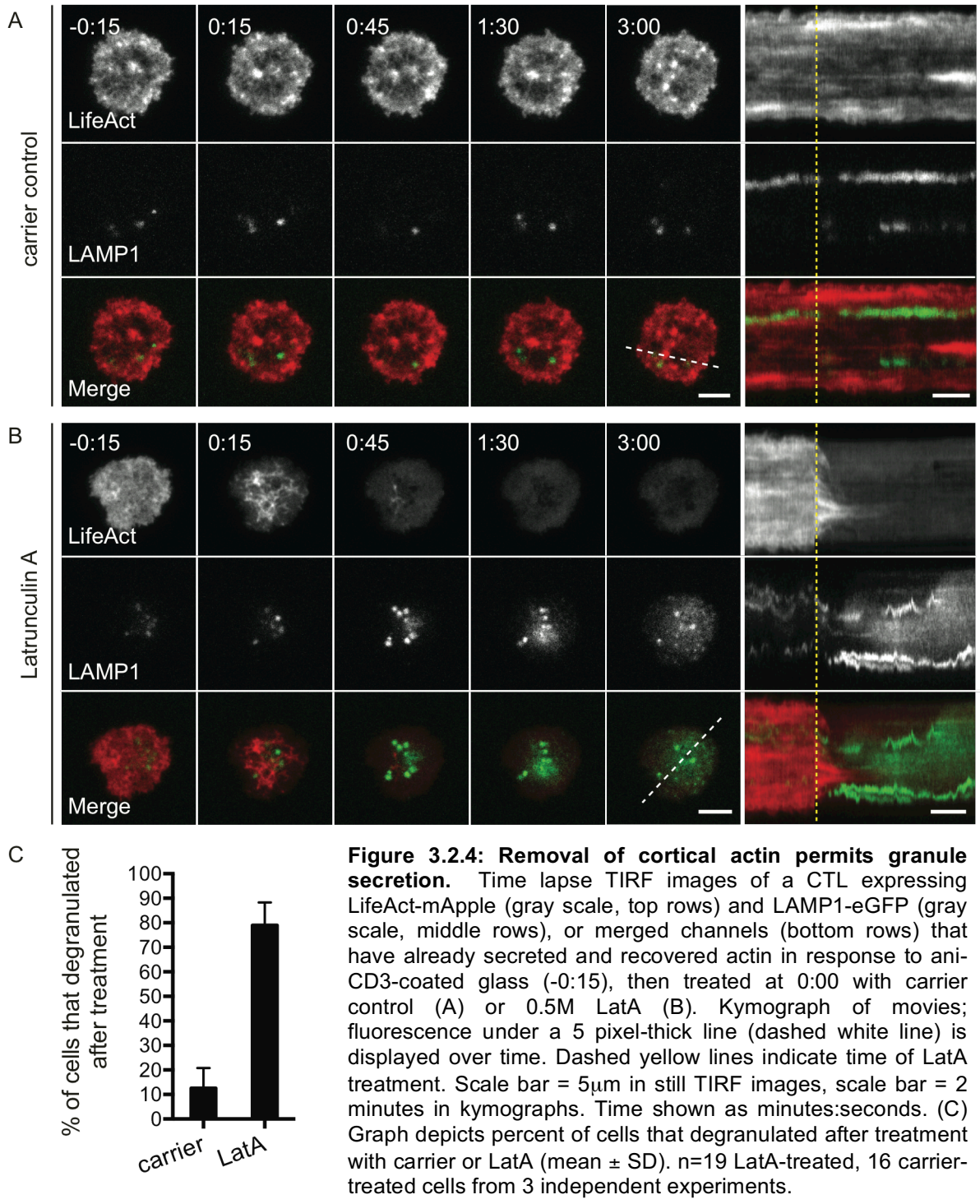

Figure 3.2.4: Removal of cortical actin permits granule secretion. Time lapse TIRF images of a CTL expressing LifeAct-mApple (gray scale, top rows) and LAMP1-eGFP (gray scale, middle rows), or merged channels (bottom rows) that have already secreted and recovered actin in response to ani-CD3-coated glass (-0:15), then treated at 0:00 with carrier control (A) or 0.5M LatA (B). Kymograph of movies; fluorescence under a 5 pixel-thick line (dashed white line) is displayed over time. Dashed yellow lines indicate time of LatA treatment. Scale bar = 5μm in still TIRF images, scale bar = 2 minutes in kymographs. Time shown as minutes:seconds. (C) Graph depicts percent of cells that degranulated after treatment with carrier or LatA (mean ± SD). n=19 LatA-treated, 16 carrier-treated cells from 3 independent experiments.

(Figure 3.2.4B). This movement and secretion of granules could also be visualized by kymographic analyses, which allowed visualization of fluorescence intensity across a region of interest over time. In carrier-treated cells, recovered actin remained relatively stable across the synapse following treatment, indicated by the maintenance of fluorescent signal over time in the kymograph. Likewise, granules could also be seen moving in and out of the TIRF field, but lines of stable intensities over time indicated that no granule fusion had occurred (Figure 3.2.4A). In contrast, LatA treatment resulted in actin depolymerization that was accompanied by granule fusion, as evidenced by the rapid increase in LAMP1-eGFP signal and diffusion of that signal through space and time (Figure 3.2.4B). Removal of the actin barrier resulted in secretion in 78.9 ± 9.4% of cells compared with secretion in only 12.5 ± 8.2% of cells treated with a carrier control (Figure 3.2.4C). These results suggest that recovered actin does indeed act as a barrier to effectively prevent further lytic granule secretion in CTLs.

PIP_2 correlates with cortical actin density at the synapse over time

The regulation of secretion by the actin cytoskeleton led us to ask what factors contribute to the control of actin cytoskeletal dynamics at the CTL:target interface. One factor known to regulate cortical actin density is phosphatidylinositol 4,5-biphosphate (PIP_2) [147-149], which can bind and activate a variety of actin regulatory proteins including, WASP, N-WASP, ADF/cofilin, and Coronin1A (reviewed in [150]). Data suggest that manipulation of PIP_2 at the plasma membrane

in Cos7 cells has direct and potentially functional outcomes on actin polymerization [151, 152] (Ritter, unpublished observations). Furthermore, it has previously been shown that the clearance of actin at the CTL synapse correlates with reduced PIP_2 [34]. To evaluate whether there was a similar spatial correlation between actin and PIP_2 at later time points during CTL:target interactions, we co-transfected CTLs with the LifeAct-mApple and a Tubby-eGFP construct expressing a PIP_2-binding domain of Tubby fused to eGFP [153]. Expression of these constructs allowed us to simultaneously visualize PIP_2 and polymerized actin in the same cell using live cell spinning disc confocal microscopy. Interestingly, actin recovery was associated with a recovery of PIP_2 levels during CTL:target interactions (Figure 3.2.5A). Farnesyl-eGFP probes appeared homogenous across the plasma membrane at all times during target interactions, confirming that the observed changes in intensity of the Tubby-eGFP probe were not the result of alterations in membrane density at the synapse (data not shown).

We were also able to confirm the association between actin and PIP_2 in TIRF microscopy. At early time points during the interaction with anti-CD3-coated surfaces, Tubby-eGFP adopted a similar ring pattern as LifeAct in CTLs. At later time points, Tubby-eGFP recovered across the synapse concomitant with LifeAct (Figure 3.2.5B). Line scans confirmed the colocalization of fluorescence intensity in each channel across the synapse at both early (cleared, 0:24) and late (recovered, 1:03) time points (Figure 3.2.5C and D). These data suggest that PIP_2 not only correlates with the TCR-triggered reduction in actin density during early interactions, but also with the recovery of cortical actin across the synapse over time.

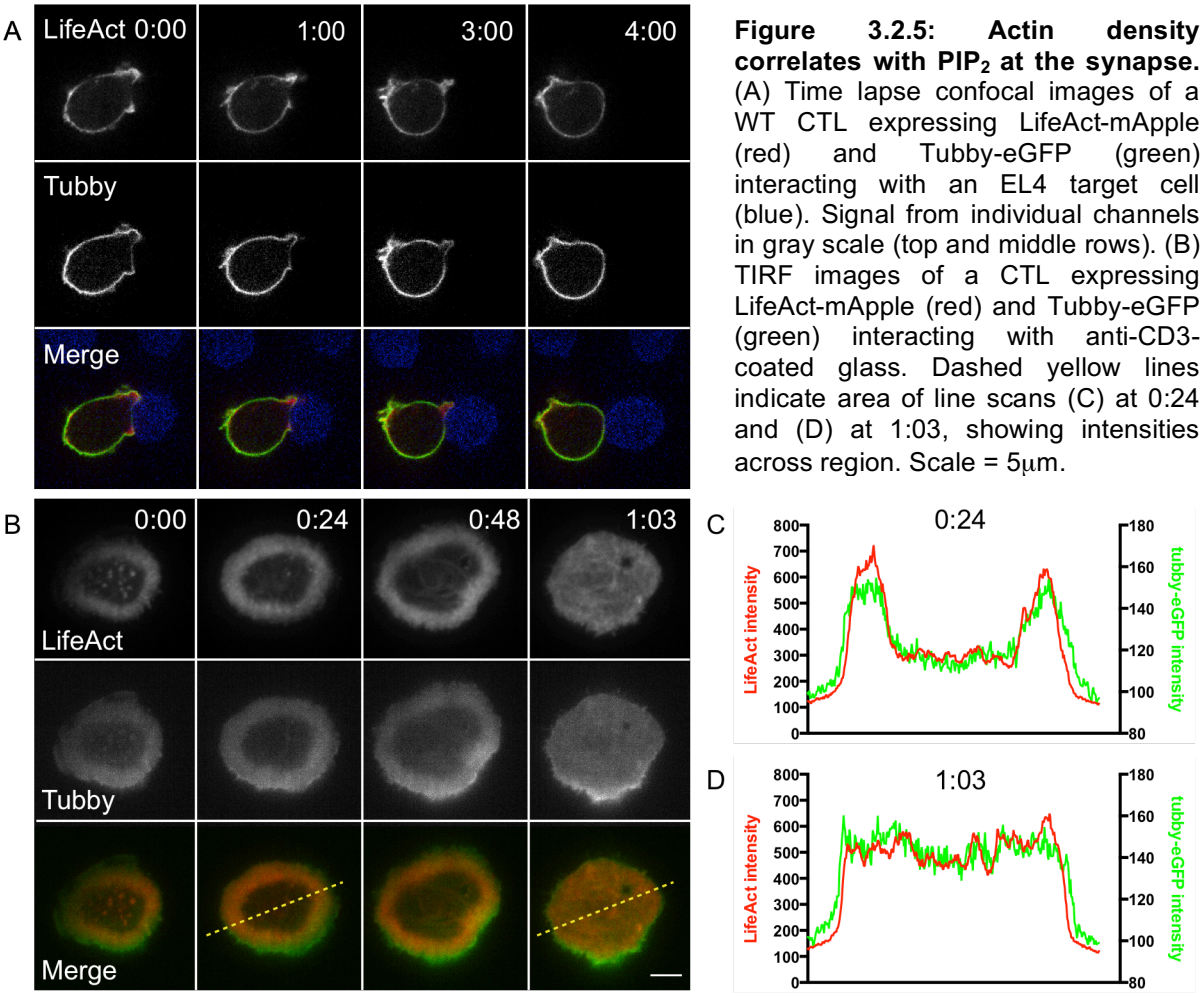

Figure 3.2.5: Actin density correlates with PIP_2 at the synapse. (A) Time lapse confocal images of a WT CTL expressing LifeAct-mApple (red) and Tubby-eGFP (green) interacting with an EL4 target cell (blue). Signal from individual channels in gray scale (top and middle rows). (B) TIRF images of a CTL expressing LifeAct-mApple (red) and Tubby-eGFP (green) interacting with anti-CD3-coated glass. Dashed yellow lines indicate area of line scans (C) at 0:24 and (D) at 1:03, showing intensities across region. Scale = 5μm.

Pharmacological inhibition of PLCγ1 and PI3K inhibits actin clearance in CTLs

The observed spatial correlation between actin and PIP_2 in CTLs led us to ask if altered PIP_2 levels play a role in cortical actin regulation in CTLs. PIP_2 is a substrate for a number of enzymes activated by T cell receptor (TCR) signaling, notably PLCγ and phosphoinositide-3-kinase (PI3K). To test whether inhibition of PLCγ1 affects actin clearance, we pretreated cells with either U-73122, an inhibitor of PLCγ1 activity, or U-73343, an inactive analog, and allowed T:target conjugates to

form before fixation. Treatment with U-73122 prevented clearance of cortical actin at the synapse, while treatment of cells with U-73343 had no effect (Figure 3.2.6A and B). These data suggest that TCR-triggered PLCγ1 activation contributes to actin cytoskeleton regulation in CTLs. However, PLCγ1 is also important for the generation of the second messengers, IP_3 and DAG, which regulate Ca^{2+} mobilization and cell polarization in CTLs, respectively. To determine whether the effect of PLCγ1 inhibition on cortical actin dynamics was due to downstream generation of these second messengers, we once again allowed CTLs to interact with target cells and then treated them with phorbol 12-myristate 13-acetate (PMA) and ionomycin to pharmacologically rescue possible downstream DAG- and Ca^{2+} flux-mediated effects, respectively. Incubation with PMA and ionomycin failed to rescue defects in cortical actin dynamics (Figure 3.2.6B). Although we cannot rule out localized effects, or some other reason why these may not rescue, these results suggest that the defect in cortical actin clearance at the synapse is distinct from PLCγ1-mediated effects on Ca^{2+} or DAG. Although less dramatic, treatment of cells with LY-294002, an inhibitor of PI3K (which also uses PIP_2 as a substrate), also reduced the clearance of actin at the synapse when compared with cells treated with a carrier control (Figure 3.2.6C).

To address whether PLCγ1 activation in CTLs is critical for clearance of both PIP_2 and actin at the synapse, we co-transfected CTLs with LifeAct-mApple and Tubby-eGFP to simultaneously monitor actin polymerization and PIP_2 in CTLs. In cells treated with the inactive analog we observed reduced PIP_2 at the synapse (Figure 3.2.6A); PLCγ1 inhibitor-treated cells showed uniform Tubby-eGFP

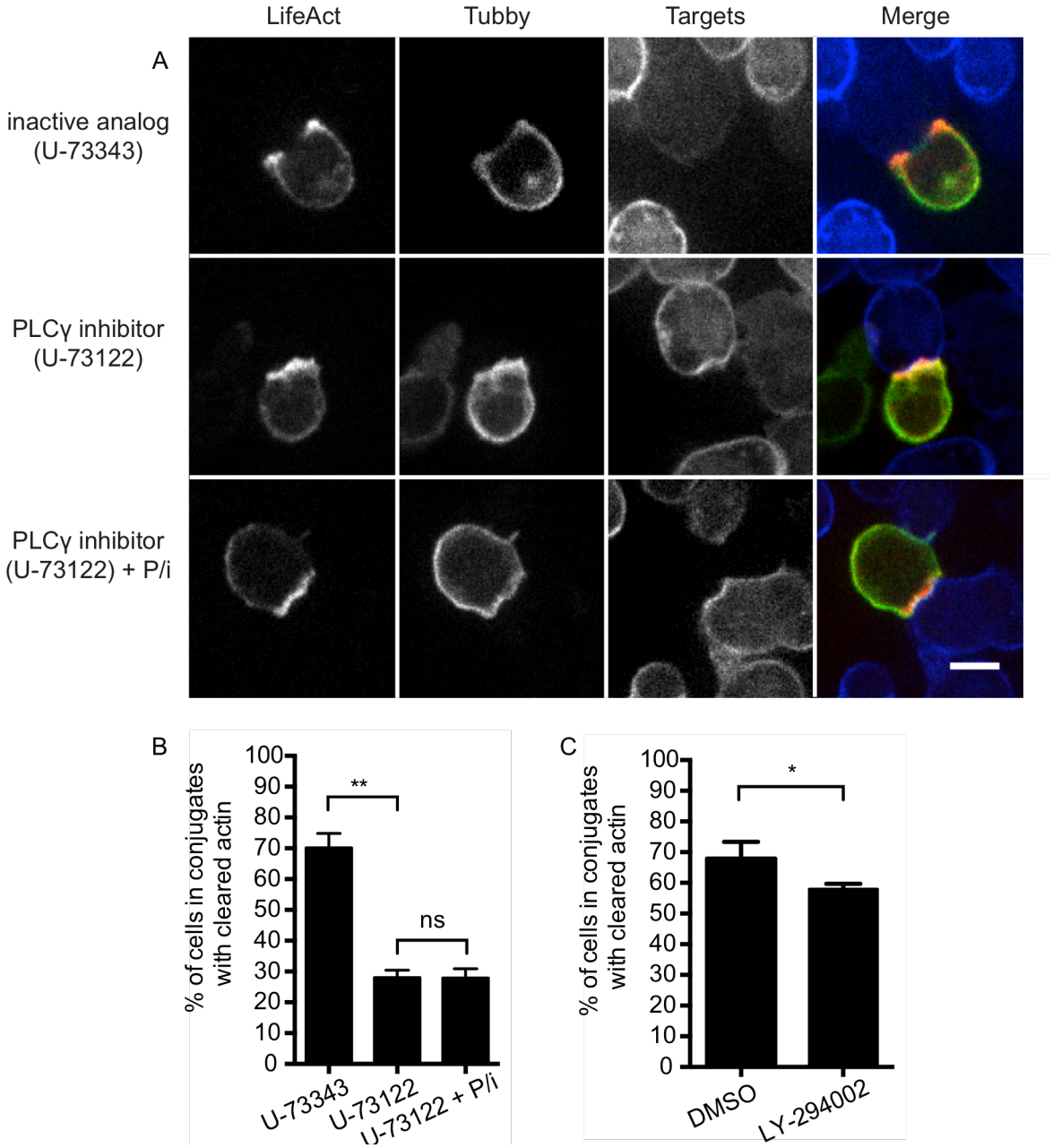

Figure 3.2.6: Pharmacological inhibition of PLCγ1 results in impaired actin clearance at the synapse in CTLs. Representative spinning disk images of WT OT-I CTLs expressing LifeAct-mApple (red) and Tubby-eGFP (green) interacting with 1μM OVA_{257-26} peptide-pulsed EL4-tagBFP target cells in the presence of (A) 1mM U-73343, 1mM U-73122, or 1mM U-73122 plus PMA and ionomycin (P/i) at 20ng/mL and 1μg/mL, respectively. LifeAct-mApple and Tubby-eGFP channels are shown in gray scale. Scale bars = 5μm. Graphs depicts the percent of cells in conjugates with actin cleared in the presence of (B) U-73343 (n=234), U-73122 (n=259), U-73122 + P/I (n=116), or (C) DMSO (n=158), LY-294002 (n=165), from at least 3 independent experiments.

fluorescence at the CTL:target interface, similar to LifeAct intensity (Figure 3.2.6A). Together this data suggests that PLCγ activation in CTLs is critical for the clearance of both PIP_2 and actin at the plasma membrane during CTL:target interactions.

Secretion-deficient *Rab27a*$^{-/-}$ CTLs have impaired actin recovery at the synapse

Our observations that actin recovers at the synapse during TCR-triggered interactions also raised the question of how actin recovery in CTLs is initiated. We noted a temporal correlation between cessation of lytic granule secretion and actin recovery at the synapse both in our live confocal and TIRF imaging (Figure 3.2.2 and 3.2.3). These observations raised the possibility that granule secretion itself may play a role in actin recovery. To test this hypothesis, we evaluated actin recovery in cells that were unable to secrete granules due to a mutation affecting RAB27a, a critical component of lytic granule fusion machinery. Activation of RAB27a-deficient cells on anti-CD3-coated glass led to the rapid reduction of cortical actin density, followed shortly by appearance of lytic granules within the TIRF field, as seen in WT CTLs. However, *Rab27a*$^{-/-}$ CTLs were unable to secrete their granules and did not recover actin at the synapse (3.2.7B). Kymographic analyses showed that the area of reduced cortical actin density persisted throughout the 20 minute duration of imaging in the context of a secretion- deficient CTL (Figure 3.2.7A and B) when compared with WTCTLs, where cortical actin density increased following secretion.

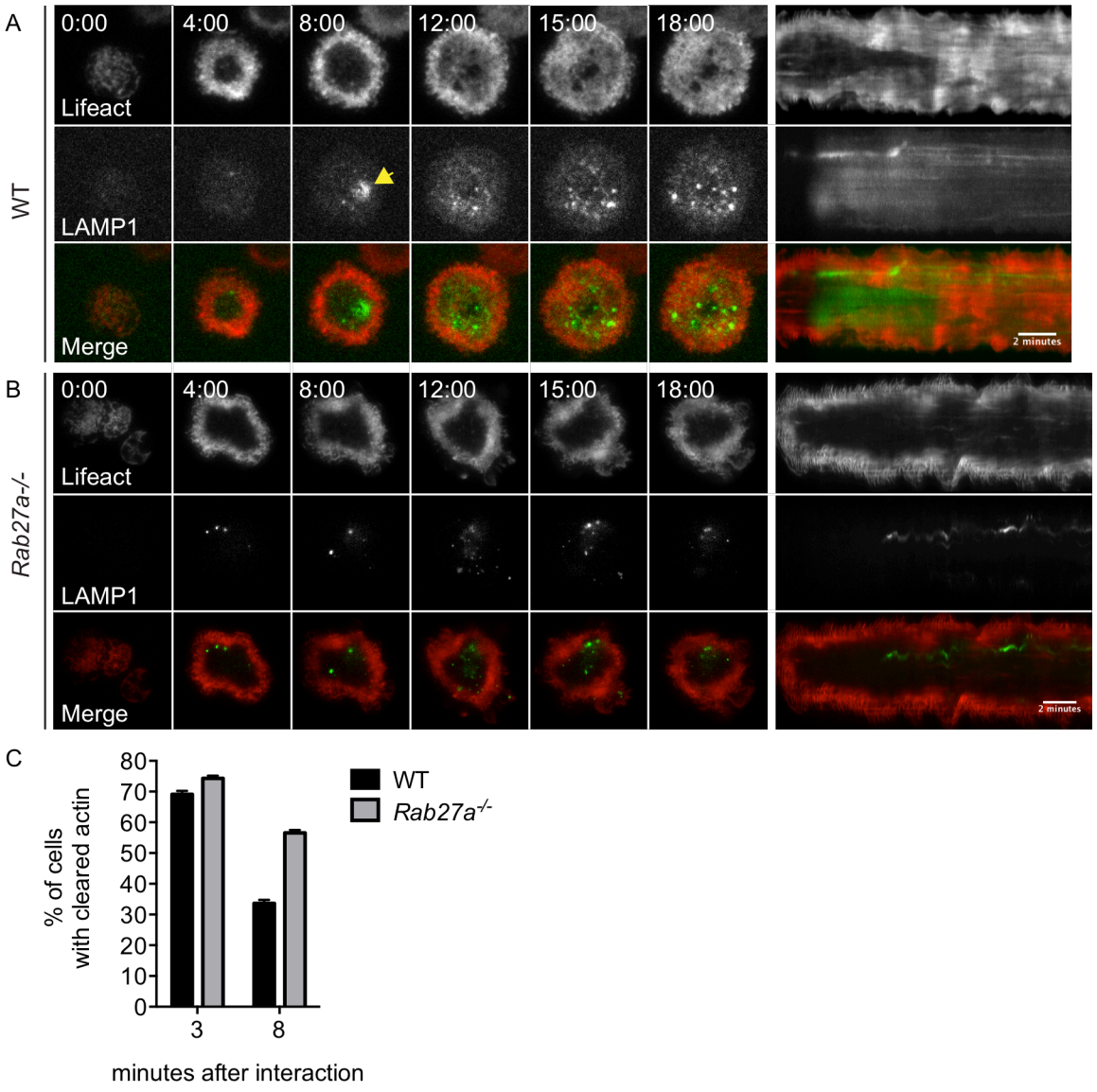

Figure 3.2.7: Secretion-deficient *Rab27a*$^{-/-}$ CTLs do not recover actin at the synapse. TIRF images and kymographs of WT (A) or *Rab27a*$^{-/-}$ (B) CTLs expressing LifeAct-mApple (red) and LAMP1-eGFP (green) interacting with anti-CD3-coated glass. Gray scale images for LifeAct (top) and LAMP1 (middle); bottom rows show merged channels. Yellow arrow in middle row highlights a secretion event. Kymographs of movies (right panels). Scale bar = 5μm in TIRF, scale bar = 2 minutes in kymographs. Time in minutes:seconds. (C) Graph represents percent of WT (black) or *Rab27a*$^{-/-}$ (gray) cells with cleared actin fixed after 3 minutes and 8 minutes after interaction with anti-CD3-coated glass.

To quantitate actin recovery in the cell population, WT or *Rab27a*$^{-/-}$ CTLs were allowed to interact with anti-CD3- coated glass and visualized at either an early (3 minute) or late (8 minute) time points. Phalloidin staining showed that while most WT CTLs had recovered actin after eight minutes, secretion-deficient RAB27a mutant CTLs failed to recover actin as well as their WT counterparts (Figure 3.2.7C). The fact that cortical actin does not recover in these cells suggests that lytic granule secretion is coupled to the mechanism that mediates cortical actin recovery in CTLs. Thus, actin cytoskeletal dynamics both regulate and are regulated by secretion, suggesting that actin recovery may be a critical step in both initiating and limiting CTL secretion.

3.3 Discussion

Actin dynamics in CTLs play an important role in signaling and overall effector function. Previous work has shown that cortical actin density is rapidly reduced after the immunological synapse forms in CTLs, and it is in those areas of reduced cortical that lytic granule secretion occurs [34, 41]. However, few studies have focused on the relationship between actin dynamics and secretion during the entire course of CTL:target interactions. Here, we monitored cortical actin throughout the duration of TCR-triggered responses in the context of secretion. We find that granule fusion is consistently followed by the recovery of cortical actin across the immunological synapse in CTLs. This recovery correlates with cessation of granule secretion. Our results suggest that recovered cortical actin acts as a barrier to

prevent further granule secretion, and that recovery itself is triggered by granule fusion. We also show that both clearance and recovery of cortical actin occurred concomitantly with PIP_2, suggesting that PIP_2 may play a role in driving actin dynamics at the synapse in CTLs. Together, our results suggest that while a reduction in cortical actin density is critical for granule fusion, the reciprocal is also true - that cortical actin recovery plays a role in regulating the cessation of granule fusion in CTLs. Thus, cortical actin both regulates, and is regulated by, secretion in CTLs, offering a new level of control of granule secretion in CTLs that may serve as a mechanism to preserve their serial killing capacity.

The role of actin in secretion has been studied in many cell types specializing in exocytosis, including NK cells [59, 75], mast cells [154], pancreatic β cells [155], and adrenal chromaffin cells [156, 157]. One model, known as the barrier model, suggests that the actin cortex acts as a physical barrier that prevents vesicles from coming in close enough proximity to the plasma membrane for fusion to occur [155]. This model is supported by evidence in chromaffin cells where ion channel clusters and SNARE complexes were associated with areas of low actin density, indicating that the actin cytoskeleton influenced the distribution of components of secretory machinery, thus influencing secretion by preventing access of granules and fusion machinery to the plasma membrane [158]. Live cell imaging of stimulated secretion in chromaffin cells showed that the depolymerization of actin permitted secretory vesicles and associated machinery access to the plasma membrane, promoting fusion [156]. Using structured illumination microscopy (SIM) combined with TIRF-based imaging (TIRF-SIM), our collaborator, Alex Ritter, found that recovered

cortical actin at the immunological synapse in CTLs appeared to form a dense wall of interconnected filaments (personal communication). Together, these observations suggest that a rich actin meshwork could act as a barrier preventing access of lytic granule to the plasma membrane, and thus preventing further secretion. This hypothesis was supported by our experiments that showed that the removal of this cortical actin barrier using the actin depolymerization agent, Latrunculin, resulted in resumed fusion of lytic granules. Thus, like in other cell types, cortical actin forms a barrier that blocks secretion in CTLs.

Two recent studies have shed light on the relationship between cortical actin density and lytic granule secretion in NK cells, which, like CTLs, rely on polarized secretion for killing. In this work, structured illumination and stimulated emission depletion microscopy of NK cells revealed that following stimulation with activating ligands, actin was reduced, but did not entirely clear at the synapse [58, 59]. On these activating surfaces, lytic granules preferentially localized and fused in areas of actin “hypodensity.” Notably, TIRF-SIM images revealed that although centralized actin density during early stages of TCR-triggered immunological synapse formation was markedly reduced, a loose network of branched actin filaments remained across the synapse (Alex Ritter, personal communication), albeit less dense than reported in NK cells [59, 75]. Differences between mechanisms regulating CTL and NK cell secretion have not been fully explored, and it remains to be seen whether the persistence of sparse actin filaments across the synapse in CTLs plays a role in granule fusion as in other cell types [154, 159-161]. Furthermore, whether denser actin networks also act as a barrier in NK cells also is not known. Nonetheless, the

current available data suggests that in CTLs, lytic granule convergence toward a docked centrosome at the plasma membrane is sufficient to bring granules in close enough proximity to the plasma membrane to promote fusion. Additionally, we now provide evidence that recovered actin in CTLs can act as a barrier to block access of granules to the plasma membrane, preventing further secretion. It will be interesting to see if similar mechanisms for cortical actin in regulating secretion hold true for directional versus non-directional secretion of other factors in CD8+ and CD4+ T cells, such as cytokines, which rely on similar stimuli but are found in different vesicular compartments.

The observation that cortical actin density recovered across the synapse during CTL:target interactions led us to explore what regulates actin dynamics in CTLs. Specifically, studies in macrophages reported that the disassembly of actin around newly formed phagosomes correlated with the loss of PIP_2 [162]. Actin cytoskeletal dynamics during phagocytosis in macrophages has been compared to immunological synapse formation in CTLs (reviewed in [163]). Interestingly, multiple reports suggest that T cells [41, 164], B cells [165, 166], and NK cells [167, 168] trogocytose, or take up surface membrane from cells with which they interact. Given these similarities, we hypothesized that like in macrophages, PIP_2 has a role in regulating actin disassembly in CTLs. In agreement with this, previous work in CTLs showed that loss of cortical actin density at the synapse correlated with a reduction in PIP_2 [34]. Our study extends this finding to reveal that the recovery of actin also coincides with the recovery of PIP_2.

During TCR engagement, PIP_2 levels at the plasma membrane in T cells are modulated primarily by PLCγ1 and PI3K activity. PLCγ1 hydrolyzes PIP_2 to generate IP_3 and DAG that lead to calcium flux and the nucleation of downstream signaling, and PI3K phosphorylates PIP_2 to generate PIP_3, creating docking sites for a number of PH domain-containing proteins. We show here that pharmacological inhibition of PLCγ1 activity, and to a lesser extent, PI3K activity, resulted in impaired TCR-triggered clearance of actin at the synapse in CTLs. Concomitantly, PIP_2 intensity at the synapse also persisted in PLCγ1 inhibitor-treated cells (data not shown). The lack of actin clearance was not rescued by the addition of ionomycin and PMA. Although there are many reasons why this rescue may not occur, these observations support the idea that reduction in cortical actin density at synapse is driven the direct activity of PLCγ1 on PIP_2 and is independent of downstream DAG- or calcium-mediated effects. Although PI3K also uses PIP_2 as a substrate, CTLs are less dependent on CD28 co-stimulation than CD4+ T cells. CD28 is a major regulator of PI3K signals in T cells and we, therefore, speculate that actin clearance in CTLs may also be less dependent on PI3K activity. In fact, while we saw some reduction in the ability of CTLs to reduce actin at the synapse, inhibition of PI3K had a far less dramatic effect than inhibition of PLCγ1, making PLCγ1 the probable major regulator of PIP_2 at the CTL membrane. Notably, PLCγ1 itself is recruited to the TCR-triggered signaling complex at the plasma membrane, where it is fully activated following phosphorylation by ITK. Thus, its activity is regulated by localized TCR signaling and restricted to the immunological synapse in CTLs, making PLCγ-mediated modulation of PIP_2 levels at the synapse a probable mechanism for regulating actin dynamics at

the synapse. The normal actin clearance in ITK-deficient CTLs, however, suggests that there is enough PLCγ1 activity to regulate actin dynamics in these cells. Whether subtle differences occur, however, may require evaluation at the super resolution level.

We further provide evidence that granule secretion itself triggers recovery of cortical actin at the synapse in CTLs. CTLs from ashen mice, which have a null mutation in the gene coding for RAB27a, are unable to secrete lytic granules and kill target cells. In these CTLs, cortical actin density remained reduced at the immunological synapse, long after WT CTLs had degranulated and recovered their cortical actin. To our knowledge, this is the first report that secretion plays a role in the recovery of actin at the synapse in CTLs. While at this time, we cannot rule out that this is a RAB27a-dependent defect independent of secretion, additional experiments using CTLs from mice with similar genetic defects in secretion due to mutations in alternative fusion machinery proteins, such as MUNC13-4, may provide additional insight into our observation. Alternatively, a washout experiment using a pharmacological inhibitor of granule fusion, such as botulinum toxin that inhibits SNARE activity, may clarify this question. Interestingly, mutations in RAB27A in humans lead to Griscelli syndrome type 2 (GS2), a primary immunodeficiency making them prone to recurrent viral infections [169]. GS2 patients also develop HLH, where an abundance of hyper-activated CD8+ T cells producing excessive IFNγ leads to the secondary activation of macrophages that, in turn, infiltrate organs and secrete damaging pro-inflammatory cytokines. Given that HLH and HLH-like symptoms are commonly associated with the inability of CTLs to control viral

infections, and RAB27A-deficient CTLs have defects in secretion-triggered recovery of cortical actin, it is possible that the hyper-activated phenotype seen in GS2 patients may not only be ascribed the inability of RAB27A-deficient CTLs to kill virally infected targets due to impaired secretion, but also the failure of CTLs to down regulate their own effector function due to their lack of granule exocytosis.

However, while we demonstrate here that secretion-impaired CTLs do not recover actin as well as secretion-sufficient CTLs, we do not fully understand how granule fusion triggers actin recovery at the synapse in CTLs. Lytic granules are estimated to be between 250 and 500nm in size [58, 170, 171], and signaling clusters imaged at the plasma membrane in activated T cells using super resolution techniques have been estimated to be between 40 and 300nm in size (reviewed in [172]). It is therefore possible that granule fusion physically disrupts remaining signaling complexes at found at the plasma membrane, terminating PLCγ signaling and allowing recovery of PIP_2 across the synapse, followed by cortical actin.

Alternatively, lytic granules may directly add membrane and membrane components, including PIP_2, that could change the composition of the membrane and influence signaling as well as actin dynamics. Lytic granules contain a number of membrane-associated components that are not found at the plasma membrane, such as lysosomal associated membrane protein 1 (LAMP1), a large and highly glycosylated receptor that can make up 50% of the lysosomal membrane [173, 174]. Therefore secretion may deliver a completely new set of granule-associated glycoproteins and phospholipids to the membrane that triggers actin recovery. The kinetic segregation model of TCR signaling suggests that clustering of TCR

complexes brings the TCR and target membranes in close proximity. This contact excludes larger inhibitory signaling components with long extracellular domains, such as CD45 phosphatase [175]. The delivery of large glycoproteins such as LAMP1 could conceivably force apart CTL and target membranes enough to disrupt TCR:MHCI interactions, allowing more inhibitory molecules access to cSMAC, from which they are normally excluded, and lead to inhibition of TCR signaling at the synapse. Discontinued PLCγ and PI3K activity could therefore result in resumed accumulation of PIP_2, through reduced enzymatic activity, delivery from lytic granule membrane, or diffusion from elsewhere. PIP_2 could then facilitate the recovery of cortical actin at the synapse following secretion, preventing further degranulation by CTLs.

Based on our data, we propose a model where when a CTL interacts with other cells, cortical actin acts as a barrier to prevent unwanted secretion. Once a CTL productively encounters a target, cortical actin must be broken down to permit lytic granule fusion for killing to occur. TCR-triggering by target cells initiates a signaling cascade that leads to the recruitment of PLCγ1 (and PI3K, to a lesser extent) to signaling complexes at the synapse, where it hydrolyzes PIP_2 in a localized fashion. The hydrolysis of PIP_2 contributes to the reduction of cortical actin at the synapse, perhaps through loss of nucleation promoting factor (NPF) activity, the release of actin severing proteins, or both. Reductions in cortical actin density promote the polarization and docking of the centrosome, delivering lytic granules to the immunological synapse in a region of reduced cortical actin density where they can efficiently fuse. In turn, secretion itself then triggers the recovery of cortical actin

across the synapse, effectively restoring the cortical actin barrier and preventing further secretion. Whether this recovered actin then alters dynamics with target cells, allowing them to move on to allow subsequent attack of new target cells, remains an intriguing question. However, we propose that this offers a mechanism through which CTLs could limit secretion and preserve their serial killing capacity.

Chapter 4: Concluding remarks and future directions

CD8+ cytotoxic T lymphocytes are critical for killing virally infected and tumorigenic cells. CTLs affect target cell killing through a tightly regulated process of granule release, after which effector molecules found in granules, such as perforin and granzymes, induce death in target cells. Given the importance of CTLs in dealing with viral infections, it is perhaps not surprising then that mutations in genes that affect the development, differentiation, or overall effector function of CTLs can lead to the development of primary immunodeficiencies that are associated with impaired viral clearance. Through the study of this growing family of primary immune disorders related to defective CTL function, we are gaining a basic appreciation of the cellular mechanisms required for CTLs to function properly, the components of which are still not fully understood.

Work in this thesis investigated the role of a proximal TCR signaling molecule, ITK, in CTL effector function. Patients with mutations in ITK, a kinase that serves as an amplifier of TCR signaling, develop lymphoproliferative disease associated with ineffective responses to EBV, and broad susceptibility to viral infections. We found CTLs from ITK-deficient mice exhibit impaired killing of several types of targets, suggesting ITK-deficiency leads to global defects in cytolysis. While *in vitro* activated CTLs from *Itk*$^{-/-}$ mice had impaired expression of granzymes and perforin, killing defects were not necessarily due to altered T cell differentiation because they could be reproduced by treating WT CTLs with an ITK-specific inhibitor during cytolysis assays. To evaluate what other steps may be affected by loss of ITK, we carefully examined the distinct stages of cytolysis. Killing by CTLs occurs when TCR signaling

triggers adherence to targets, formation of the immunological synapse, centrosome and granule polarization, and release of lytic granules inducing cytolysis of targets. Although early events such as adhesion, actin ring formation, and cell polarization were normal in ITK-deficient murine CTLs, granule secretion was defective suggesting ITK may play an unappreciated role in the final stages of killing. Surprisingly, prolonged culture of ITK-deficient CTLs in IL-2 could rescue defects in degranulation. This is similar to what has been observed for other mutants with defective NK cell function, where cytotoxicity is enhanced in culture after IL-2 stimulation. Together these experiments provide clues to novel roles for ITK and proximal TCR signaling in regulating the late stages of CTL function that may account for reduced viral clearance in patients with mutations in ITK.

While my efforts to mechanistically link the activation-independent contribution of ITK to secretion were not successful, more extensive work examining the granule fusion stage in ITK-deficient CTLs will provide additional information on how secretion can be regulated by proximal TCR signaling components, such as ITK. For example, the precise contribution of ion flux to degranulation in CTLs remains poorly understood. Studies in chromaffin cells have reported patches of fusion machinery colocalized with clusters of L- and P/Q type calcium channels [158]. As defects in cytolysis of targets by ITK-deficient CTLs are associated with impaired secretion, and ITK-deficiency can lead to profound defects in calcium flux, more extensive studies exploring the specific channels contributing to secretion, as well as their association or activation of fusion machinery, warrants additional research. More broadly, phosphoproteomics studies performed on WT CTLs versus

WT CTLs treated with an ITK-inhibitor would provide insight into TCR-triggered post-translational modifications, such as phosphorylation, that directly effect degranulation and cytolysis in CTLs.

We also found that prolonged culture in IL-2 augments degranulation and cytolysis in the absence of ITK; exactly how IL-2 enables the complete activation of CTLs in the absence of optimal TCR signaling remains an intriguing question. One possibility is that over time, IL-2 signaling activates transcriptional or translational programs, through persistent STAT5 signaling or activation of mTOR-related pathways, that supplement suboptimal signals received through the TCR in the absence of ITK. To explore this, microarray or RNAseq experiments examining the transcriptional profile in WT versus ITK-deficient CTLs at different time points following TCR stimulation and IL-2 administration may offer clues to help address how and where IL-2 and TCR signaling pathways converge to enable complete activation of CTLs. It may also be of interest to examine molecules and pathways affected in specific genetic disorders in which degranulation has been rescued by IL-2 to determine whether these might provide additional insight.

To further understand what regulates cytotoxic granule release in CTLs, we also examined the role of actin in regulating degranulation. This work was performed in collaborative work with Alex Ritter, a graduate student co-mentored by Gillian Griffiths at the Cambridge Institute for Medical Research, and Jennifer Lippincott-Schwartz at the National Institutes of Health. Similar to the previously reported role of actin in controlling the initiation of secretion, we show here that actin recovery can affect the termination of secretion, most likely by acting as barrier to prevent access

of lytic granules to the plasma membrane. We also provide evidence that granule secretion itself triggers the recovery of cortical actin density across the synapse in CTLs and speculate that mechanisms such as this have evolved in CTLs in order to conserve a limited number of lytic granules for multiple target cell encounters.

A number of potential mechanisms may regulate the TCR-triggered density of cortical actin at the synapse. Our experiments reveal a spatial and temporal correlation between the recovery of actin and PIP_2 and the synapse, suggesting that the distribution of phosphatidylinositols in the plasma membrane represent a potential way through which CTLs regulate the density of cortical actin during T:target interactions. These observations fit well with the known ability of PIP_2 to activate a number of actin regulatory proteins. Together this work provides new insight into actin-related mechanisms that regulate the cessation of secretion in CTLs, and the preservation of serial killing capacity during an immune response. Future work dissecting the relationship between PIP_2 and actin dynamics at the synapse will reveal new roles for specific known and perhaps even novel nucleation promoting factors and actin severing proteins important for the down regulation of CTL responses. It will also be interesting to examine how the delivery of new protein and lipid components to the plasma membrane during secretion contributes to CTL behavior at the termination of T:target interactions.

Experiments described in this thesis using mouse models of immunodeficiency have provided us with clues to novel roles for ITK ad TCR signaling in regulating secretion and killing in CTLs. Additionally, I've presented data that implicates actin as a major contributor to the termination of secretion during

CTL:target interactions. I hope this work will help us better understand the defects that we see in immunodeficient patients with mutations in genes that effect CTL effector function.

Chapter 5: Materials and Methods

5.1 Solutions

Complete medium for culture of primary T and B cells (RPMI 10): Roswell Park Memorial Institute (RPMI) 1640 (Thermo Fisher Scientific) supplemented with 10% fetal bovine calf serum or human serum (FBS), 2mM L-glutamine, 100U/mL Penicillin, 100µg/mL Streptomycin, and 50uM β-mercaptoethanol.

Cell line medium (DMEM 10 and EMEM 10): Dulbecco's Modified Eagle Medium (DMEM, Thermo Fisher Scientific) or Eagles Minimum Essential Medium (EMEM) supplemented with 10% fetal bovine calf serum (FBS), 2mM L-glutamine, 100U/mL Penicillin, and 100µg/mL Streptomycin.

Killing assay medium: phenol-red free RPMI 1640 supplemented with 2% FBS, 100U/mL Penicillin, and 100µg/mL Streptomycin.

Imaging medium: phenol-red free RPMI 1640 supplemented with 5% FBS.

Fluorescence activated cell sorting (FACS) buffer: 1x phosphate buffered saline (PBS, Thermo Fisher Scientific) supplemented with 1% FBS, 100U/mL Penicillin, and 100µg/mL Streptomycin.

Magnetic activated cell sorting (MACS) buffer: 1x PBS containing 2mM ethylene-

diamine-tetra-acetic acid (EDTA), and 0.5% bovine serum albumin (BSA, Sigma-Aldrich), sterile-filtered.

Phospho-staining buffer: 1x PBS containing 1% Triton-X, and 0.5% BSA.

5.2 Mice

Wild-type (WT) OT-I [122], *Itk*$^{-/-}$ [176] OT-I TCR transgenic, and C57Bl/6 (Jackson Laboratories) mice were between 7-10 weeks of age. LifeAct-mRuby mice, the generous gift of Roberto Weigert, were crossed to WT OT-I and *Itk*$^{-/-}$ OT-I TCR transgenic mice to generate LifeAct-mRuby WT and ITK-deficient OT-I mice. *Rab27a*$^{-/-}$ (ashen) mice were generous gifts from both John Hammer and Gillian Griffiths [80]. Animal husbandry and experiments were performed in accordance with approved protocols by the National Human Genome Research Institute Animal Use and Care Committee at the National Institutes of Health.

5.3 Antibodies and dyes

Tables 5.3.1 and 5.3.2. list the dyes and antibodies used.

Table 5.3.1: Dyes

Dye	Concentration or dilution	Application	Source
CellTrace Violet	0.1μM	FC, IF	Life Technologies
CFSE	1μM	FC, IF	eBioscience
Lysotracker	50nM	FC, IF	Life Technologies
Live/Dead, green	1:2500	FC	Life Technologies

Table 5.3.2: Antibodies

Antigen	Clone	Host	Reactivity	Isotype	Application	Dilution	Source
actin	AC-40	Rb, Ms	Ms, Rt, Hu	IgG2a	IF, WB	1:2000	Sigma
β-actin	AC-15	Ms	Ms, Rt, Hu	IgG1	WB	1:10000	Sigma
CD3ε	2C11	Ar Ham	Ms	IgG1	FC	1:500	eBio, BD
CD4	RM4-5	Rt	Ms	IgG2a	FC	1:1000	Miltenyi
CD8α	53-6.7	Rt	Ms	IgG2a	FC	1:500	Miltenyi
CD11a	2D7	Rt	Ms	IgG2a	FC	1:250	eBio, BD
CD16					FC		BioXCell
CD19	1D3	Rt	Ms	IgG2a	FC	1:500	eBio, BD
CD25	7D4	Rt	Ms	IgM	FC	1:250	eBio, BD
CD44	IM7	Rt	Ms	IgG2b	FC	1:1000	eBio, BD
CD62L	MEL-14	Ms	Ms	IgG2a	FC	1:250	eBio, BD
CD69	H1.2F3	Ar Ham	Ms	IgG1	FC	1:250	eBio, BD
CD107a	1D4B	Rt	Ms	IgG2a	FC	1:500	Cell Sig
CD178	MFL3	Ar Ham	Ms	IgG	FC	1:200	BioLegend
EEA1	C45B10	Rb	Ms, Rt, Hu	IgG1	IF	1:500	Cell Sig
γ-tubulin	poly	Rb	Ms, Rt, Hu		IF, WB	1:200, 1:1000	Sigma
GM130	mono	Rb	Ms, Rt, Hu	IgG	IF	1:1000	abcam
AF488		Gt, Dn	Ms, Rb, Rt		IF	1:1000	Life Tech
AF568		Gt, Dn	Ms, Rb, Rt		IF	1:1000	Life Tech
AF647		Gt, Dn	Ms, Rb, Rt		IF	1:1000	Life Tech
granz B	GB11	Ms	Hu	IgG1	FC	1:250	BD
granz B	poly	Rb	Ms, Rt, Hu	IgG	WB	1:500	Abcam
LAMP1	poly	Rb	Ms, Rt, Hu	IgG	IF, WB		Abcam
LCK	3A5	Ms	Ms, Rt, Hu		IF	1:200	Millipore
IFNγ	XMG1.2	Rt	Ms	IgG1	FC	1:250	BD
IL-2	JES6-5H4	Ms	Ms	IgG2b	FC	1:100	BD
MUNC13-4	poly	Gt	Ms, Hu		IF, WB	1:500	Novus Biol
MUNC18-2	poly	Rb	Ms, Hu		IF, WB	1:200	Synaptic Sys
perforin	poly	Rb	Ms		WB	1:1000	Cell Sig
pS6			Ms				
pY	4G10	Ms	Ms	IgG2b	WB	1:2000	Millipore
SNAP23						1:100	Roche lab (NIH)
SYTI					IF, WB	1:1000	Synaptic Sys
SYTVII	poly	Rb	Ms, Rt, Hu		IF, WB	1:150, 1:1000	Synaptic Sys
STX11	poly	Rb	Ms, Rt, Hu		IF, WB	1:150, 1:1000	Synaptic Sys
talin	8D4	Ms	Ms, Rt, Hu		IF		Sigma
TCRβ	H57-957	Ar Ham	Ms	IgG2	FC	1:500	eBio, BD
TNFα	MP6XT22	Rt	Ms	IgG1	FC	1:200	eBio
Vα2	B20.1	Rt	Ms	IgG2a	FC	1:500	eBio, BD

Abbreviations: FC, flow cytometry; IF, immunofluorescence; WB, Western blotting

5.4 Cell culture

in vitro activated mouse CTLs and primary B cells

To generate *in vitro* activated mouse CTLs, whole splenocytes from naïve WT or *Itk*$^{-/-}$ OT-I mice were harvested and stimulated at 0.5x10^6 cells/mL with 10nM $OVA_{257-264}$ peptide (AnaSpec) for 3 days in RPMI 10 at 37C with 5% CO_2. Cells were then washed once and resuspended at 0.5x10^6 cells/mL in RPMI 10 plus 10 IU/mL recombinant human IL-2 (rHIL-2) and seeded in fresh media plus rhIL-2 every 48 hours. All experiments were performed with CTLs between 6 and 8 days after primary *in vitro* stimulation, unless otherwise indicated. Resting B cells were purified by negative selection with αCD43 microbeads (Miltenyi) and activated with 1μg/mL LPS from *E. coli* (Enzo Life Sciences) in RPMI 10 for 2-3 days before use as targets in all assays.

Cell lines

MC57 and P815 cell lines were maintained in DMEM10. EL4 cell lines were maintained in RPMI 10. Stably transduced EL4-tagRFP-MEM and EL4-GCaMP6 cell lines were a generous gift of the Lippincott-Schwartz lab and maintained in RPMI10. 293T cell lines were maintained in EMEM10.

Human allo-activated CD8+ T cells

Blood from healthy donors was obtained at the NIH Clinical Center under approved protocols. Peripheral blood mononuclear cells (PBMCs) were isolated from whole blood by density-gradient centrifugation using Lymphocyte Separation Medium (MP Biomedical), washed twice in phosphate buffered saline (PBS), and resuspended at $1x10^6$ cells/mL. One mL of cells was then added to each well of a 24-well plate and placed at 37° C. Mixed buffy coats for anti-allogeneic stimulation were irradiated and resuspended at $1x10^6$ cells/mL, and phytohemagglutinin (PHA)was added to the buffy coats at 2μg/mL. To stimulate lymphocytes, 1mL of activated buffy coat was added to each well for a final ratio of 1:1 stimulators:responders in 1μg/mL PHA. PHA blasts were split as needed, and CD8+ T cells isolated using a CD8+ T cell isolation kit (MACS Miltenyi). Bulk CD8+ T cells were cultured for use in experiments. For inhibition experiments, previously activated WT OT-I CTLs or human CD8+ T cells were pre-treated for 10 minutes at 37°C with ITK inhibitor (gift of Craig Thomas) at indicated concentrations and used directly in assays without washing.

5.5 Flow Cytometry

Data were acquired on a FACS Calibur, LSRII, or AriaII (all BD Biosciences) and analyzed using FlowJo software (Tree Star).

Cell surface and intracellular staining

To stain surface markers cells were washed once in fluorescence activated cell sorting (FACS) buffer (PBS plus 2% FBS) and samples were incubated at 4°C in the presence of Fc block (BioXCell) for 10 minutes to reduce non-specific antibody binding. Cells were stained in 50μL of FACS buffer containing the appropriate antibodies for 20 minutes at 4°C. For antibodies not directly conjugated to fluorophores, primary antibody staining was followed by a second 20-minute incubation at 4°C with the appropriate species-specific fluorophore-conjugated secondary antibody. After staining, cells were washed twice in FACS buffer and fixed with 2% paraformaldehyde (PFA, Sigma-Aldrich). For intracellular staining, surface staining was followed by a fixation/permeabilization step using BD CytoFix/CytoPerm, 35 minutes at 4°C. Cells were then washed once in 1X Permeabilization Buffer (eBioscience) and stained in 50μL of Permeabilization Buffer containing the appropriate fluorophore-conjugated antibodies at 4°C for 35 minutes. After staining, cell were washed twice and resuspended in FACS buffer for analysis. For phospho-antibody staining, cells were fixed with 4% paraformaldehyde, methanol-permeabilized at -20 C, stained for 60 minutes at 4 C with indicated phospho-antibodies in PBS plus 1% Triton X-100 and 0.5% bovine serum albumin (BSA), and resuspended in PBS for analysis.

Fluorescence Activated Cell Sorting

To prepare cells for sorting, samples were washed once and resuspended in fluorescence-activated cell sorting (FACS) buffer at a concentration of $10x10^6$

cells/mL. If surface marker staining was required, samples were stained as described above. Cells were sorted directly into 10% complete medium plus IL-2, spun down for 10 minutes, and plated at $1x10^6$ cells/mL plus 10 IU/mL IL-2 for culture.

Proliferation assays

To evaluate cell proliferation, splenocytes were stained with 1μM Cell Trace Violet (CTV, Life Technologies) in PBS at 37 C for 10 minutes. Stained cells were washed three times with complete media and then stimulated in the presence of $OVA_{257-264}$. Cells were collected at indicated time points, stained with anti-CD8 antibodies, and evaluated via flow cytometry.

5.6 Cytotoxicity assays

Lactate dehydrogenase release

Cytolytic activity was determined *in vitro* using CytoTox Non-radioactive Cytotoxicity Assays (Promega) according to the manufacturer's instructions. Briefly, targets were pulsed with 1μM $OVA_{257-264}$ peptide for 1 hour at 37°C, washed twice, and resuspended in phenol red-free RPMI with 2% FBS (assay buffer). Activated CTLs were washed and resuspended in assay buffer, added to 96 well plates and titrated in assay buffer. Targets or assay buffer were added to wells to achieve appropriate effector:target ratios and control groups, and plates were incubated for 4

hours at 37°C. Twenty minutes before the completion of the assay, lysis buffer was added to control wells for maximum lactate dehydrogenase (LDH) release from target cells. Supernatants were then transferred to plates containing chromogenic assay substrate and the OD read at 490nm on a Thermomax plate reader to measure lactate dehydrogenase (LDH) release. Percent cytotoxicity was calculated as $\{[(E-M_{bkgnd})-(CTL_{sp}-M_{bkgnd})-(T_{sp}-M_{bkgnd})]/[T_{max}-(T_{sp}-M_{bkgnd})-V_c]\}$ x100, where E is the measured LDH release value, CTL_{sp} represents the spontaneous LDH release from CTLs alone, T_{sp} is the spontaneous release of LDH from targets alone, T_{max} is the maximum value of LDH release from lysed target cells, M_{bkgnd} is the assay buffer background, and V_c is the volume correction control for the addition of lysis buffer to obtain maximum LDH release.

FACS-based cytotoxicity

In vitro cytolytic activity was also evaluated by FACS. Targets were stained with 1μM Cell Trace Violet (CTV, Life Technologies) as previously described. Targets were either left unpulsed as a control, or pulsed with 1μM $OVA_{257-264}$ peptide for 1 hour at 37°C, washed twice, and resuspended in 10% complete medium. Activated CTLs were washed and resuspended in assay buffer, added to 96 well round bottom plates and titrated in 10% complete medium. Control, non-pulsed, or pulsed targets were added to wells with T cells to achieve appropriate effector:target ratios, and additional wells set up with target cells alone to control for spontaneous target cell death. Plates were centrifuged at 500RPM for one minute, and incubated

at 37°C. After 4-6 hours, plates were centrifuged, and supernatants discarded. Cells were then stained with αCD8-PECy7 antibodies and LiveDead green for 20 minutes at 4C, and washed once with FACS buffer before analysis. For more sensitive measurement of cell death, some samples were labeled with Annexin V. For AnnexinV staining, an additional single wash in 1x AnnexinV staining buffer (BioLegend) was performed, and cells were resuspended in 1x AnnexinV buffer plus allophycocyanin (APC)-conjugated AnnexinV. Plates were incubated in the dark at room temperature for 20 minutes, and additional 1x AnnexinV buffer was added to each well. Plates were read within the hour on a LSRII instrument using a high throughput sampler. For analysis, the CTV+ LiveDead+ (or AnnexinV-) population represents the target cells that have been killed, while the CTV+ LiveDead- (or AnnexinV+) population represents the remaining viable target cells in each well. Percent cytotoxicity was calculated as: 100 – [(viable CTV+ cells in sample)/(viable CTV+ cells in control)] x 100, where CTV+ cells in sample are cells in experimental wells, and viable CTV+ cells in control are cells in wells without T cells.

in vivo cytotoxicity

To examine cytolytic activity *in vivo*, indicated numbers of either WT or ITK-deficient CTLs were adoptively transferred via retro-orbital injection into naïve WT C57BL/6 hosts. LPS-activated B cell targets from WT GFP mice were labeled with either 0.2μM or 2μM Cell Trace Violet (CTV, eBioscience). 0.2μM-dyed B cell targets were left unpulsed as a control, and 2μM-dyed target were pulsed with 1μM OVA_{257-}

$_{264}$ peptide for 1 hour at 37°C. B cells were then mixed at a 1:1 ratio and transferred via retro-orbital injection into mice 24 hours after injection of CTLs. Spleens were harvested at indicated time points and populations analyzed via flow cytometry. Transferred B cells were distinguished from recipient B cells by gating on the GFP-positive population, and peptide pulsed versus non-pulsed targets were distinguished by the intensity of CTV fluorescence. Percent cytotoxicity was calculated as = 100 – {[(T_{pulsed}/$T_{non\text{-}pulsed}$)/(C_{pulsed}/$C_{non\text{-}pulsed}$)] x 100}, where T_{pulsed} is the percentage of peptide-pulsed targets harvested from spleens of recipients, $T_{non\text{-}pulsed}$ is the percentage of non-pulsed targets harvested from spleens of recipients, C_{pulsed} is the percentage of peptide-pulsed targets harvested from spleens of PBS recipients, and $C_{non\text{-}pulsed}$ is the percentage of non-pulsed targets harvested from spleens of PBS recipients.

5.7 T:target conjugate assays

For FACS-based conjugate assays, LPS-activated primary B cells, EL4, or MC57 targets were stained with 0.1μM carboxyfluorescein diacetate succinimidyl ester (CFSE), and pulsed with peptide at the concentrations indicated for 1 hour at 37°C or left unpulsed as a control. After washing, targets were mixed with previously activated CTLs at a 2:1 T:target ratio in 96-well round bottom plates, centrifuged, and incubated for 20 minutes at 37°C. Cells were washed and stained with α-CD8α-PerCPCy5.5 or –APC and conjugates enumerated via flow cytometry, where the CD8+CFSE double positive population represented T cells forming conjugates with targets.

5.8 Degranulation assays

For degranulation assays, activated CTLs were stimulated in plates coated with αCD3ε (BioXCell) or mixed at a 1:1 ratio with peptide-pulsed or unpulsed targets at 37°C in the presence of αCD107a-PE or –APC labeled antibody. At indicated time points, plates were placed on ice and cells transferred into cold PBS, stained with αCD8α and αCD107a-FITC antibodies, and analyzed via flow cytometry.

5.9 Intracellular cytokine production

To measure intracellular cytokine production, cells were stimulated with plate-bound αCD3ε or mixed at a 1:1 ratio with peptide-pulsed or non-pulsed targets at 37°C for 4-6 hours in the presence of 1μL/mL Golgi Stop containing monensin (BD Biosciences). Surface and intracellular staining was then done as described above.

5.10 Biochemistry

Preparation of total T cell lysates and immunoblotting

To obtain total lysates, naïve or previously activated CD8+ T cells were washed twice in PBS, resuspended in serum-free medium, and rested at 37C for two hours. Cells were then spun down and $1x10^6$ to $5x10^6$ cells were resuspended in 50μL. For lysis, 50μL of 2x loading buffer plus 2-mercaptoethanol heated to 99C was added to cells and transferred to a 99C heating block for 5 minutes. A size standard

and lysates were loaded onto Tris-glycine gels and run between 90V and 120V for two hours, transferred to nitrocellulose membranes using an iBlot dry blotting system (Thermo Fisher Scientific), and incubated for one hour at room temperature in 1% BSA in Tris-buffered saline plus 0.1% Tween (TBS-T), to block non-specific antibody binding. Membranes were blotted overnight at 4C with primary antibody in TBS-T, washed 4x for five minutes each with TBS-T and blotted with the appropriate secondary antibody for one hour at room temperature, protected from light. Following four washes in TBS-T, blots were imaged using an Odyssey Infrared Imaging System (LICOR Biosciences).

5.11 T cell transfections

The Amaxa Mouse T Cell Nucleofector kit (Lonza) was used to transfect primary T cells. Briefly, 2mL per reaction of proprietary rescue medium was supplemented with 10% FBS, 2mM L-glutamine, and 10µL/mL of proprietary Medium Supplement A and B, and incubated at 37C with 5% CO_2 for a minimum of 1 hour before use. For each reaction, 85µL of Nucleofector solution was mixed with 19µL of proprietary Supplement 2 provided with the kit, and 2µg of the plasmid of interest. Between $5x10^6$ and $10x10^6$ CD8+ T cells were centrifuged at 600RPM for 5 minutes, and resuspended gently, using a wide-bore tip, in the supplemented Nucleofector solution. Cells were then transferred into an electroporation cuvette, and transfected using X-001 CD8 T cell program on a Nucleofector 2b Device (Lonza). Immediately after electroporation, cells were transferred to the rescue

medium for 2-3 hours before being split into additional wells containing pre-warmed RPMI 10 containing 10IU rhIL-2 for continued culture.

5.12 Retroviral transductions

Plasmids

The LifeAct-mApple construct and LAMP1-eGFP cloned into the pMIGR retroviral expression vector were gifts from the Lippincott-Schwartz lab (NICHD, NIH). Constructs coding for the lipid binding domains of Tubby and AKT fused to eGFP were provided by Tamas Balla (NICHD, NIH). The pCL-Eco retroviral packaging vector has been previously described [177].

Generation of retroviral supernatants

Retroviral supernatants were generated through the transient transfection of HEK293T cells using TransIT-293 Transfection Reagent (Mirus). Eighteen to 24 hours before transfection, $1.5x10^6$ HEK293T cells were plated in 2.5mL complete 10% EMEM per well in a six well plate. Immediately before transfection, TransIT-293 Reagent was warmed to room temperature and vortexed gently. For each well of the six well plate, 2μg of plasmid DNA, 1μg of packaging plasmid, and 9μL of TransIT-293 Reagent were added to 300μL of Opti-MEM Reduced-Serum Medium and mixed by pipetting. After incubation at room temperature for 15-30 minutes, the TransIT-293 Reagent:DNA complex was added drop wise to different areas of the

each well in the six well plate, gently rocked, and plates were incubated for 48 hours before supernatants were harvested.

Transductions

30 hours prior to transduction, whole splenocytes from naïve WT or *Itk*$^{-/-}$ OT-I mice were harvested and stimulated at 0.5x10^6 cells/mL with 10nM $OVA_{257-264}$ peptide (AnaSpec) in 10% complete RPMI. Cells were washed and 2x10^6 activated OT-I T cells were plated per well in a 24-well plate. Viral supernatants were harvested and centrifuged for 10 minutes at 2000 RPM to remove cell debris. Supernatants were transferred to a fresh conical tube, and Polybrene and IL2 were added at a final concentration of 8μg/mL and 10IU/mL, respectively. 1mL per well of viral supernatants were added per well and plates were spun down at 2000 RPM for 90 minutes at 37°C. After transduction, supernatants were removed and replaced with fresh media plus IL2 for continued culture.

5.13 Microscopy

All microscopy used an Axio Observer Z1 microscope (Carl Zeiss Inc.) with oil immersion Plan-Apochromat 40x, 63x, or 100x objectives. Spinning disc images were acquired with a Zeiss Yokogawa Spinning Disk system mounted on the microscope using a 16-bit Photometrics Evolve EMCCD camera (Photometrics); TIRF images were acquired on the same microscope, without the spinning disk attachment and using a cMOS camera (PCO Edge). Image acquisition was

controlled using Zeiss Zen Blue Software. Data were analyzed with Imaris Scientific Image Processing and Analysis Software (Bitplane Scientific Software) and ImageJ (NIH) software.

Confocal microscopy of fixed cells

To prepare conjugates for immunofluorescence microscopy, targets were pulsed with 1μM $OVA_{257-264}$ at 37°C for 1 hour, washed twice, and resuspended in pre-warmed phenol red-free RPMI (imaging media). Activated CTLs were washed and resuspended in imaging medium and mixed with peptide-pulsed targets at a 1:1 ratio. Cells were incubated at 37°C for 15 minutes to allow conjugate formation and then plated on glass multi-well slides on previously coated with 0.01% poly-L-lysine for 5 minutes at 37°C. Cells were fixed and permeabilized with cold methanol on ice or fixed at room temperature with 2% paraformaldehyde for 5 minutes, followed by several washes in PBS. Methanol-fixed cells were blocked for 30 minutes at room temperature in 1% BSA in PBS plus Fc block (blocking buffer). PFA-fixed cells were quenched for 10 minutes with 5mM glycine, and permeabilized and blocked with 0.2% saponin in blocking buffer for 30 minutes at room temperature. Cells were incubated with primary antibodies in blocking buffer for 1 hour at room temperature, washed in either blocking buffer or blocking buffer containing 0.2% saponin, followed by a 45-minute incubation with secondary antibodies at room temperature, and washed several times. Samples were preserved using ProLong Gold with DAPI (Life

Technologies) and no. 1.5 cover glass (VWR), and imaged using an Axio Observer Z1 microscope (Carl Zeiss Inc.).

Spinning disc live confocal imaging

To prepare cells for live imaging, previously activated and transduced cells were sorted on a BD Aria III instrument. Samples were washed once and resuspended in FACS buffer at a concentration of $10x10^6$ cells/mL. Cells were sorted directly into 10% complete medium, spun down for 10 minutes, and plated at $1x10^6$ cells/mL plus 10 IU/mL rhIL-2 for culture. Alternatively, activated CTLs were transfected using a Mouse T Cell Nucleofector kit (see above) and immediately transferred into manufacturer-provided rescue medium plus rhIL-2 for 18 hours before imaging. Cells were imaged within 6 to 24 hours after transfection, depending on the plasmid. For imaging, peptide-pulsed targets were resuspended in serum-free imaging medium at $1\text{-}2x10^6$ cells/mL and allowed to settle at 37C in chambers (Nunc, Lab-Tek) previously coated overnight at 4C with 0.5µg/mL ICAM-1/FC (R&D Systems). After 5 minutes, chambers were gently washed with imaging medium and placed on the microscope with heat and CO_2. Transfected or transduced CTLs were resuspended at $10x10^6$-$20x10^6$ cells/mL in 150uL of imaging medium and added drop wise into the chamber containing the plated target cells. Serial confocal 1µm z stacks were taken at 25-second intervals, and imaging began within minutes of addition of the CTLs to each chamber.

Total internal reflection fluorescence microscopy

For total internal reflection fluorescence (TIRF) microscopy imaging, CTLs were plated on #1.5 cover glass 8-well imaging chambers (Lab-Tek) previously coated with 0.01% poly-L-lysine (Sigma) and anti-CD3ε in pre-warmed imaging media. Retrovirally transduced and sorted or transfected cells were added drop wise into chambers, and images were acquired every 3 seconds using the Axio Observer Z1 microscope (Carl Zeiss Inc.) with TIRF fiber illuminator and oil immersion 100x TIRF objective.

Transmission electron microscopy

To prepare cells for transmission electron microscopy (TEM), WT and *Itk*$^{-/-}$ OT-I splenocytes were activated for three days in the presence of $OVA_{257-264}$ as previously described, and frozen before shipment to the Griffiths lab where Dr. Jane Stinchcombe performed all TEM and analysis. For TEM, vial contents were thawed into medium plus IL-2 for 48 hours to allow for the recovery and expansion of CTLs, after which they were labeled overnight with horseradish peroxidase (HRP, Boehringer Ingelheim) to load secretory lysosomes. The following day, EL-4 targets were pulsed with either 1μM or 10nM $OVA_{257-264}$ to generate conjugates with CTLs for TEM. Cells were fixed, processed, and imaged as previously described [41, 67].

5.14 Statistical analysis

All statistical analysis (Student's t tests and two-way ANOVA) was performed using Microsoft Excel or GraphPad Prism software. p values less than 0.05 were considered statistically significant.

References

1. Doudna, JA and E Charpentier (2014). "Genome editing. The new frontier of genome engineering with CRISPR-Cas9." Science 346(6213): 1258096.

2. Saito, T, F Hochstenbach, S Marusic-Galesic, AM Kruisbeek, M Brenner, and RN Germain (1988). "Surface expression of only gamma delta and/or alpha beta T cell receptor heterodimers by cells with four (alpha, beta, gamma, delta) functional receptor chains." J Exp Med 168(3): 1003-20.

3. Clevers, H, B Alarcon, T Wileman, and C Terhorst (1988). "The T cell receptor/CD3 complex: a dynamic protein ensemble." Annu Rev Immunol 6: 629-62.

4. van der Merwe, PA and O Dushek (2011). "Mechanisms for T cell receptor triggering." Nat Rev Immunol 11(1): 47-55.

5. Call, ME and KW Wucherpfennig (2005). "The T cell receptor: critical role of the membrane environment in receptor assembly and function." Annu Rev Immunol 23: 101-25.

6. Huang, YH and K Sauer (2010). "Lipid signaling in T-cell development and function." Cold Spring Harb Perspect Biol 2(11): a002428.

7. Berg, LJ, LD Finkelstein, JA Lucas, and PL Schwartzberg (2005). "Tec family kinases in T lymphocyte development and function." Annu Rev Immunol 23: 549-600.

8. Andreotti, AH, PL Schwartzberg, RE Joseph, and LJ Berg (2010). "T-cell signaling regulated by the Tec family kinase, Itk." Cold Spring Harb Perspect Biol 2(7): a002287.

9. Min, L, W Wu, RE Joseph, DB Fulton, L Berg, and AH Andreotti (2010). "Disrupting the intermolecular self-association of Itk enhances T cell signaling." J Immunol 184(8): 4228-35.

10. Joseph, RE, L Min, R Xu, ED Musselman, and AH Andreotti (2007). "A remote substrate docking mechanism for the tec family tyrosine kinases." Biochemistry 46(18): 5595-603.

11. Schaeffer, EM and PL Schwartzberg (2000). "Tec family kinases in lymphocyte signaling and function." Curr Opin Immunol 12(3): 282-8.

12. Liu, KQ, SC Bunnell, CB Gurniak, and LJ Berg (1998). "T cell receptor-initiated calcium release is uncoupled from capacitative calcium entry in Itk-deficient T cells." The Journal of Experimental Medicine 187(10): 1721-7.

13. Fowell, DJ, K Shinkai, XC Liao, AM Beebe, RL Coffman, DR Littman, and RM Locksley (1999). "Impaired NFATc translocation and failure of Th2 development in Itk-deficient CD4+ T cells." Immunity 11(4): 399-409.

14. Grasis, JA and CD Tsoukas (2011). "Itk: the rheostat of the T cell response." J Signal Transduct 2011: 297868.

15. Hogan, PG, RS Lewis, and A Rao (2010). "Molecular basis of calcium signaling in lymphocytes: STIM and ORAI." Annu Rev Immunol 28: 491-533.

16. Berrebi, G, H Takayama, and MV Sitkovsky (1987). "Antigen-receptor interaction requirement for conjugate formation and lethal-hit triggering by cytotoxic T lymphocytes can be bypassed by protein kinase C activators and Ca2+ ionophores." Proc Natl Acad Sci U S A 84(5): 1364-8.

17. Au-Yeung, BB, SD Katzman, and DJ Fowell (2006). "Cutting edge: Itk-dependent signals required for CD4+ T cells to exert, but not gain, Th2 effector function." J Immunol 176(7): 3895-9.

18. Boyman, O and J Sprent (2012). "The role of interleukin-2 during homeostasis and activation of the immune system." Nat Rev Immunol 12(3): 180-90.

19. Kundig, TM, H Schorle, MF Bachmann, H Hengartner, RM Zinkernagel, and I Horak (1993). "Immune responses in interleukin-2-deficient mice." Science 262(5136): 1059-61.

20. Pipkin, ME, JA Sacks, F Cruz-Guilloty, MG Lichtenheld, MJ Bevan, and A Rao (2010). "Interleukin-2 and inflammation induce distinct transcriptional programs that promote the differentiation of effector cytolytic T cells." Immunity 32(1): 79-90.

21. Voisinne, G, BG Nixon, A Melbinger, G Gasteiger, M Vergassola, and G Altan-Bonnet (2015). "T Cells Integrate Local and Global Cues to Discriminate between Structurally Similar Antigens." Cell Rep 11(8): 1208-19.

22. Powell, JD, KN Pollizzi, EB Heikamp, and MR Horton (2012). "Regulation of immune responses by mTOR." Annu Rev Immunol 30: 39-68.

23. Finlay, DK, E Rosenzweig, LV Sinclair, C Feijoo-Carnero, JL Hukelmann, J Rolf, AA Panteleyev, K Okkenhaug, and DA Cantrell (2012). "PDK1 regulation of mTOR and hypoxia-inducible factor 1 integrate metabolism and migration of CD8+ T cells." The Journal of Experimental Medicine 209(13): 2441-53.

24. Takemoto, N, AM Intlekofer, JT Northrup, EJ Wherry, and SL Reiner (2006). "Cutting Edge: IL-12 inversely regulates T-bet and eomesodermin expression during pathogen-induced CD8+ T cell differentiation." J Immunol 177(11): 7515-9.

25. Kaech, SM and W Cui (2012). "Transcriptional control of effector and memory CD8+ T cell differentiation." Nat Rev Immunol 12(11): 749-61.

26. Cruz-Guilloty, F, ME Pipkin, IM Djuretic, D Levanon, J Lotem, MG Lichtenheld, Y Groner, and A Rao (2009). "Runx3 and T-box proteins cooperate to establish the transcriptional program of effector CTLs." J Exp Med 206(1): 51-9.

27. Joshi, NS, W Cui, CX Dominguez, JH Chen, TW Hand, and SM Kaech (2011). "Increased numbers of preexisting memory CD8 T cells and decreased T-bet expression can restrain terminal differentiation of secondary effector and memory CD8 T cells." J Immunol 187(8): 4068-76.

28. Intlekofer, AM, N Takemoto, C Kao, A Banerjee, F Schambach, JK Northrop, H Shen, EJ Wherry, and SL Reiner (2007). "Requirement for T-bet in the aberrant differentiation of unhelped memory CD8+ T cells." J Exp Med 204(9): 2015-21.

29. Pearce, EL, AC Mullen, GA Martins, CM Krawczyk, AS Hutchins, VP Zediak, M Banica, CB DiCioccio, DA Gross, CA Mao, H Shen, N Cereb, SY Yang, T Lindsten, J Rossant, CA Hunter, and SL Reiner (2003). "Control of effector CD8+ T cell function by the transcription factor Eomesodermin." Science 302(5647): 1041-3.

30. Pachlopnik Schmid, J, M Cote, MM Menager, A Burgess, N Nehme, G Menasche, A Fischer, and G de Saint Basile (2010). "Inherited defects in lymphocyte cytotoxic activity." Immunol Rev 235(1): 10-23.

31. Kupfer, A and G Dennert (1984). "Reorientation of the microtubule-organizing center and the Golgi apparatus in cloned cytotoxic lymphocytes triggered by binding to lysable target cells." J Immunol 133(5): 2762-6.

32. Cannon, JL and JK Burkhardt (2002). "The regulation of actin remodeling during T-cell-APC conjugate formation." Immunol Rev 186: 90-9.

33. Stinchcombe, JC, E Majorovits, G Bossi, S Fuller, and GM Griffiths (2006). "Centrosome polarization delivers secretory granules to the immunological synapse." Nature 443(7110): 462-5.

34. Ritter, AT, Y Asano, JC Stinchcombe, NM Dieckmann, BC Chen, C Gawden-Bone, S van Engelenburg, W Legant, L Gao, MW Davidson, E Betzig, J Lippincott-Schwartz, and GM Griffiths (2015). "Actin depletion initiates events leading to granule secretion at the immunological synapse." Immunity 42(5): 864-76.

35. Dennert, G and ER Podack (1983). "Cytolysis by H-2-specific T killer cells. Assembly of tubular complexes on target membranes." J Exp Med 157(5): 1483-95.

36. Masson, D and J Tschopp (1987). "A family of serine esterases in lytic granules of cytolytic T lymphocytes." Cell 49(5): 679-85.

37. Masson, D and J Tschopp (1985). "Isolation of a lytic, pore-forming protein (perforin) from cytolytic T-lymphocytes." J Biol Chem 260(16): 9069-72.

38. Henkart, P, M Henkart, P Millard, P Frederikse, J Bluestone, R Blumenthal, C Yue, and C Reynolds (1985). "The role of cytoplasmic granules in cytotoxicity by large granular lymphocytes and cytotoxic T lymphocytes." Advances in Experimental Medicine and Biology 184: 121-38.

39. Paul, WE and RA Seder (1994). "Lymphocyte responses and cytokines." Cell 76(2): 241-51.

40. Monks, CR, BA Freiberg, H Kupfer, N Sciaky, and A Kupfer (1998). "Three-dimensional segregation of supramolecular activation clusters in T cells." Nature 395(6697): 82-6.

41. Stinchcombe, JC, G Bossi, S Booth, and GM Griffiths (2001). "The immunological synapse of CTL contains a secretory domain and membrane bridges." Immunity 15(5): 751-61.

42. Purbhoo, MA, DJ Irvine, JB Huppa, and MM Davis (2004). "T cell killing does not require the formation of a stable mature immunological synapse." Nat Immunology 5(5): 524-30.

43. Grakoui, A, SK Bromley, C Sumen, MM Davis, AS Shaw, PM Allen, and ML Dustin (1999). "The immunological synapse: a molecular machine controlling T cell activation." Science 285(5425): 221-7.

44. Ehrlich, LI, PJ Ebert, MF Krummel, A Weiss, and MM Davis (2002). "Dynamics of p56lck translocation to the T cell immunological synapse following agonist and antagonist stimulation." Immunity 17(6): 809-22.

45. Bunnell, SC, DI Hong, JR Kardon, T Yamazaki, CJ McGlade, VA Barr, and LE Samelson (2002). "T cell receptor ligation induces the formation of dynamically regulated signaling assemblies." J Cell Biol 158(7): 1263-75.

46. Lee, KH, AD Holdorf, ML Dustin, AC Chan, PM Allen, and AS Shaw (2002). "T cell receptor signaling precedes immunological synapse formation." Science 295(5559): 1539-42.

47. Varma, R, G Campi, T Yokosuka, T Saito, and ML Dustin (2006). "T cell receptor-proximal signals are sustained in peripheral microclusters and terminated in the central supramolecular activation cluster." Immunity 25(1): 117-27.

48. Ksionda, O, A Saveliev, R Kochl, J Rapley, M Faroudi, JE Smith-Garvin, C Wulfing, K Rittinger, T Carter, and VL Tybulewicz (2012). "Mechanism and function of Vav1 localisation in TCR signalling." J Cell Sci 125(Pt 22): 5302-14.

49. Perica, K, JG Bieler, M Edidin, and J Schneck (2012). "Modulation of MHC binding by lateral association of TCR and coreceptor." Biophys J 103(9): 1890-8.

50. Zhao, F, JL Cannons, M Dutta, GM Griffiths, and PL Schwartzberg (2012). "Positive and Negative Signaling through SLAM Receptors Regulate Synapse Organization and Thresholds of Cytolysis." Immunity 36(6): 1003-16.

51. Kupfer, A and SJ Singer (1989). "Cell biology of cytotoxic and helper T cell functions: immunofluorescence microscopic studies of single cells and cell couples." Annu Rev Immunol 7: 309-37.

52. Sept, D and JA McCammon (2001). "Thermodynamics and kinetics of actin filament nucleation." Biophys J 81(2): 667-74.

53. Ochs, HD and AJ Thrasher (2006). "The Wiskott-Aldrich syndrome." J Allergy Clin Immunol 117(4): 725-38; quiz 739.

54. Goley, ED and MD Welch (2006). "The ARP2/3 complex: an actin nucleator comes of age." Nat Rev Mol Cell Biol 7(10): 713-26.

55. Pollard, TD (2007). "Regulation of actin filament assembly by Arp2/3 complex and formins." Annu Rev Biophys Biomol Struct 36: 451-77.

56. Gomez, TS, K Kumar, RB Medeiros, Y Shimizu, PJ Leibson, and DD Billadeau (2007). "Formins regulate the actin-related protein 2/3 complex-independent polarization of the centrosome to the immunological synapse." Immunity 26(2): 177-90.

57. Mace, EM and JS Orange (2014). "Lytic immune synapse function requires filamentous actin deconstruction by Coronin 1A." Proc Natl Acad Sci U S A 111(18): 6708-13.

58. Brown, AC, S Oddos, IM Dobbie, JM Alakoskela, RM Parton, P Eissmann, MA Neil, C Dunsby, PM French, I Davis, and DM Davis (2011). "Remodelling of cortical actin where lytic granules dock at natural killer cell immune

synapses revealed by super-resolution microscopy." PLoS Biol 9(9): e1001152.

59. Rak, GD, EM Mace, PP Banerjee, T Svitkina, and JS Orange (2011). "Natural killer cell lytic granule secretion occurs through a pervasive actin network at the immune synapse." PLoS Biol 9(9): e1001151.

60. Griffiths, GM, A Tsun, and JC Stinchcombe (2010). "The immunological synapse: a focal point for endocytosis and exocytosis." J Cell Biol 189(3): 399-406.

61. Fukata, M, T Watanabe, J Noritake, M Nakagawa, M Yamaga, S Kuroda, Y Matsuura, A Iwamatsu, F Perez, and K Kaibuchi (2002). "Rac1 and Cdc42 capture microtubules through IQGAP1 and CLIP-170." Cell 109(7): 873-85.

62. Combs, J, SJ Kim, S Tan, LA Ligon, EL Holzbaur, J Kuhn, and M Poenie (2006). "Recruitment of dynein to the Jurkat immunological synapse." Proc Natl Acad Sci U S A 103(40): 14883-8.

63. Geiger, B, D Rosen, and G Berke (1982). "Spatial relationships of microtubule-organizing centers and the contact area of cytotoxic T lymphocytes and target cells." J Cell Biol 95(1): 137-43.

64. Lowin-Kropf, B, VS Shapiro, and A Weiss (1998). "Cytoskeletal polarization of T cells is regulated by an immunoreceptor tyrosine-based activation motif-dependent mechanism." J Cell Biol 140(4): 861-71.

65. Kuhne, MR, J Lin, D Yablonski, MN Mollenauer, LI Ehrlich, J Huppa, MM Davis, and A Weiss (2003). "Linker for activation of T cells, zeta-associated protein-70, and Src homology 2 domain-containing leukocyte protein-76 are required for TCR-induced microtubule-organizing center polarization." J Immunol 171(2): 860-6.

66. Tsun, A, I Qureshi, JC Stinchcombe, MR Jenkins, M de la Roche, J Kleczkowska, R Zamoyska, and GM Griffiths (2011). "Centrosome docking at the immunological synapse is controlled by Lck signaling." J Cell Biol 192(4): 663-74.

67. Jenkins, MR, A Tsun, JC Stinchcombe, and GM Griffiths (2009). "The strength of T cell receptor signal controls the polarization of cytotoxic machinery to the immunological synapse." Immunity 31(4): 621-31.

68. Au-Yeung, BB, SE Levin, C Zhang, LY Hsu, DA Cheng, N Killeen, KM Shokat, and A Weiss (2010). "A genetically selective inhibitor demonstrates a function for the kinase Zap70 in regulatory T cells independent of its catalytic activity." Nat Immunol 11(12): 1085-92.

69. Huse, M, LO Klein, AT Girvin, JM Faraj, QJ Li, MS Kuhns, and MM Davis (2007). "Spatial and temporal dynamics of T cell receptor signaling with a photoactivatable agonist." Immunity 27(1): 76-88.

70. Quann, EJ, E Merino, T Furuta, and M Huse (2009). "Localized diacylglycerol drives the polarization of the microtubule-organizing center in T cells." Nat Immunol 10(6): 627-35.

71. Liu, X, TM Kapoor, JK Chen, and M Huse (2013). "Diacylglycerol promotes centrosome polarization in T cells via reciprocal localization of dynein and myosin II." Proceedings of the National Academy of Sciences of the United States of America.

72. Martin-Cofreces, NB, J Robles-Valero, JR Cabrero, M Mittelbrunn, M Gordon-Alonso, CH Sung, B Alarcon, J Vazquez, and F Sanchez-Madrid (2008). "MTOC translocation modulates IS formation and controls sustained T cell signaling." J Cell Biol 182(5): 951-62.

73. Quann, EJ, X Liu, G Altan-Bonnet, and M Huse (2011). "A cascade of protein kinase C isozymes promotes cytoskeletal polarization in T cells." Nat Immunol 12(7): 647-54.

74. Fontana, S, S Parolini, W Vermi, S Booth, F Gallo, M Donini, M Benassi, F Gentili, D Ferrari, LD Notarangelo, P Cavadini, E Marcenaro, S Dusi, M Cassatella, F Facchetti, GM Griffiths, A Moretta, LD Notarangelo, and R Badolato (2006). "Innate immunity defects in Hermansky-Pudlak type 2 syndrome." Blood 107(12): 4857-64.

75. Clark, RH, JC Stinchcombe, A Day, E Blott, S Booth, G Bossi, T Hamblin, EG Davies, and GM Griffiths (2003). "Adaptor protein 3-dependent microtubule-mediated movement of lytic granules to the immunological synapse." Nature Immunology 4(11): 1111-20.

76. Kurowska, M, N Goudin, NT Nehme, M Court, J Garin, A Fischer, G de Saint Basile, and G Menasche (2012). "Terminal transport of lytic granules to the immune synapse is mediated by the kinesin-1/Slp3/Rab27a complex." Blood 119(17): 3879-89.

77. Menasche, G, E Pastural, J Feldmann, S Certain, F Ersoy, S Dupuis, N Wulffraat, D Bianchi, A Fischer, F Le Deist, and G de Saint Basile (2000). "Mutations in RAB27A cause Griscelli syndrome associated with haemophagocytic syndrome." Nature genetics 25(2): 173-6.

78. Wilson, SM, R Yip, DA Swing, TN O'Sullivan, Y Zhang, EK Novak, RT Swank, LB Russell, NG Copeland, and NA Jenkins (2000). "A mutation in Rab27a causes the vesicle transport defects observed in ashen mice." Proceedings of

the National Academy of Sciences of the United States of America 97(14): 7933-8.

79. Stinchcombe, JC, DC Barral, EH Mules, S Booth, AN Hume, LM Machesky, MC Seabra, and GM Griffiths (2001). "Rab27a is required for regulated secretion in cytotoxic T lymphocytes." The Journal of Cell Biology 152(4): 825-34.

80. Haddad, EK, X Wu, JA Hammer, 3rd, and PA Henkart (2001). "Defective granule exocytosis in Rab27a-deficient lymphocytes from Ashen mice." J Cell Biol 152(4): 835-42.

81. Holt, O, E Kanno, G Bossi, S Booth, T Daniele, A Santoro, M Arico, C Saegusa, M Fukuda, and GM Griffiths (2008). "Slp1 and Slp2-a localize to the plasma membrane of CTL and contribute to secretion from the immunological synapse." Traffic 9(4): 446-57.

82. Menasche, G, MM Menager, JM Lefebvre, E Deutsch, R Athman, N Lambert, N Mahlaoui, M Court, J Garin, A Fischer, and G de Saint Basile (2008). "A newly identified isoform of Slp2a associates with Rab27a in cytotoxic T cells and participates to cytotoxic granule secretion." Blood 112(13): 5052-62.

83. de Saint Basile, G, G Menasche, and A Fischer (2010). "Molecular mechanisms of biogenesis and exocytosis of cytotoxic granules." Nat Rev Immunol 10(8): 568-79.

84. Feldmann, J, I Callebaut, G Raposo, S Certain, D Bacq, C Dumont, N Lambert, M Ouachee-Chardin, G Chedeville, H Tamary, V Minard-Colin, E Vilmer, S Blanche, F Le Deist, A Fischer, and G de Saint Basile (2003). "Munc13-4 is essential for cytolytic granules fusion and is mutated in a form of familial hemophagocytic lymphohistiocytosis (FHL3)." Cell 115(4): 461-73.

85. Crozat, K, K Hoebe, S Ugolini, NA Hong, E Janssen, S Rutschmann, S Mudd, S Sovath, E Vivier, and B Beutler (2007). "Jinx, an MCMV susceptibility phenotype caused by disruption of Unc13d: a mouse model of type 3 familial hemophagocytic lymphohistiocytosis." J Exp Med 204(4): 853-63.

86. Menager, MM, G Menasche, M Romao, P Knapnougel, CH Ho, M Garfa, G Raposo, J Feldmann, A Fischer, and G de Saint Basile (2007). "Secretory cytotoxic granule maturation and exocytosis require the effector protein hMunc13-4." Nat Immunol 8(3): 257-67.

87. zur Stadt, U, S Schmidt, B Kasper, K Beutel, AS Diler, JI Henter, H Kabisch, R Schneppenheim, P Nurnberg, G Janka, and HC Hennies (2005). "Linkage of familial hemophagocytic lymphohistiocytosis (FHL) type-4 to chromosome 6q24 and identification of mutations in syntaxin 11." Human Molecular Genetics 14(6): 827-34.

88. Bryceson, YT, E Rudd, C Zheng, J Edner, D Ma, SM Wood, AG Bechensteen, JJ Boelens, T Celkan, RA Farah, K Hultenby, J Winiarski, PA Roche, M Nordenskjold, JI Henter, EO Long, and HG Ljunggren (2007). "Defective cytotoxic lymphocyte degranulation in syntaxin-11 deficient familial hemophagocytic lymphohistiocytosis 4 (FHL4) patients." Blood 110(6): 1906-15.

89. Hata, Y, CA Slaughter, and TC Sudhof (1993). "Synaptic vesicle fusion complex contains unc-18 homologue bound to syntaxin." Nature 366(6453): 347-51.

90. zur Stadt, U, J Rohr, W Seifert, F Koch, S Grieve, J Pagel, J Strauss, B Kasper, G Nurnberg, C Becker, A Maul-Pavicic, K Beutel, G Janka, G Griffiths, S Ehl, and HC Hennies (2009). "Familial hemophagocytic lymphohistiocytosis type 5 (FHL-5) is caused by mutations in Munc18-2 and impaired binding to syntaxin 11." Am J Hum Genet 85(4): 482-92.

91. Cote, M, MM Menager, A Burgess, N Mahlaoui, C Picard, C Schaffner, F Al-Manjomi, M Al-Harbi, A Alangari, F Le Deist, AR Gennery, N Prince, A Cariou, P Nitschke, U Blank, G El-Ghazali, G Menasche, S Latour, A Fischer, and G de Saint Basile (2009). "Munc18-2 deficiency causes familial hemophagocytic lymphohistiocytosis type 5 and impairs cytotoxic granule exocytosis in patient NK cells." J Clin Invest 119(12): 3765-73.

92. Takayama, H and MV Sitkovsky (1987). "Antigen receptor-regulated exocytosis in cytotoxic T lymphocytes." J Exp Med 166(3): 725-43.

93. Maul-Pavicic, A, SC Chiang, A Rensing-Ehl, B Jessen, C Fauriat, SM Wood, S Sjoqvist, M Hufnagel, I Schulze, T Bass, WW Schamel, S Fuchs, H Pircher, CA McCarl, K Mikoshiba, K Schwarz, S Feske, YT Bryceson, and S Ehl (2011). "ORAI1-mediated calcium influx is required for human cytotoxic lymphocyte degranulation and target cell lysis." Proc Natl Acad Sci U S A 108(8): 3324-9.

94. Chapman, ER (2008). "How does synaptotagmin trigger neurotransmitter release?" Annu Rev Biochem 77: 615-41.

95. Fowler, KT, NW Andrews, and JW Huleatt (2007). "Expression and function of synaptotagmin VII in CTLs." J Immunol 178(3): 1498-504.

96. Koh, TW and HJ Bellen (2003). "Synaptotagmin I, a Ca2+ sensor for neurotransmitter release." Trends Neurosci 26(8): 413-22.

97. Sugita, S, W Han, S Butz, X Liu, R Fernandez-Chacon, Y Lao, and TC Sudhof (2001). "Synaptotagmin VII as a plasma membrane Ca(2+) sensor in exocytosis." Neuron 30(2): 459-73.

98. Trenn, G, R Taffs, R Hohman, R Kincaid, EM Shevach, and M Sitkovsky (1989). "Biochemical characterization of the inhibitory effect of CsA on cytolytic T lymphocyte effector functions." J Immunol 142(11): 3796-802.

99. Dutz, JP, DA Fruman, SJ Burakoff, and BE Bierer (1993). "A role for calcineurin in degranulation of murine cytotoxic T lymphocytes." J Immunol 150(7): 2591-8.

100. Grybko, MJ, JP Bartnik, GA Wurth, AT Pores-Fernando, and A Zweifach (2007). "Calcineurin activation is only one calcium-dependent step in cytotoxic T lymphocyte granule exocytosis." J Biol Chem 282(25): 18009-17.

101. Heyeck, SD and LJ Berg (1993). "Developmental regulation of a murine T-cell-specific tyrosine kinase gene, Tsk." Proc Natl Acad Sci U S A 90(2): 669-73.

102. Siliciano, JD, TA Morrow, and SV Desiderio (1992). "itk, a T-cell-specific tyrosine kinase gene inducible by interleukin 2." Proc Natl Acad Sci U S A 89(23): 11194-8.

103. August, A, A Sadra, B Dupont, and H Hanafusa (1997). "Src-induced activation of inducible T cell kinase (ITK) requires phosphatidylinositol 3-kinase activity and the Pleckstrin homology domain of inducible T cell kinase." Proc Natl Acad Sci U S A 94(21): 11227-32.

104. Shan, X and RL Wange (1999). "Itk/Emt/Tsk activation in response to CD3 cross-linking in Jurkat T cells requires ZAP-70 and Lat and is independent of membrane recruitment." J Biol Chem 274(41): 29323-30.

105. Bunnell, SC, M Diehn, MB Yaffe, PR Findell, LC Cantley, and LJ Berg (2000). "Biochemical interactions integrating Itk with the T cell receptor-initiated signaling cascade." J Biol Chem 275(3): 2219-30.

106. Heyeck, SD, HM Wilcox, SC Bunnell, and LJ Berg (1997). "Lck phosphorylates the activation loop tyrosine of the Itk kinase domain and activates Itk kinase activity." The Journal of Biological Chemistry 272(40): 25401-8.

107. Andreotti, AH, SC Bunnell, S Feng, LJ Berg, and SL Schreiber (1997). "Regulatory intramolecular association in a tyrosine kinase of the Tec family." Nature 385(6611): 93-7.

108. Schaeffer, EM, J Debnath, G Yap, D McVicar, XC Liao, DR Littman, A Sher, HE Varmus, MJ Lenardo, and PL Schwartzberg (1999). "Requirement for Tec kinases Rlk and Itk in T cell receptor signaling and immunity." Science 284(5414): 638-41.

109. Dombroski, D, RA Houghtling, CM Labno, P Precht, A Takesono, NJ Caplen, DD Billadeau, RL Wange, JK Burkhardt, and PL Schwartzberg (2005). "Kinase-independent functions for Itk in TCR-induced regulation of Vav and the actin cytoskeleton." J Immunol 174(3): 1385-92.

110. Hao, S, Q Qi, J Hu, and A August (2006). "A kinase independent function for Tec kinase ITK in regulating antigen receptor induced serum response factor activation." FEBS Lett 580(11): 2691-7.

111. Gomez-Rodriguez, J, N Sahu, R Handon, TS Davidson, SM Anderson, MR Kirby, A August, and PL Schwartzberg (2009). "Differential expression of interleukin-17A and -17F is coupled to T cell receptor signaling via inducible T cell kinase." Immunity 31(4): 587-97.

112. Singleton, KL, M Gosh, RD Dandekar, BB Au-Yeung, O Ksionda, VL Tybulewicz, A Altman, DJ Fowell, and C Wulfing (2011). "Itk controls the spatiotemporal organization of T cell activation." Sci Signal 4(193): ra66.

113. Sahu, N, AM Venegas, D Jankovic, W Mitzner, J Gomez-Rodriguez, JL Cannons, C Sommers, P Love, A Sher, PL Schwartzberg, and A August (2008). "Selective expression rather than specific function of Txk and Itk regulate Th1 and Th2 responses." Journal of Immunology 181(9): 6125-31.

114. Gomez-Rodriguez, J, F Meylan, R Handon, ET Hayes, SM Anderson, MR Kirby, RM Siegel, and PL Schwartzberg (2016). "Itk is required for Th9 differentiation via TCR-mediated induction of IL-2 and IRF4." Nat Commun 7: 10857.

115. Bachmann, MF, DR Littman, and XC Liao (1997). "Antiviral immune responses in Itk-deficient mice." J Virol 71(10): 7253-7.

116. Atherly, LO, MA Brehm, RM Welsh, and LJ Berg (2006). "Tec kinases Itk and Rlk are required for CD8+ T cell responses to virus infection independent of their role in CD4+ T cell help." J Immunol 176(3): 1571-81.

117. Mansouri, D, SA Mahdaviani, S Khalilzadeh, SA Mohajerani, M Hasanzad, S Sadr, SA Nadji, S Karimi, A Droodinia, N Rezaei, RM Linka, K Bienemann, A Borkhardt, MR Masjedi, and AA Velayati (2012). "IL-2-inducible T-cell kinase deficiency with pulmonary manifestations due to disseminated Epstein-Barr virus infection." Int Arch Allergy Immunol 158(4): 418-22.

118. Linka, RM, SL Risse, K Bienemann, M Werner, Y Linka, F Krux, C Synaeve, R Deenen, S Ginzel, R Dvorsky, M Gombert, A Halenius, R Hartig, M Helminen, A Fischer, P Stepensky, K Vettenranta, K Kohrer, MR Ahmadian, HJ Laws, B Fleckenstein, H Jumaa, S Latour, B Schraven, and A Borkhardt (2012). "Loss-of-function mutations within the IL-2 inducible kinase ITK in patients with EBV-associated lymphoproliferative diseases." Leukemia.

119. Huck, K, O Feyen, T Niehues, F Ruschendorf, N Hubner, HJ Laws, T Telieps, S Knapp, HH Wacker, A Meindl, H Jumaa, and A Borkhardt (2009). "Girls homozygous for an IL-2-inducible T cell kinase mutation that leads to protein deficiency develop fatal EBV-associated lymphoproliferation." The Journal of Clinical Investigation 119(5): 1350-8.

120. Ghosh, S, K Bienemann, K Boztug, and A Borkhardt (2014). "Interleukin-2-inducible T-cell kinase (ITK) deficiency - clinical and molecular aspects." J Clin Immunol 34(8): 892-9.

121. Palendira, U, C Low, A Chan, AD Hislop, E Ho, TG Phan, E Deenick, MC Cook, DS Riminton, S Choo, R Loh, F Alvaro, C Booth, HB Gaspar, A Moretta, R Khanna, AB Rickinson, and SG Tangye (2011). "Molecular pathogenesis of EBV susceptibility in XLP as revealed by analysis of female carriers with heterozygous expression of SAP." PLoS Biol 9(11): e1001187.

122. Hogquist, KA, SC Jameson, WR Heath, JL Howard, MJ Bevan, and FR Carbone (1994). "T cell receptor antagonist peptides induce positive selection." Cell 76(1): 17-27.

123. Atherly, LO, JA Lucas, M Felices, CC Yin, SL Reiner, and LJ Berg (2006). "The Tec family tyrosine kinases Itk and Rlk regulate the development of conventional CD8+ T cells." Immunity 25(1): 79-91.

124. Labno, CM, CM Lewis, D You, DW Leung, A Takesono, N Kamberos, A Seth, LD Finkelstein, MK Rosen, PL Schwartzberg, and JK Burkhardt (2003). "Itk functions to control actin polymerization at the immune synapse through localized activation of Cdc42 and WASP." Curr Biol 13(18): 1619-24.

125. Anikeeva, N, K Somersalo, TN Sims, VK Thomas, ML Dustin, and Y Sykulev (2005). "Distinct role of lymphocyte function-associated antigen-1 in mediating effective cytolytic activity by cytotoxic T lymphocytes." Proc Natl Acad Sci U S A 102(18): 6437-42.

126. Betts, MR, JM Brenchley, DA Price, SC De Rosa, DC Douek, M Roederer, and RA Koup (2003). "Sensitive and viable identification of antigen-specific CD8+ T cells by a flow cytometric assay for degranulation." Journal of Immunological Methods 281(1-2): 65-78.

127. Trinchieri, G, M Matsumoto-Kobayashi, SC Clark, J Seehra, L London, and B Perussia (1984). "Response of resting human peripheral blood natural killer cells to interleukin 2." J Exp Med 160(4): 1147-69.

128. Rohr, J, K Beutel, A Maul-Pavicic, T Vraetz, J Thiel, K Warnatz, I Bondzio, U Gross-Wieltsch, M Schundeln, B Schutz, W Woessmann, AH Groll, B Strahm, J Pagel, C Speckmann, G Janka, G Griffiths, K Schwarz, U zur Stadt, and S Ehl (2010). "Atypical familial hemophagocytic lymphohistiocytosis due to

mutations in UNC13D and STXBP2 overlaps with primary immunodeficiency diseases." Haematologica 95(12): 2080-7.

129. Miller, AT and LJ Berg (2002). "Defective Fas ligand expression and activation-induced cell death in the absence of IL-2-inducible T cell kinase." J Immunol 168(5): 2163-72.

130. Orange, JS, S Roy-Ghanta, EM Mace, S Maru, GD Rak, KB Sanborn, A Fasth, R Saltzman, A Paisley, L Monaco-Shawver, PP Banerjee, and R Pandey (2011). "IL-2 induces a WAVE2-dependent pathway for actin reorganization that enables WASp-independent human NK cell function." J Clin Invest 121(4): 1535-48.

131. Ruffo, E, V Malacarne, SE Larsen, R Das, L Patrussi, C Wulfing, C Biskup, SM Kapnick, K Verbist, P Tedrick, PL Schwartzberg, CT Baldari, I Rubio, KE Nichols, AL Snow, G Baldanzi, and A Graziani (2016). "Inhibition of diacylglycerol kinase alpha restores restimulation-induced cell death and reduces immunopathology in XLP-1." Sci Transl Med 8(321): 321ra7.

132. Pattu, V, M Halimani, M Ming, C Schirra, U Hahn, H Bzeih, HF Chang, L Weins, E Krause, and J Rettig (2013). "In the crosshairs: investigating lytic granules by high-resolution microscopy and electrophysiology." Front Immunol 4: 411.

133. Suzuki, K and IM Verma (2008). "Phosphorylation of SNAP-23 by IkappaB kinase 2 regulates mast cell degranulation." Cell 134(3): 485-95.

134. Feske, S, Y Gwack, M Prakriya, S Srikanth, SH Puppel, B Tanasa, PG Hogan, RS Lewis, M Daly, and A Rao (2006). "A mutation in Orai1 causes immune deficiency by abrogating CRAC channel function." Nature 441(7090): 179-85.

135. Picard, C, CA McCarl, A Papolos, S Khalil, K Luthy, C Hivroz, F LeDeist, F Rieux-Laucat, G Rechavi, A Rao, A Fischer, and S Feske (2009). "STIM1 mutation associated with a syndrome of immunodeficiency and autoimmunity." N Engl J Med 360(19): 1971-80.

136. Liu, D, JA Martina, XS Wu, JA Hammer, 3rd, and EO Long (2011). "Two modes of lytic granule fusion during degranulation by natural killer cells." Immunol Cell Biol 89(6): 728-38.

137. James, AM, HT Hsu, P Dongre, G Uzel, EM Mace, PP Banerjee, and JS Orange (2013). "Rapid activation receptor- or IL-2-induced lytic granule convergence in human natural killer cells requires Src, but not downstream signaling." Blood 121(14): 2627-37.

138. Gerosa, F, M Tommasi, C Benati, G Gandini, M Libonati, G Tridente, G Carra, and G Trinchieri (1993). "Differential effects of tyrosine kinase inhibition in CD69 antigen expression and lytic activity induced by rIL-2, rIL-12, and rIFN-alpha in human NK cells." Cell Immunol 150(2): 382-90.

139. Halle, S, KA Keyser, FR Stahl, A Busche, A Marquardt, X Zheng, M Galla, V Heissmeyer, K Heller, J Boelter, K Wagner, Y Bischoff, R Martens, A Braun, K Werth, A Uvarovskii, H Kempf, M Meyer-Hermann, R Arens, M Kremer, G Sutter, M Messerle, and R Forster (2016). "In Vivo Killing Capacity of Cytotoxic T Cells Is Limited and Involves Dynamic Interactions and T Cell Cooperativity." Immunity 44(2): 233-45.

140. Bossi, G, C Trambas, S Booth, R Clark, J Stinchcombe, and GM Griffiths (2002). "The secretory synapse: the secrets of a serial killer." Immunological Reviews 189: 152-60.

141. Beemiller, P and MF Krummel (2013). "Regulation of T-cell receptor signaling by the actin cytoskeleton and poroelastic cytoplasm." Immunol Rev 256(1): 148-59.

142. Ritter, AT, KL Angus, and GM Griffiths (2013). "The role of the cytoskeleton at the immunological synapse." Immunol Rev 256(1): 107-17.

143. Riedl, J, AH Crevenna, K Kessenbrock, JH Yu, D Neukirchen, M Bista, F Bradke, D Jenne, TA Holak, Z Werb, M Sixt, and R Wedlich-Soldner (2008). "Lifeact: a versatile marker to visualize F-actin." Nat Methods 5(7): 605-7.

144. Keefe, D, L Shi, S Feske, R Massol, F Navarro, T Kirchhausen, and J Lieberman (2005). "Perforin triggers a plasma membrane-repair response that facilitates CTL induction of apoptosis." Immunity 23(3): 249-62.

145. Chen, TW, TJ Wardill, Y Sun, SR Pulver, SL Renninger, A Baohan, ER Schreiter, RA Kerr, MB Orger, V Jayaraman, LL Looger, K Svoboda, and DS Kim (2013). "Ultrasensitive fluorescent proteins for imaging neuronal activity." Nature 499(7458): 295-300.

146. Sneller, MC, J Wang, JK Dale, W Strober, LA Middelton, Y Choi, TA Fleisher, MS Lim, ES Jaffe, JM Puck, MJ Lenardo, and SE Straus (1997). "Clinical, immunologic, and genetic features of an autoimmune lymphoproliferative syndrome associated with abnormal lymphocyte apoptosis." Blood 89(4): 1341-8.

147. Raucher, D, T Stauffer, W Chen, K Shen, S Guo, JD York, MP Sheetz, and T Meyer (2000). "Phosphatidylinositol 4,5-bisphosphate functions as a second messenger that regulates cytoskeleton-plasma membrane adhesion." Cell 100(2): 221-8.

148. Shibasaki, Y, H Ishihara, N Kizuki, T Asano, Y Oka, and Y Yazaki (1997). "Massive actin polymerization induced by phosphatidylinositol-4-phosphate 5-kinase in vivo." J Biol Chem 272(12): 7578-81.

149. Gilmore, AP and K Burridge (1996). "Regulation of vinculin binding to talin and actin by phosphatidyl-inositol-4-5-bisphosphate." Nature 381(6582): 531-5.

150. Yin, HL and PA Janmey (2003). "Phosphoinositide regulation of the actin cytoskeleton." Annu Rev Physiol 65: 761-89.

151. Varnai, P, B Thyagarajan, T Rohacs, and T Balla (2006). "Rapidly inducible changes in phosphatidylinositol 4,5-bisphosphate levels influence multiple regulatory functions of the lipid in intact living cells." J Cell Biol 175(3): 377-82.

152. Kwik, J, S Boyle, D Fooksman, L Margolis, MP Sheetz, and M Edidin (2003). "Membrane cholesterol, lateral mobility, and the phosphatidylinositol 4,5-bisphosphate-dependent organization of cell actin." Proc Natl Acad Sci U S A 100(24): 13964-9.

153. Balla, T and P Varnai (2009). "Visualization of cellular phosphoinositide pools with GFP-fused protein-domains." Curr Protoc Cell Biol Chapter 24: Unit 24 4.

154. Wollman, R and T Meyer (2012). "Coordinated oscillations in cortical actin and Ca2+ correlate with cycles of vesicle secretion." Nat Cell Biol 14(12): 1261-9.

155. Orci, L, KH Gabbay, and WJ Malaisse (1972). "Pancreatic beta-cell web: its possible role in insulin secretion." Science 175(4026): 1128-30.

156. Giner, D, P Neco, M Frances Mdel, I Lopez, S Viniegra, and LM Gutierrez (2005). "Real-time dynamics of the F-actin cytoskeleton during secretion from chromaffin cells." J Cell Sci 118(Pt 13): 2871-80.

157. Villanueva, J, CJ Torregrosa-Hetland, V Garcia-Martinez, M del Mar Frances, S Viniegra, and LM Gutierrez (2012). "The F-actin cortex in chromaffin granule dynamics and fusion: a minireview." J Mol Neurosci 48(2): 323-7.

158. Torregrosa-Hetland, CJ, J Villanueva, D Giner, I Lopez-Font, A Nadal, I Quesada, S Viniegra, G Exposito-Romero, A Gil, V Gonzalez-Velez, J Segura, and LM Gutierrez (2011). "The F-actin cortical network is a major factor influencing the organization of the secretory machinery in chromaffin cells." J Cell Sci 124(Pt 5): 727-34.

159. Kogel, T, R Rudolf, E Hodneland, A Hellwig, SA Kuznetsov, F Seiler, TH Sollner, J Barroso, and HH Gerdes (2010). "Distinct roles of myosin Va in

membrane remodeling and exocytosis of secretory granules." Traffic 11(5): 637-50.

160. Rudolf, R, T Kogel, SA Kuznetsov, T Salm, O Schlicker, A Hellwig, JA Hammer, 3rd, and HH Gerdes (2003). "Myosin Va facilitates the distribution of secretory granules in the F-actin rich cortex of PC12 cells." J Cell Sci 116(Pt 7): 1339-48.

161. Varadi, A, T Tsuboi, and GA Rutter (2005). "Myosin Va transports dense core secretory vesicles in pancreatic MIN6 beta-cells." Mol Biol Cell 16(6): 2670-80.

162. Scott, CC, W Dobson, RJ Botelho, N Coady-Osberg, P Chavrier, DA Knecht, C Heath, P Stahl, and S Grinstein (2005). "Phosphatidylinositol-4,5-bisphosphate hydrolysis directs actin remodeling during phagocytosis." J Cell Biol 169(1): 139-49.

163. Niedergang, F, V Di Bartolo, and A Alcover (2016). "Comparative Anatomy of Phagocytic and Immunological Synapses." Front Immunol 7: 18.

164. Huang, JF, Y Yang, H Sepulveda, W Shi, I Hwang, PA Peterson, MR Jackson, J Sprent, and Z Cai (1999). "TCR-Mediated internalization of peptide-MHC complexes acquired by T cells." Science 286(5441): 952-4.

165. Batista, FD, D Iber, and MS Neuberger (2001). "B cells acquire antigen from target cells after synapse formation." Nature 411(6836): 489-94.

166. Batista, FD and MS Neuberger (2000). "B cells extract and present immobilized antigen: implications for affinity discrimination." EMBO J 19(4): 513-20.

167. Zimmer, J, V Ioannidis, and W Held (2001). "H-2D ligand expression by Ly49A+ natural killer (NK) cells precludes ligand uptake from environmental cells: implications for NK cell function." J Exp Med 194(10): 1531-9.

168. Carlin, LM, K Eleme, FE McCann, and DM Davis (2001). "Intercellular transfer and supramolecular organization of human leukocyte antigen C at inhibitory natural killer cell immune synapses." J Exp Med 194(10): 1507-17.

169. Bizario, JC, J Feldmann, FA Castro, G Menasche, CM Jacob, L Cristofani, EB Casella, JC Voltarelli, G de Saint-Basile, and EM Espreafico (2004). "Griscelli syndrome: characterization of a new mutation and rescue of T-cytotoxic activity by retroviral transfer of RAB27A gene." J Clin Immunol 24(4): 397-410.

170. Ming, M, C Schirra, U Becherer, DR Stevens, and J Rettig (2015). "Behavior and Properties of Mature Lytic Granules at the Immunological Synapse of Human Cytotoxic T Lymphocytes." PLoS One 10(8): e0135994.

171. Martina, JA, XS Wu, M Catalfamo, T Sakamoto, C Yi, and JA Hammer, 3rd (2011). "Imaging of lytic granule exocytosis in CD8+ cytotoxic T lymphocytes reveals a modified form of full fusion." Cell Immunol 271(2): 267-79.

172. Sherman, E, V Barr, and LE Samelson (2013). "Super-resolution characterization of TCR-dependent signaling clusters." Immunol Rev 251(1): 21-35.

173. Wilke, S, J Krausze, and K Bussow (2012). "Crystal structure of the conserved domain of the DC lysosomal associated membrane protein: implications for the lysosomal glycocalyx." BMC Biol 10: 62.

174. Carlsson, SR and M Fukuda (1989). "Structure of human lysosomal membrane glycoprotein 1. Assignment of disulfide bonds and visualization of its domain arrangement." J Biol Chem 264(34): 20526-31.

175. Davis, SJ and PA van der Merwe (2006). "The kinetic-segregation model: TCR triggering and beyond." Nat Immunol 7(8): 803-9.

176. Liao, XC and DR Littman (1995). "Altered T cell receptor signaling and disrupted T cell development in mice lacking Itk." Immunity 3(6): 757-69.

177. Naviaux, RK, E Costanzi, M Haas, and IM Verma (1996). "The pCL vector system: rapid production of helper-free, high-titer, recombinant retroviruses." J Virol 70(8): 5701-5.

Biographical Sketch

SENTA KAPNICK

EDUCATION

2010 – 2016 **Ph.D., Cell Signaling and Immunology**
National Institutes of Health/Johns Hopkins University Graduate Partnership Program
Bethesda, MD

Degree conferral date: 8/2016

Advisor: Dr. Pam Schwartzberg

Thesis title: Understanding cytotoxic T lymphocyte effector function using models of primary immunodeficiencies

2007 – 2008 **M.H.S., Molecular Microbiology and Immunology**
Vaccine Science and Policy Certificate
Johns Hopkins University Bloomberg School of Public Health
Baltimore, MD

Thesis title: Tuberculosis Drug Development – Current Drugs and Promising Targets

2001 –2005 **B.A., Biology**
The University of Texas at Austin
Austin, TX

RESEARCH EXPERIENCE

2010 – 2016 **Pre-doctoral Trainee**
NHGRI/GDRB/Cell Signaling and Immunity Section
Bethesda, MD

Advisor: Dr. Pam Schwartzberg

Research synopsis: Investigation of the role of proximal T cell receptor signaling components and the actin cytoskeleton in regulating proper $CD8^+$ T lymphocyte cytolytic effector function using models of primary immunodeficiencies

2008 – 2010 **Oak Ridge Institute for Science and Education (ORISE) Research Fellow**
FDA/CBER/Division of Viral Products
Bethesda, MD

Advisors: Drs. Hana Golding and Marina Zaitseva

Research synopsis: Application of bioluminescence imaging to characterize vaccinia virus dissemination and evaluate novel passive immunotherapies in the mouse model

2005 – 2007 **Microbiologist**
Texas Department of State Health Services/Division of Mycology and Mycobacteriology
Austin, TX

Advisor: Ken Jost, Jr. and Denise Dunbar

Description of work: *Mycobacterium* culture and microscopy, biochemical assays, high-performance liquid chromatography, drug susceptibility testing, maintenance of CDC Tuberculosis Genotyping Database, prevalence surveys

2005 **Public Health Research Intern**
Texas Department of State Health Services/Division of Consumer Microbacteriology
Austin, TX

Advisors: Drs. Suzanne Barth and Monica Kingsley

Research synopsis: Environmental analysis of Texas bay waters for *Vibrio* species to determine public health exposure risks

2004 – 2005 **Behavioral Science Research Assistant**
The University of Texas at Austin
Austin, TX

Advisor: Dr. Christopher Ellison

Research synopsis: Investigation of intrinsic, extrinsic, and quest religious relationship's impact on academic interests among college students

TEACHING AND MENTORING EXPERIENCE

Spring 2016 **Teaching Fellow, Bioinformatics short course, Genes and Genomes (HLSC322)**
Integrated Life Sciences Program, Honors College, U of Maryland, College Park, MD

Fall 2015 **Instructor, Research Tools for Studying Disease (BIOL262)**
Foundation for Advanced Education in the Sciences (FAES), NIH, Bethesda, MD

Spring 2015 **Teaching Fellow, Bioinformatics short course, Genes and Genomes (HLSC322)**
Integrated Life Sciences Program, Honors College, U of Maryland, College Park, MD

Summer 2014 **Lead, Fundamentals in Cellular & Molecular Immunology Journal Club**
National Institutes of Health, Bethesda, MD

Summer 2012 **Judge, NIH Post Baccalaureate Poster Day**
National Institutes of Health, Bethesda, MD

2011 **Scientists Teaching Science Workshop**
National Institutes of Health, Bethesda, MD

Spring 2011 **Teaching Assistant, Developmental Biology laboratory**
Johns Hopkins University, Baltimore, MD

Fall 2010 **Teaching Assistant, Biochemistry laboratory**
Johns Hopkins University, Baltimore, MD

2005 – 2006 **Teaching Assistant, math and science courses**
Webb Middle School/Austin Independent School District, Austin, TX

2003 - 2005 **Tutor, Biology**
The University of Texas at Austin, Austin, TX

AWARDS

2015	**Three-Minute-Talk (TmT) Competition Finalist** NHGRI, Bethesda, MD
2015	**Genome Recognition of Employee Accomplishment & Talents (GREAT) Award** National Human Genome Research Institute (NHGRI), Bethesda, MD
2014	**Fellows Award for Research Excellence (FARE) Award** NIH, Bethesda, MD
2014	**American Association of Immunologists (AAI) Trainee Abstract Award** Baltimore, MD
2011	**Dupont Award for Excellence in Teaching, Developmental Biology Laboratory** Johns Hopkins University, Baltimore, MD

LEADERSHIP

2015 – 2016	**Organization Committee, NIH 2016 Career Symposium** National Institutes of Health, Bethesda, MD
2014 – 2015	**Representative, Genome Trainee Advisory Committee** National Human Genome Research Institute, Bethesda, MD
2013 – 2014	**Co-chair of the Outreach and Mentoring Committee, Graduate Student Council** National Institutes of Health, Bethesda, MD

PUBLICATIONS

1. **Kapnick SM**, Stinchcombe JC, Griffiths GM, Schwartzberg PL. Inducible T cell kinase regulates degranulation and expression of cytolytic effectors in CD8+ cytotoxic T cells. *In preparation.*
2. Ritter AT*, **Kapnick SM***, Griffiths GM, Lippincott-Schwartz J, Schwartzberg PL. Dynamic regulation of cortical actin and secretion controls cytolytic activity of CD8 cells. *In preparation.* *first co-authors
3. Ruffo E, Malacarne V, Larsen SE, Das R, Patrussi L, Wülfing C, Biskup C, **Kapnick SM**, Verbist K, Tedrick P, Schwartzberg PL, Baldari CT, Rubio I, Nichols KE, Snow AL, Baldanzi G, Graziani A. (2016) Inhibition of diacylglycerol kinase α restores restimulation-induced cell death and reduced immunopathology in XLP-1. *Sci Trans Med*. 8(321):321ra7
4. Afonso PV, McCann CP, **Kapnick SM**, Parent CA. (2013) Discoidin domain receptor 2 regulates neutrophil chemotaxis in 3D collagen matrices. *Blood*. 121(9):1644-50.
5. Zaitseva M, **Kapnick S,** Golding H. (2012) Measurements of vaccinia virus dissemination using whole-body imaging: approaches for predicting lethality in challenge models and testing of vaccines and antiviral treatments. *Methods Mol Biol.* 890:161-76.
6. Golden JW, Zaitseva M, **Kapnick S,** Fisher RW, Mikolajczyk MG, Ballantyne J, Golding H, Hooper JW. (2011) Polyclonal antibody cocktails generated using DNA vaccine technology protect in murine models of orthopoxvirus disease. *Virol J*. 8(1): 441.
7. Zaitseva M, **Kapnick SM**, Meseda CM, Shotwell E, King LR, Manischewitz J, Scott J, Kodihalli S, Merchlinsky M, Nielsen H, Lantto J, Weir J, Golding H. (2011) Passive immunotherapies protect WRvFire and IHD-J-Luc vaccinia virus-infected mice from lethality

by reducing viral loads in the upper respiratory tract and internal organs. *J Virol.* 85(17): 9147-58.

8. Zaitseva M, **Kapnick SM**, Scott J, King LR, Manischewitz J, Sirota L, Kodihalli S, Golding H. (2009) Application of bioluminescence imaging to the prediction of lethality in vaccinia virus infected mice. *J Virol.* 83(20): 10437-47.
9. **Kapnick SM**, Zhang Y. (2008) New tuberculosis drug development: targeting the shikimate pathway. *Expert Opin. Drug Discov.* 3(5): 565-77.

INVITED ORAL PRESENTATIONS

1. Understanding cytotoxic T lymphocyte effector function using models of primary immunodeficiencies. *Johns Hopkins University Trainee Retreat*. St. Michaels, MD. October 2015.
2. Investigating CD8+ T cell cytolytic function in a model of a primary immunodeficiency. *National Human Genome Research Institute Symposium,* Bethesda, MD. December 2014.
3. Inducible T cell kinase controls $CD8^+$ cytolytic T lymphocyte effector function. *Annual Meeting of the American Association of Immunologists.* Pittsburgh, PA. May 2014.
4. Investigating the role of inducible T cell kinase in cytotoxic T lymphocyte effector function. *Clinical Immunology Society: Primary Immune Deficiency Diseases North American Conference.* Baltimore, MD. April 2014. (selected presenter for "guided poster session")
5. Investigating the role of inducible T cell kinase in cytotoxic T lymphocyte effector function. *National Institutes of Health Immunology Interest Group Retreat*. Bethesda, MD. September 2013.

POSTER PRESENTATIONS

1. **Kapnick SM,** Schwartzberg PL. Inducible T cell kinase regulates the final stage of cytolysis in CD8+ cytotoxic T lymphocytes. *FASEB Signal Transduction in the Immune System.* Big Sky, MT. June 2015.
2. **Kapnick SM,** Schwartzberg PL. Investigating $CD8^+$ T cell cytolytic function in a model of a primary immunodeficiency. *National Human Genome Research Institute Symposium.* Bethesda, MD. December 2014.
3. **Kapnick SM**, Schwartzberg PL. Investigating the role of inducible T cell kinase in cytotoxic T-lymphocyte effector function. *Annual Meeting of the American Association of Immunologists.* Pittsburgh, PA. May 2014.
4. **Kapnick SM**, Schwartzberg PL. Investigating the role of inducible T cell kinase in cytotoxic T-lymphocyte effector function. *Clinical Immunology Society: Primary Immune Deficiency Diseases North American Conference.* Baltimore, MD. April 2014.
5. **Kapnick SM**, Schwartzberg PL. Investigating the role of inducible T cell kinase in cytotoxic T lymphocyte effector function. *National Institutes of Health Immunology Interest Group Retreat*. Bethesda, MD. September 2013.
6. **Kapnick SM**, Schwartzberg PL. Investigating the role of inducible T cell kinase in cytotoxic T lymphocyte effector function. *FASEB Signal Transduction in the Immune System.* Nassau, Bahamas. June 2013.
7. **Kapnick SM**, Schwartzberg PL. Investigating the role of inducible T cell kinase in cytotoxic T lymphocyte effector function. *National Institutes of Health Graduate Student Symposium.* Bethesda, MD. January 2013.
8. **Kapnick SM**, Schwartzberg PL. Investigating the role of inducible T cell kinase in cytotoxic T lymphocyte effector function. *Johns Hopkins University Cellular, Molecular, Developmental Biology and Biophysics Retreat.* Cumberland, MD. October 2012.

9. **Kapnick SM**, Zaitseva M, Scott J, Meseda C, Nielsen H, Merchilinsky M, Weir J, Golding H. Quantitative bioimaging of WRvFire and IHD-J-Luc vaccinia virus dissemination in mice and the effects of prophylactic and therapeutic treatments with IgG and antivirals. *Annual Meeting of the American Association of Immunologists*. Baltimore, MD. May 2010.
10. **Kapnick SM**, Zaitseva M, Meseda C, Manischewitz J, Nielson H, Merchilinsky M, Weir J, Golding H. Quantitative bioimaging of vaccinia virus infections in live mice: prophylactic immunoglobulin treatments protected from lethal infection and reduced viral dissemination in internal organs. *National Institutes of Health Immunology Interest Group Retreat*. Gettysburg, PA. September 2009.